Biomedical Application of Hyaluronic Acid Nanoparticles

By

Amir Fakhari

Submitted to graduate degree program in Bioengineering
and the Graduate Faculty of the University of Kansas in
partial fulfillment of the requirements for the degree of
Doctor of Philosophy

Committee members:

_____

Chairperson: Dr. Cory J. Berkland

_____

Dr. Michael Detamore

_____

Dr. Laird Forrest

_____

Dr. Stevin Gehrke

_____

Dr. Sarah Kieweg

Date Defended: January 19, 2012

The Dissertation Committee for Amir Fakhari

certifies that this is the approved version of the following dissertation:

Biomedical Application of Hyaluronic Acid Nanoparticles

_____

Chairperson: Dr. Cory J. Berkland

Date approved: January 19, 2012

Abstract

Hyaluronic acid (HA) is a naturally occurring biodegradable polymer with a variety of applications in medicine including tissue engineering, dermatological fillers, and viscosupplementation for osteoarthritis treatment. The cytotoxicity of crosslinking techniques for scaffold fabrication and the high viscosity of viscosupplements have been issues impeding the development of products from HA. Thus, novel HA biomaterials for tissue engineering and improved properties of viscosupplements are in demand. Nanotechnology can be a useful tool to address these needs. The aim of this dissertation was to synthesize HA nanoparticles and use the fabricated nanoparticles to develop colloidal systems for these proposed biomedical applications. First, nanoparticles were successfully synthesized using a technique free of an oil and surfactant. Nanoparticles then were employed to develop colloidal gels and suspensions. Several methods were used to characterize nanoparticles, colloidal gels, and colloidal suspensions including dynamic light scattering, uniaxial compression testing, and rheometry. Factors such as polymer type, concentration of polymer, and molecular weight of polymer (17, 741, and 1500 kDa) influenced nanoparticle properties. In addition, mixing nanoparticles composed of 17 kDa HA in deionized water at different concentrations (15%, 30%, and 45% w/v) formed a stable 3-D colloidal gel as a result of physical entanglement of free polymer chains on the surfaces of nanoparticles. Mechanical and rheological investigation showed that Young's modulus, shear modulus, viscosity, and viscoelasticity of colloidal gels are concentration dependent. These investigations also indicated that the colloidal gels had recoverable and dynamic properties. Viscous suspensions were also formed via addition of nanoparticles (17kDa or 1500 kDa) to either deionized water or to hyaluronic acid solution (1500 kDa). Rheological investigations showed that the viscosity

and the viscoelasticity of the suspensions can be controlled via interactions between polymer in solution and free polymer chains on the surfaces of nanoparticles. These interactions were shown to be influenced by type of the nanoparticles (17 kDa or 1500 kDa). Overall, a variety of HA nanoparticle formulations were discovered that enable new strategies in tissue scaffolding, dermatological filling, and viscosupplementation.

To the supreme God and my wonderful family

Without your help, kindness, and support I would never have arrived at this destination

Acknowledgments

I would like to sincerely and gratefully thank my advisor, Dr. Cory Berkland, for all of his support, guidance, patience, understanding, and most importantly, his friendship during my graduate studies at The University of Kansas. I have been fortunately blessed to have an advisor who gave me a great opportunity to develop my own individuality by being allowed to work with such independence and at the same time his guidance. He encouraged me to not only grow as a researcher but as an independent thinker to use scientific approaches to face the challenges in my future research carrier. For everything you have done for me, Dr. Berkland, I sincerely appreciate.

I would also like to thank members of my dissertation committee: Dr. Michael Detamore, Dr. Laird Forrest, Dr. Stevin Gehrke, and Dr. Sarah Kieweg for their commitment to my dissertation and for their helpful suggestions at different stages of my research. I would like to thank all faculty members in The Bioengineering Graduate Program for numerous discussions and lectures that helped me to improve my knowledge in this area.

I would also like to thank all of my colleagues and collaborators at The University of Kansas especially, Dr. David Moore, Dr. Sheng-Xue Xie, Dr. Huili Guan, Dr. Nashwa El Gendy, Dr. Kristin Aillon, Dr. Xiang Wang, Dr. Abdul Baoum, Dr. Supang Khondee, Dr. Chuda Chittasupho, Dr. Qun Wang, Dr. Zahra Mohammadi, Dr. Joshua Sestak, Dr. Ahmed Badawi, Dr. Parthiban Selvam, Heather Shinogle, Sarah Neuenswander, Justin Douglas, Chris Kuehl, Sharadvi Thati, Adel Alghaith, Nabil Alhakamy, Connor Dennis, Warangkana Pornputtapitak, for their friendship, valuable discussions in science and help in the lab. I would like to acknowledge all staff in The Bioengineering Graduate Program and department of Pharmaceutical Chemistry especially, Leigh Ann Fulkerson, Destiny

Poole, Karen Hall, and Nicole Brooks for all of their assistance and support. Additionally, the years spent in Lawrence would not have been as wonderful without my friends. I greatly value their friendship and I deeply appreciate their belief in me.

To my past mentors, teachers, and colleagues, Dr. Ramazan Asmatulu at Wichita State University, Dr. Vikas Sharma, and Dr. Tom Patapoff at Genentech Inc., who encouraged, inspired, and helped facilitate my pursuit of a graduate science career.

Most importantly, none of this would have been possible without the wonderful love and support of my family. My special thanks to the persons whom I owe everything I am today, my parents, Mohammad Mahdi Fakhari and Nahid Tavassoli, for their unlimited love, concern, support and strength all these years. I would also like to thank my lovely sister, Shiva Fakhari for her great love and support. Their faith and confidence in my abilities and in me is what has shaped me to be the person I am today.

Amir Fakhari
December 2011

Table of content:

Chapter 1

Introduction

Chapter 1: Introduction

1.1. Introduction to hyaluronic acid

Hyaluronic acid (HA), also named hyaluronan, is a high molecular weight (10^5-10^7 Da) naturally occurring biodegradable polymer. HA is an unbranched non-sulfated glycosaminoglycan (GAG) composed of repeating disaccharides (β-1,4-D-glucuronic acid (known as uronic acid) and β-1,3-*N*-acetyl-*D*-glucosamide) (Figure 1-1) (1, 2). HA can include several thousand sugar molecules in the backbone. HA is a polyanion that can self-associate and that can also bind water molecules (when not bound to other molecules) giving it a stiff, viscous quality similar to 'Jello' (3).

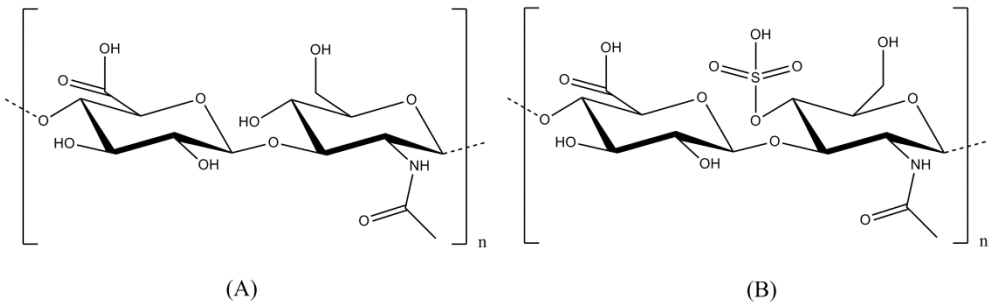

Figure (1-1) Chemical structure of two glycosaminoglycans (GAGs) made of disaccharide repeats of *N*-acetylglucosamine and glucuronic acid. (A) Hyaluronic acid (HA). (B) Chondroitin sulfate (CS).

Hyaluronic acid is one of the major elements in the extracellular matrix (ECM) of vertebrate tissues. It is found in almost all body fluids and tissues, such as the synovial fluid, the vitreous humor of the eye, and hyaline cartilage (Table 1-1) (4-7). This biopolymer works as a scaffold, binding other matrix molecules including aggrecan (2). It is also involved in several important biological functions, such as regulation of cell

adhesion and cell motility, manipulation of cell differentiation and proliferation, and providing biomechanical properties of tissues (5). Several cell surface receptors such as CD44, RHAMM, and ICAM-1 interact with HA influencing cellular processes including morphogenesis, wound repair, inflammation, and metastasis (8-11). Moreover, HA is responsible for supporting the viscoelasticity of biofluids (synovial fluid and vitreous humor of the eye) and controlling tissue hydration and water transport (3). In addition, HA has been found during embryonic development, suggesting materials composed of HA may persuade favorable conditions for tissue regeneration and growth (Table 1-1) (12-16).

Table (1-1) Examples of body tissues/fluids that contain HA. Table was regenerated with permission (2, 17).

Tissue or body fluid	Concentration (µg/g; µg/ml)	Remarks
Umbilical cord	4100	Primary high molecular weight HA.
Joint (synovial) fluid	1400-3600	Decreasing HA concentration occurs due to increasing the synovial fluid volume under inflammatory conditions.
Vitreous body	140-500	During tissue maturation, HA concentration increases.
Cartilage	-	HA works as a scaffold for the binding of other matrix molecules such as aggrecan.
Dermis	200-500	HA is used as a "rejuvenating" agent in cosmetic dermatology.
Epidermis	100	High HA concentration was observed around the cells that synthesized dermis.
Thoracic lymph	0.2-50	HA molecular weight affects inflammatory response and cell binding.

HA's characteristics including its consistency, biocompatibility, and hydrophilicity have made it an excellent moisturizer in cosmetic dermatology and skin-care products (3). Moreover, its unique viscoelasticity and limited immunogenicity have led it to be used in several biomedical applications such as viscosupplementation in osteoarthritis treatment, as a surgical aid in ophthalmology, and for surgical wound

regeneration in dermatology (3, 4). In addition, HA has currently been explored as a drug delivery agent for different routes such as nasal, pulmonary, ophthalmic, topical and parenteral (3, 18).

1.1.1. History of hyaluronic acid

In 1934, Karl Meyer and his colleague John Palmer were the first investigators who discovered and isolated HA from the vitreous body of cows' eyes (2, 3). In the 1950s, the chemical structure of HA was solved by this group. They found that HA is composed of two sugar molecules (*D*-glucuronic acid (known as uronic acid) and *D*-*N*-acetyl glucosamine) and called it hyaluronic acid (hyaluronan). This name is derived from "hyalos" (the Greek word for glass + uric acid). Initially, they isolated HA as an acid but it behaved like a salt in physiological conditions (sodium hyaluronate) (2-4). At the time, they did not fully appreciate their discovery of one of the most interesting and important biological macromolecules. Several years after them in 1942, Endore Balazs patented the first application of HA as a substitute for egg white in bakery products (3).

The first biomedical application of HA took place in late 1950s when HA was used for a vitreous substitution/replacement during eye surgery. For medical applications, HA was initially isolated from umbilical cord and shortly afterward, from rooster combs (3, 4). Later on, HA was isolated from other sources and the structural/biological characteristics of this polysaccharide were investigated more deeply in several laboratories (3).

1.1.2. Properties of hyaluronic acid

1.1.2.1. Chemical properties of hyaluronic acid

Structural studies showed that the two sugar molecules, *D*-glucuronic acid and *D*-*N*-acetyl glucosamine, in the HA disaccharide structure are connected together through alternative beta-1,4 and beta-1,3 glycosidic bonds (Figure 1-1) (2, 3). The hyaluronic acid backbone is stiffened in physiological solution via a combination of internal hydrogen bonds, interactions with solvents, and the chemical structure of the disaccharide. HA molecular investigations suggested that the axial hydrogen atoms form a non-polar face (relatively hydrophobic) and the equatorial side chains form a more polar face (hydrophilic) led to a twisted ribbon structure for HA called a coiled structure (3).

HA's structural characteristics hinge on this random coiled structure in solution. At very low concentrations, chains entangle each other, leading to a mild viscosity (molecular weight dependent). On the other hand, HA solutions at higher concentrations have a higher than expected viscosity due to greater HA chain entanglement that is shear-dependent. For instance, a 1% solution of high molecular weight HA (Mw > ~1000 kDa) can behave like jelly, but when shear stress is applied it will easily shear thin and can be administered via a thin needle (3). As such, HA is known as a "pseudo-plastic" material. This rheological property (concentration and molecular weight dependent) of HA solutions has made HA ideal for lubrication in biomedical applications (3).

In addition to the unique viscosity of HA, viscoelasticity is another characteristic of HA resulting from entanglement and self-association of HA random coils in solution (2). It was suggested that the molecular self-association of HA occurs by forming anti-

parallel double helices, bundles and ropes. Further experiments verified that HA chain–chain association occured in solution. Moreover, studies proposed that hydrogen bonding between adjacent saccharides occurred alongside mutual electrostatic repulsion between carboxyl groups, thus stiffening HA (3, 6, 19). Viscoelasticity of HA can be tied to these molecular interactions which are also dependent on concentration and molecular weight.

Electrostatic and ionic effects on HA were evaluated as a function of counter-ion type and valency. Studies suggested that these greatly affect rheological and hydrodynamic properties of HA. In one study, the effect of electrostatic and ionic interactions was investigated by comparing HA solution properties in deionized water (D.I.), 0.5 M NaCl, and 0.5 M NaOH. This study showed that solution properties affect the hydrogen bonding and electrostatic interaction between the solution and HA resulting in a change in HA chain stiffness (2, 20). Moreover, the hydrodynamic radius of HA was found to be greater in D.I. water than in 0.5 M NaCl or 0.5 NaOH (D.I. water > 0.5M NaCl > 0.5M NaOH) (2).

1.1.2.2. Biological properties of hyaluronic acid

As mentioned before, hyaluronic acid performs several structural tasks in the extracellular matrix (ECM) as it binds with cells and other biological components through specific and non-specific interactions. Several extracellular matrix proteins are stabilized upon binding to HA. Specific molecules and receptors that interact with HA are involved in cellular signal transduction; molecules such as aggrecan, versican, and neurocan, and receptors including CD44, RHAMM, TSG6, GHAP, and LYVE-1 are examples of cell components that bind to HA (3). Between these receptors, CD44 and

RHAMM seem to have received more attention since they are found to be involved in cancer metastases (3, 21-23). CD44 is a structurally variable and multifunctional cell surface glycoprotein on most cell types and is perhaps the best characterized transmembrane HA receptor so far. Due to its wide distribution and based on current knowledge, CD44 is considered to be the primary HA receptor on most cell types (3, 24).

Hyaluronic acid also stimulates gene expression in macrophages, endothelial cells, eosinophils, and certain epithelial cells. High molecular weight HA does not seem to be involved in gene expression and only low/intermediate molecular weight HA (2×10^4-4.5×10^5 Da) is known to promote gene expression (3, 25, 26). As an example, HA is also known to have an important role in wound healing and scar formation. Products of HA degradation (low molecular weight HA) are identified to contribute in the scar formation process. Moreover, scar formation was minimized when high molecular weight HA was found in wound fluid during fetal wound healing. These results suggested that the molecular weight of HA plays a significant role in wound healing and scar formation. The findings also suggested that high molecular weight HA favored cell quiescence and supported tissue integrity, whereas production of HA fragments signaled injury and initiated the inflammatory response (2, 3, 27).

1.2. Synthesis of hyaluronic acid

Hyaluronic acid is a natural polymer biologically synthesized by cells in the body via an enzymatic process. HA production is a unique, highly controlled, and continuous process in which HA is produced and secreted by fibroblasts, keratinocytes, or chondrocytes. The Golgi network is the production site for most glycosaminoglycans. In tissues such as skin and cartilage where HA comprises a large portion of the tissue mass, the level of HA synthesis is very high. HA is naturally synthesized by hyaluronan synthases (HAS1, HAS2, and HAS3), a class of integral membrane proteins (3, 28). In HA production by hyaluronan synthase enzymes, large linear polymers of the repeating disaccharide units are made. The mechanism of HA synthesis involves chain extension by addition of a monosaccharide (alternating addition of glucuronic acid and *N*-acetyl glucosamine) to the reducing end of the chain (2). The number of repeat disaccharides in a completed HA molecule can reach as high as 10,000 or more and a molecular weight of around 4 million Daltons (molecular weight of each disaccharide is about 400 Daltons). Since the average length of a disaccharide is about 1 nm, a HA molecule of 10,000 repeats could extend 10 μm if stretched from end to end (approximately equal to the diameter of a human erythrocyte) (3, 29).

1.3. Degradation of hyaluronic acid

Degradation of HA is a step-wise process that can occur via enzymatic or non-enzymatic reactions. Three types of enzymes (hyaluronidase, β-*D*-glucuronidase, and β–*N*-acetyl-hexosaminidase) are involved in enzymatic degradation of hyaluronic acid.

These enzymes are found in various forms, in the intercellular space and in serum. Hyaluronidase cleaves high molecular weight HA into smaller fragments while the other two enzymes degrade the fragments by removing non-reducing terminal sugars (3, 17, 30). It was observed that cleavage can occur in a single glycosidic bond on the HA backbone causing fragmentation or the enzyme can remove a single monosaccharide unit from the HA backbone (30). Enzymes not only help to degrade HA but also play an important role defining HA. For instance, enzymes available in the cytosol of cells are involved in basic biological processes including trimming of oligosaccharides (30).

Non-enzymatic mechanisms often degrade HA via thermal or shear stress. In addition, chemical reactions such as acidic/alkaline hydrolysis and degradation by oxidants are categorized as non-enzymatic degradation pathways for HA (17, 30, 31). Ultrasonication degrades HA in a non-random fashion. Studies suggested that high molecular weight HA chains degrade slower than low molecular weight HA chains subjected to ultrasonication (2, 30). Heat is another type of stress leading to HA degradation. Rheological studies on HA solutions showed that increasing temperature resulted in degradation and decreased viscosity exponentially as a function of temperature (30).

Similar to other polysaccharides, acid and alkaline conditions can hydrolyze HA. This type of degradation occurs in a random fashion often resulting in disaccharide fragment production. Acidic hydrolysis degrades the glucuronic acid moiety. On the other hand, alkaline hydrolysis occurs on *N*-acetylglucosamine units (30). HA can also degrade via oxidation. Reactive oxygen species (ROS) can be generated from cells as a consequence of aerobic respiration. Superoxide anions, hydroxyl radicals, and

hypochloride are examples of these species that cause HA chain cleavage. ROS are proposed to be involved in several inflammatory and biodegenerative processes such as arthritis but their mechanism of action in the disease are myriad and still largely unknown (2, 30).

1.4. Turnover and possible pathways for elimination of hyaluronic acid

Studies showed that the concentration of HA in the human body varies from a high concentration of 4 g/kg in umbilical cord, 2-4 g/L in synovial fluid, 0.2 g/kg in dermis, and about 10 mg/L in thoracic lymph, to a low concentration of 0.1-0.01 mg/L in normal serum. In a normal human body (70 kg), the total HA body content is approximately 15 g (2, 3). From this 15 g, the largest amount was found in the extracellular matrix (ECM) of skin and musculoskeletal tissue. Depending on the location of HA in the body, most of the HA is catabolized within days. Studies suggested that the normal half-life of HA varies from 1-3 weeks in inert tissues such as cartilage, 1-2 days in the epidermis of skin, to 2-5 minutes in blood circulation. Besides enzymatic degradation and non-enzymatic degradation pathways described previously, two more pathways are engaged in HA catabolism: turnover (internalization and degradation within tissue) and release from the tissue matrix, drainage into the vasculature, and clearance via lymph nodes, liver, and kidney (Figure 1-2) (2).

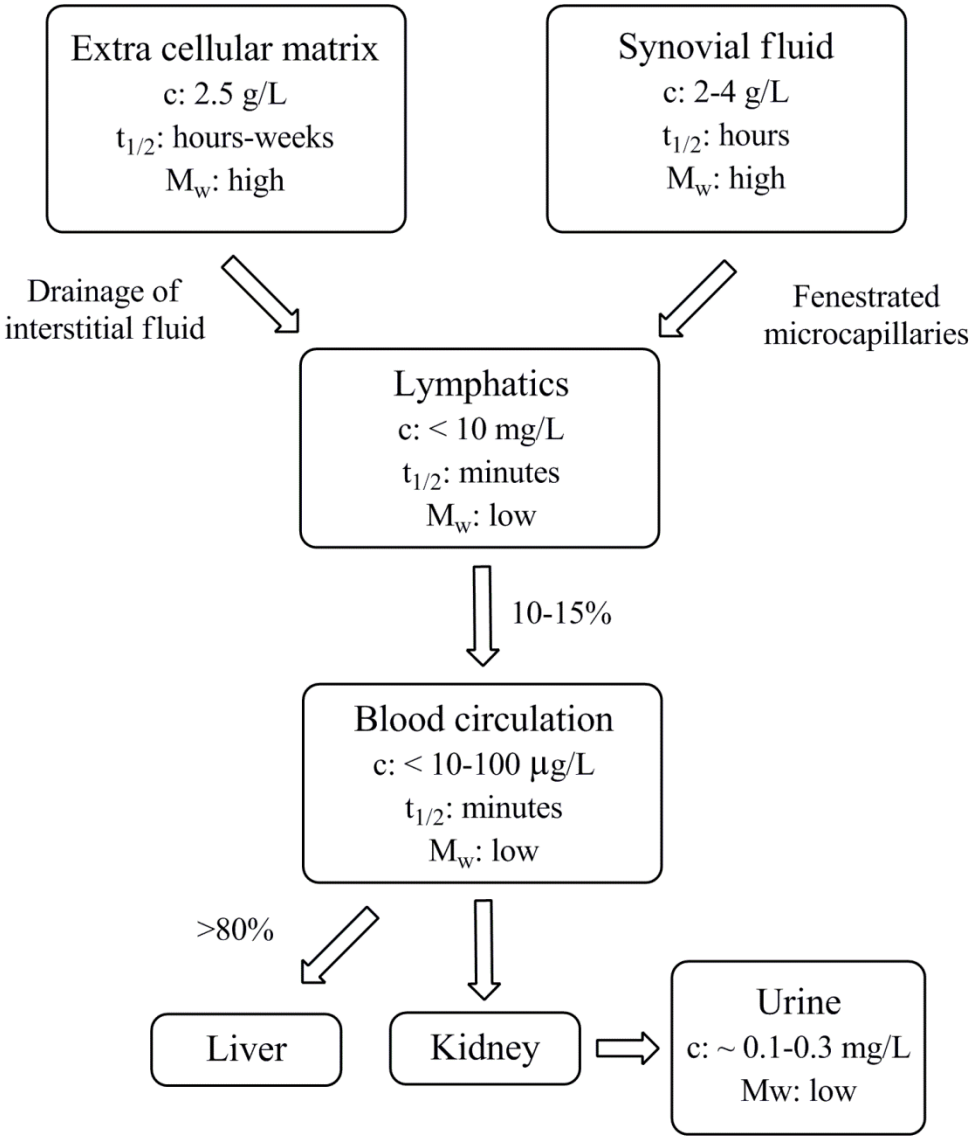

Figure (1-2) HA catabolic pathway in the body. Arrows show the flow of HA. Concentration (c), half-life ($t_{1/2}$), and molecular weight (M_w) of HA within the organ systems are indicated. Figure was regenerated with permission (2). High Mw > ~1000 kDa and low Mw < ~450 kDa.

In structural tissues like bone or cartilage with no or little lymphatic drainage, HA degradation occurs *in situ* with other ECM molecules such as collagens and proteoglycans. On the other hand, in skin and joints, a minimal fraction (approximately 20-30%) of HA degrades *in situ.* Approximately, 50% of HA in the body is available in

skin tissue. Since HA is restricted to the small intracellular space of skin tissue, its half-life is a bit longer at days and weeks (2, 17).

HA can also be eliminated through the lymphatic system draining the extracellular space of relatively dense tissues. First, high molecular weight HA is partially degraded before it releases from the tissue matrix. Upon release from the tissue matrix, degraded HA enters the lymphatic system. HA metabolic degradation mostly takes place in the lymphatic system as HA goes through peripheral tissues to the blood circulation (2). One of the functions of the lymphatic system is to collect filtered plasma and interstitial fluid and transport them back to the blood circulation. Studies showed that most of the subcutaneously injected radio-labeled HA is picked up and degraded in lymphatic tissue (2, 17). Remaining HA enters into the blood circulation and is rapidly removed in the liver by sinusoidal endothelial cells or eliminated via kidneys. In the blood circulation, the liver eliminates about 80% of HA and kidneys clear 10% of HA from bloodstream (Figure 1-2). As mentioned before, the daily turnover of HA is on the order of one-third (5 g) of the total HA body content (15 g) (2).

Synovial fluid is one of the body fluids containing high molecular weight HA. Lubrication and viscoelasticity are properties of high molecular weight HA in synovial fluid. In a healthy joint, high levels (2-4 g/L) of HA with high molecular weight (approximately 6-7 MDa) are required for synovial fluid to function properly. In order to have synovial fluid lubrication and viscoelasticity, macromolecules including HA are secreted by synoviocytes continuously into the synovial fluid. Every time pressure is increased, fluid is pushed out of the joint cavity into micro-capillaries embedded in the synovium. Therefore, HA escapes through the interstitial drainage pores in the synovial

lining (diameter 30-90 nm). It is also suggested that high molecular weight HA can form a layer at the tissue-fluid interface forming a “shell” that is not drained into micro-capillaries. The normal intra-articular turnover time for HA is found to be less than 40 hours. Both HA molecular weight and concentration are decreased in patients with arthritis resulting in a significant reduction in synovial fluid functionality. Moreover, studies showed that production and secretion of ROS in arthritic joints degraded the HA in synovial fluid and cartilage (2, 3, 32-34).

1.5. Biomedical application of hyaluronic acid

1.5.1. Application of hyaluronic acid in tissue engineering

Since hyaluronic acid is one of the main components of body tissues, its potential for tissue engineering applications has been highly touted. HA is highly soluble at room temperature and has a high rate of elimination and turnover depending on its molecular weight and location in the body. Each of these properties could be a barrier for HA scaffold fabrication and structural integrity. To overcome these limitations, crosslinking of hyaluronic acid has been proposed (4, 35, 36). Currently, water-soluble carbodiimide crosslinking (37), polyvalent hyadrazide crosslinking (38), divinyl sulfone crosslinking (39), disulfide crosslinking (40), and photocrosslinking of hydrogels through glycidyl methacrylate-HA conjugation (41) have been introduced for tissue engineering applications of HA. Chemical crosslinking of HA provides the ability to combine the desirable biological and mechanical properties, even for bone or cartilage tissue engineering (4, 35). Moreover, crosslinking extends the HA degradation process *in vivo*

and provides long-term stability. Crosslinking HA at various densities has been used for multiple applications including orthopedics, cardiovascular medicine, and dermatology (35).

Studies have suggested positive results for cell growth on photocrosslinked HA networks incorporated with chondrocytes. Chondrocytes within the HA hydrogel retained viability and were able to generate cartilage within the porous network (35, 42). This type of photopolymerization has also been used in heart valve applications to mimic cardiac valve development (21). HA has also been combined with other polymers such as polypyrrole to develop multifunctional copolymers. HA functionalized with polypyrrole is electronically conductive and supports cell growth. This copolymerization could have potential for tissue engineering applications (43, 44). Benzyl derivatives of HA is another category of polymeric scaffolds used for tissue engineering of cartilage with predictable degradation rates. Studies on these derivatives suggested the potential of benzyl esters of HA as a delivery scaffold for chondrocytes in cartilage tissue engineering (35, 45). Since HA is a biocompatible natural polymer, development of scaffolds based on HA appears to be suitable for surfaces contacting blood. For example, HA crosslinked with divinyl sulfone (DVS) in the presence of ultraviolet light has been suggested to develop "non-activating" surfaces for cell adhesion in heart valve tissue engineering (35, 46, 47).

Auto-crosslinked and *in situ* crosslinked HA hydrogels are another category of crosslinking used for tissue engineering. The requirement for surgical implantation is the major limitation of most scaffolds used for tissue engineering. Application of HA that crosslinks after injection has been introduced for three main reasons. First, the injectable HA could be filled into any desirable shape and crosslinked *in situ*. Second, crosslinkable

HA may adhere to the native tissue resulting in mechanical or chemical interlocking and a cohesive scaffold-tissue interface. Third, injection and laparoscopic methods can be used to reduce the invasiveness of the surgical procedure (48). Studies showed that *in situ* crosslinked HA hydrogel using adipic acid dihydrazide and aldehyde chemistry could form a flexible hydrogel *in situ* upon mixing (49). In another study, poly(lactic-co-glycolic acid) nanoparticles were mixed with HA of similar chemistry to develop an *in situ* crosslinkable system with drug delivery potential. Although such *in situ* crosslinking has been shown to form flexible hydrogels with reasonable mechanical properties, potential toxicity of the reactions used in these techniques are still an important issue to consider (50).

1.5.2. Application of hyaluronic acid as a dermal filler

The influence of sun exposure, gravity, and years of facial muscle movements starts to appear as wrinkles on the skin. During the aging process, basic changes in the skin, soft tissue, and skeletal support of the face occur resulting in a breakdown of the tissues under the skin leaving lines or other facial defects (51, 52). Skin aging can be divided in two categories: internal aging and external aging.

Internal aging of skin causes various histological changes in different skin layers such as flattening of the epidermal-dermal interface, a decrease in the number of melanocytes and Langerhans cells in the epidermis, a loss of dermal papillae, dermal atrophy, a decrease in the number of mast cells, fibroblasts, and blood vessels, a loss of elastic tissue in the fine subepidermal elaunin network, and abnormal thickening and

fragmentation of elastic tissue in the reticular dermis (52). Internal aging also reduces several skin functions such as type I and type III collagen production, the epidermal turnover rate, and melanocyte activity (52, 53).

External aging is influenced by sun exposure and UV radiation and also causes histological changes which are different from other changes caused by internal aging. External aging is typified by damage of elastic tissue and decrease in cellularity. Photodamage induces elastosis, the overgrowth of abnormal elastic fibers, and an increase in population of histiocytes, fibroblasts, and mast cells (52, 53). In both internal and external aging, collagen content and melanocyte activity are decreased and wound healing is abnormal (52).

To address age-related changes in skin quality and appearance, several treatments have been proposed (Table 1-2). Development of soft-tissue fillers (dermal fillers) can help lines and wrinkles to be filled temporarily (or permanently) (51). It seems an ideal dermal filler should be temporary but long-lasting, having minimum side effects and no allergenic effect, easy to administer, having minimum pain or no pain upon injection, and a reasonable cost for both the physician and the patient (51).

Table (1-2) Treatments proposed to enhance age-related changes in skin quality (52).

Treatment	Remarks
Skin protections and skin cares	Sunscreens help to enhance changes in skin quality and appearance caused by sun exposure. Daily skin care is recommended to improve the quality and appearance of aged skin.
Chemical peels	Chemical peels applied directly to the skin use alpha-hydroxy acid, salicylic acid, trichloroacetic acid, or phenol can improve the appearance of aged skin.
Nonablative therapies	In nonablative therapies, light or thermal energy from various sources (visible and infrared lasers, intense pulsed light, light-emitting diodes, and radiofrequency) are used to improve skin texture, discoloration, and scarring.
Ablative therapies	Ablative therapies are laser treatments in which the laser induces ablation of water-containing tissue (epidermal tissue).
Botulium toxin type A injection	Local injection of botulinum toxin causes temporary muscle denervation, resulting in relaxation of hyperfunctional facial muscles and smoothing of the skin overlying these muscles.
Dermal fillers	Dermal fillers are used to recover soft-tissue volume of the skin and remove skin wrinkles.

Depending on the residence time in tissue, dermal fillers are categorized as temporary, semipermanent (at least 18 months), and permanent. They are also classified based on their composition with the primary ingredients such as collagen (bovine, porcine, or human), animal or synthetic hyaluronic acid, poly-*L*-lactic acid, calcium hydroxyapatite, polymethyl methacrylate, and polyacrylamide gel (Table 1-2) (52, 54-56).

Hyaluronic acid has been approved by the Food and Drug Administration (FDA) as a dermal filler. In 2006, cosmetic injections of HA were known to be the second most popular non-surgical procedure for women and the third most popular procedure for men (57-60). HA has a very short half-life and, therefore, is chemically crosslinked to extend duration as a dermal filler (61). HA is not involved in the structure of collagen and does not enhance tissue, the shortage of HA, in aged skin, but simply works by augmenting volume (51, 57). The development of dermal filler products with enhanced injectability and longer duration is desired.

Table (1-3) Different types of dermal fillers and some of the commercially available products (52, 54, 56, 59).

Material	Brand name	Description	Duration	Biodegradability
Autologous fat	Viable Fat	-	Temporary	Biodegradable
Hyaluronic acid	Restylene®	Cross-linked HA (20 mg/mL)	Temporary 6-12 months	Biodegradable
	Prelane®	Cross-linked HA (20 mg/mL)	Temporary 6-12 months	
	Juvéderm®	Cross-linked HA (24 mg/mL)	Temporary up to 12 months	
	Elevess®	Cross-linked HA (28 mg/mL)	Temporary months	
	Hylaform®	Cross-linked HA (5 mg/mL)	Temporary 3-6 months	
Collagen	Zyderm®	3.5% bovine collagen+0.3% lidocaine	Temporary 3-4 months	Biodegradable
	Zyplast®	3.5% crosslinked bovine collagen +0.3% lidocaine	Temporary 3-6 months	
	CosmoDerm®	3.5% human collagen+0.3% lidocaine	Temporary 3-5 months	
	CosmoPlast®	3.5% crosslinked human collagen+0.3% lidocaine	Temporary 3-5 months	
	ArteFill®	20% PMMA microsphers+80% bovine collagen (3.5%)+0.3% lidocaine	Permanent	Not biodegradable
Calcium hydroxyapatite	Radiessa®	Calcium hydroxyapatite microspheres in aqueous gel	Semipermanent 2-5 years	Biodegradable
Poly-*L*-lactic acid	Sculptra®	Injectable PLLA microspheres suspended in sodium carboxymethylcellulose gel	Semipermanent 18-24 months	Biodegradable
β-tricalcium phosphate with hyaluronic acid	Atlean®	-	Semipermanent	Biodegradable
Polyacrylamide gel	Aquamid®	-	Permanent	Not biodegradable
	Bio-Alcamid®			
Polymethyl methacrylate	Arteplast®	-	Semipermanent	Not biodegradable
	Artecoll®			
	Artefill®			
	Dermalive®			
	Dermadeep®			
Dimenthylsiloxane polymers	Silicone	-	Permanent	Not biodegradable

1.4.3. Application of hyaluronic acid in osteoarthritis treatment

Osteoarthritis (OA) is the most common disease associated with aging, affecting approximately 33 million Americans with about 70% of these individuals aged 65 and over. OA is characterized by the slow degradation of cartilage, pain, and increasing disability. The disease can have an impact on several aspects of a patient's life, including functional and social activities (62, 63). Current pharmacological therapies target palliation of pain and include analgesics (i.e. acetaminophen, cyclooxygenase-2-specific inhibitors, non-steroidal anti-inflammatory drugs, tramadol, opioids), intra-articular therapies (glucocorticoids and hyaluronan), and topical treatments (i.e. capsaicin, methylsalicylate). If none of these therapies work, surgical joint replacement is the last option, which is costly and highly invasive (63).

Synovial spaces are the cavities of the joints that facilitate movement of adjacent bones. Synovial spaces are formed by a surface of cartilage, synovium, and synovial fluid. The synovial fluid is a clear, colorless or sometimes yellowish liquid secreted into the joint cavity by the synovioum. The synovial fluid volume is approximately 2 mL in normal human knee joints and contains electrolytes, low molecular weight organic molecules, and macromolecules such as glycosaminoglycans (GAGs). GAGs present in the synovial fluid are chondrotin-4-sulfate (2%), with the remaining 98% made up of HA (62).

The mechanical function of the synovial fluid can be attributed to its rheological properties, more specifically its viscoelastic properties. Synovial fluid viscoelasticity may be ascribed to the concentration, molecular weight, and molecular weight distribution, and to the physical and non-covalent interactions within the HA molecule as well as with

other molecules such as proteins and ions (4). HA molecules overlap and interact though physical entanglement or temporary crosslinking interactions with ions and proteins at physiological conditions. These interactions, which are dependent on HA molecular weight and concentration, determine the formation of the transient network structure that is responsible for the viscoelasticity of synovial fluid (62, 63). In OA, HA loses these functionalities as a result of reduced HA molecular weight and concentration; thus, decreasing the viscoelastic properties of synovial fluid (32, 62, 64).

The viscoelastic behavior of synovial fluid can be described by the elastic modulus (G´) and viscous modulus (G˝) as a function of frequency (32, 65, 66). The degradation of synovial fluid is evident from its rheological properties. Generally, aging is the main reason for a reduction in HA molecular weight or HA concentration (Table 1-4). After damage or aging, synovial fluid cannot provide the required viscoelastic response to compression and tangential forces arising in everyday life, allowing cartilage-cartilage contact and increasing wear of the joint surface (62, 63). Intra-articular treatment with HA and hylans (uncrosslinked HA and crosslinked HA, respectively) has recently been accepted as a common therapy for reducing pain associated with OA (62, 63). Currently, FDA-approved products such as Hyalgan® (HA), Orthovisc® (HA) and Synvisc® (hylan GF 20) are available as viscosupplements for intra-synovial injection in osteoarthritis treatment Table (1-5) (62, 65, 67, 68).

Table (1-4) Properties of healthy synovial fluid and osteoarthritic synovial fluid (65, 67, 69, 70).

	HA molecular weight (MDa)	HA concentration (mg/mL)	Viscoelastic properties		Zero shear viscosity (Pa.s)
			Elastic modulus (G') (Pa) at 2.5 Hz	Viscous modulus (G'') (Pa) at 2.5 Hz	
Healthy Young Synovial Fluid	6.3-7.6	2.5-4	23	7	6-175
Osteoarthritic Synovial Fluid	1.6-3.48	1-2	7	5	0.01-1

Table (1-5) Some of the HA viscosupplements available in the North American market. Table was regenerated with permission (62, 65, 67, 68, 71).

Brand name (Generic name)	Molecular weight (kDa)	Approved dosing*	Amount per injection (mL)	Approved indications
Durolane® (Hyaluronic acid, 2%)	1000	1 injection	3	Knee or hip, mild or moderate
Fermathron® (Sodium hyaluronate, 1%)	1000	3-5 injections	2	Knee, mild or moderate
Hyalgan® (Sodium hyaluronate, 1%)	500-730	3-5 injections	2	Knee, shoulder, or hip
NeoVisc® (Sodium hyaluronate, 1%)	1000	3-5 injections	2	Synovial fluid replacement following arthrocentesis
Orthovisc® (Sodium hyaluronate, 1.4%)	1000-2900	3 injections	2	Knee
Ostenil® (Sodium hyaluronate, 1%)	1000-2000	3 injections	2	Degenerative or traumatic synovial joint disorders, including knee joint
Supartz® (Sodium hyaluronate, 1%)	620-1170	3-5 injections	2.5	Knee nonresponsive to conservative therapy
Suplasyn® (Sodium hyaluronate, 1%)	500-730	3-6 injections	2	Synovial fluid replacement following arthrocentesis
Synvisc® (Hylan G-F 20; Crosslinked HA)	6000-7000	3 injections	2	Knee nonresponsive to 0.8% conservative therapy

* The number of weekly intra-articular injections per treatment course, excluding Durolane®, which is given as a single injection.

Several clinical trials have demonstrated the efficacy and tolerability of intra-articular HA for the treatment of pain associated with OA. These studies have shown three injections of Synvisc® (crosslinked HA) can provide relief of knee pain up to 6 months. A competing product, Hyalgan® (sodium hyaluronate solution), requires 6 injections to reach the same efficacy of Synvisc® (34, 67, 72, 73). While Synvisc® was shown to be more efficient in reducing pain, its structure (high molecular weight HA due

to crosslinking) has made this difficult to inject (Table 1-6). Unlike Synvisc®, Hyalgan® has a lower viscosity, making injection easier, but Hyalgan® is not as effective as Synvisc® due to lower viscoelastic properties (elastic and viscous moduli) (65, 67, 73). Moreover, Orthovisc®, one of the viscosupplements with the highest HA concentration, has lower viscosity than Synvisc® but it is not reported to be as effective as Synvisc® (65, 67, 73). This creates a need for development of products with enhanced injectability and yet reasonable viscoelastic behavior (Synvisc® elastic and viscous moduli values).

Table (1-6) Properties of Hyalgan® and Synvisc®. Data were adapted from Hyalgan® product information, Orthovisc® product information, Synvisc® product information, and references (65, 67, 70).

Brand name	**Molecular weight (kDa)**	**Viscoelastic properties**		Number of injections	Duration of pain relief
		Elastic modulus (G') (Pa) at 2.5 Hz	**Viscous modulus (G'') (Pa) at 2.5 Hz**		
Hyalgan® (Uncrosslinked)	500-730	0.6	3	3-5	6 months
Orthovisc® (Uncrosslinked)	1000-2900	60	46	3	6 months
Synvisc® (Crosslinked polymer)	6000-7000	111± 13	25±2	3	6 months

1.6. Introduction of thesis

Due to the prevalence of hyaluronic acid in the body, HA has been deemed as a suitable material for biomedical applications. Three applications of HA were introduced; tissue engineering, dermal filling, and viscosupplementation. In each application, difficulties such as potential toxicity of *in situ* crosslinking techniques, high viscosity of HA solutions, and rapid elimination have been raised as limitations to develop biomedical products from HA. Nanotechnology may provide an approach to resolve these limitations. Studies suggested that fabrication of nanoparticles from polymers can effect bulk properties (physical, mechanical, rheological, and etc.) of ensuing materials (74, 75). In this work, a nanoparticle fabrication technique for HA has been introduced. Then, the use of HA nanoparticles to modify viscosity and viscoelasticity of HA solutions or suspensions was explored. This study is focused on the application of HA nanoparticles to develop materials for tissue engineering, dermal filling, and viscosupplementation.

As mentioned, crosslinking is a common technique employed for HA scaffold fabrication. Almost all of the crosslinking reactions used for this purpose are toxic to cells; however, the desired mechanical properties can be achieved for tissue engineering applications (18, 63). In addition to that, injectability of viscous HA is another desired property that can help physicians to fill a defect site without invasive surgery (5, 49). This thesis aimed to develop a new type of colloidal material based on HA nanoparticles, which can be used as a self-assembled scaffold without utilizing chemical reactions. The injectability of the colloidal material and its behavior under shear stress was evaluated to determine applicability as an injectable scaffold for tissue engineering.

HA nanoparticles may also be used to enhance the properties of dermal fillers. HA based dermal fillers are one of the most popular for temporary treatment within a duration of up to 12 months (52, 54, 56). These crosslinked HA solutions are viscous and difficult to administer with fine needles. Modifying these supplements with HA nanoparticles may extend the residency of the HA *in vivo* and increase the treatment duration to more than 12 months. Moreover, nanoparticles may also help to reduce the viscosity of these solutions for easy injection via fine needles. In this thesis, HA nanoparticles were used to modify HA polymer solutions and the effect on viscosity was evaluated.

Modification of viscosupplements used for osteoarthritis treatment is another area in which HA nanoparticles may be employed. High viscosity of viscosupplements such as Synvisc® has always been an issue (65, 67, 68). In this research, reducing the viscosity of HA solutions by using HA nanoparticles was investigated. Viscoelastic behavior (change in elastic and viscous moduli), another characteristic of HA solutions (and suspensions), was evaluated to determine the effect of nanoparticles in HA solutions (and suspensions). An outline of the design characteristics and rationale of this thesis are shown in Table 1-7.

Table (1-7) Outline of the design characteristics and rationale of the thesis.

Hyaluronic acid		**Remarks**	**Applications**
Polymer solution		The viscosity of solution is high at high Mw of HA even at low concentrations	Dermal fillers, osteoarthritis viscosupplements
Nanoparticle in colloidal suspension	**Nanoparticle**	Reducing the viscosity and viscoelastic properties (elastic and viscous moduli) compared to the polymer solution	Dermal fillers, osteoarthritis viscosupplements
	Nanoparticle & Polymer	Reducing or increasing the viscosity and viscoelastic properties (elastic and viscous moduli) compared to the polymer solution	
Nanoparticle in colloidal gel		Developing 3-D HA scaffold	Scaffold fabrication

1.7. Design of the thesis

The studies outlined in this thesis include nanoparticle fabrication, nanoparticle characterization, development of colloidal systems based on nanoparticles, and finally characterization of these colloidal systems including physical, mechanical, and rheological characterization.

Chapter 2: Fabrication of hyaluronic acid nanoparticles

Nanoparticles were synthesized using a technique free of oil and surfactant. In this method, nanoparticles were fabricated by crosslinking HA polymer chains through their carboxyl groups via carbodiimide chemistry (76). The crosslinking reaction was validated via Fourier transform infrared spectroscopy (FTIR). The effect of polymer type (hyaluronic acid or chondroitin sulfate), polymer concentration, HA molecular weight, reaction time, and the ratio between polymer to crosslinker was evaluated. To understand the morphology of the nanoparticles, cryo-transmission electron microscopy was used.

Chapter 3: Application of hyaluronic acid nanoparticles for colloidal gel fabrication

HA nanoparticles (chapter 2) were used to form colloidal gels in this chapter. Colloidal gels were made by mixing nanoparticles with deionized water at different concentrations. First, the effect of the type of nanoparticles (hyaluronic acid or chondroitin sulfate nanoparticles), concentration of nanoparticles, and the molecular weight of HA used for nanoparticle fabrication was tested. Then, the swelling ratio of

colloidal gels was measured in deionized water and 0.1 M PBS to understand the behavior of colloidal gels compared to a classic HA hydrogel. Uniaxial compression testing was employed to evaluate mechanical properties of colloidal gels at different conditions. Rheological properties (viscosity and viscoelastic properties (elastic and viscous moduli)) of the colloidal gels were also determined. Finally, structural recoverability and dynamic behavior of colloidal gels were examined using uniaxial compression testing and rheometry.

Chapter 4: Application of hyaluronic acid nanoparticles in colloidal suspensions as a potential osteoarthritis treatment

To evaluate the potential of HA nanoparticles for osteoarthritis treatment and the effect of nanoparticles on rheological behavior (viscosity and viscoelasticity) of HA, two experiments were designed. For both experiments, HA (HA Mw=1500 kDa) at 1.4% w/v was prepared as a model of the Orthovisc® viscosupplement for osteoarthritis treatment (or dermal filler). The rheological effect of mixing HA polymer with HA nanoparticles at different ratios (maintaining HA concentration of 1.4% w/v) was studied. The interaction between nanoparticles and HA polymer was observed to affect the viscosity and viscoelasticity of the HA suspension. The effect of nanoparticle concentration on the rheological properties of HA nanoparticle suspensions was examined. Here, the effect of nanoparticle fabrication to reduce the viscosity of HA suspensions was explored. All the experiments aimed to determine the effect of nanoparticles on injectable viscosupplements.

1.8. References

1. Kurisawa M, Chung J, Yang Y, Gao S, Uyama H., Injectable biodegradable hydrogels composed of hyaluronic acid–tyramine conjugates for drug delivery and tissue engineering, Chemical communications, 2005(34):4312-4.
2. Garg, H.G. and C.A. Hales, Chemistry and biology of hyaluronan, 2004, Elsevier Science.
3. Necas J, Bartosikova L, Brauner P, Kolar J., Hyaluronic acid (hyaluronan): a review, Veterinarni Medicina. 2008;53(8):397-411.
4. Falcone S, Palmeri D, Berg R, editors., Biomedical applications of hyaluronic acid, 2006, ACS Publications.
5. Zheng Shu X, Liu Y, Palumbo F, Luo Y, Prestwich G., In situ crosslinkable hyaluronan hydrogels for tissue engineering, Biomaterials, 2004;25(7-8):1339-48.
6. Vejlens L., Glycosaminoglycans of human bone tissue. Calcified Tissue International, 1971;7(1):175-90.
7. Dumitriu S., Polymeric biomaterials, 2002, New York, Marcel Dekker Inc..
8. Segura T, Anderson B, Chung P, Webber R, Shull K, Shea L., Crosslinked hyaluronic acid hydrogels: a strategy to functionalize and pattern, Biomaterials, 2005;26(4):359-71.
9. Toole B., Hyaluronan: from extracellular glue to pericellular cue, Nature Reviews Cancer, 2004;4(7):528-39.
10. Cai S, Xie Y, Bagby T, Cohen M, Forrest M., Intralymphatic chemotherapy using a hyaluronan-cisplatin conjugate, The Journal of surgical research, 2008;147(2):247.
11. Underhill C., CD44: the hyaluronan receptor, Journal of Cell Science, 1992;103(2):293.
12. Eng, D., et al., Hyaluronan scaffolds: A balance between backbone functionalization and bioactivity, Acta Biomaterialia, 2010;6(7):2407-2414.
13. Kim J, Kim I, Cho T, Lee K, Hwang S, Tae G, et al, Bone regeneration using hyaluronic acid-based hydrogel with bone morphogenic protein-2 and human mesenchymal stem cells, Biomaterials, 2007;28(10):1830-7.
14. Luo Y, Kirker K, Prestwich G., Cross-linked hyaluronic acid hydrogel films: new biomaterials for drug delivery, Journal of controlled release, 2000;69(1):169-84.
15. Lee K, Mooney D., Hydrogels for tissue engineering, Chem Rev. 2001;101(7):1869-80.
16. Drury J, Mooney D., Hydrogels for tissue engineering: scaffold design variables and applications, Biomaterials, 2003;24(24):4337-51.
17. Volpi N, Schiller J, Stern R, Soltes L., Role, metabolism, chemical modifications and applications of hyaluronan, Current medicinal chemistry, 2009;16(14):1718-45.
18. Burdick JA, Prestwich GD, Hyaluronic Acid Hydrogels for Biomedical Applications, Advanced Materials, 2011(23):H41–H56.
19. Whelan J., The Biology of hyaluronan, 1989, John Wiley & Sons.
20. Sheehan J, Arundel C, Phelps C., Effect of the cations sodium, potassium and calcium on the interaction of hyaluronate chains: a light scattering and viscometric study, International Journal of Biological Macromolecules, 1983;5(4):222-8.
21. Toole BP, Hyaluronan in morphogenesis, 2001, Elsevier.
22. Toole BP, Wight TN, Tammi MI., Hyaluronan-cell interactions in cancer and vascular disease, Journal of Biological Chemistry, 2002;277(7):4593.
23. Noble PW., Hyaluronan and its catabolic products in tissue injury and repair, Matrix biology, 2002;21(1):25-9.
24. Toole B., Hyaluronan in morphogenesis, Journal of internal medicine, 1997;242(1):35-40.

25. McKee CM, Penno MB, Cowman M, Burdick MD, Strieter RM, Bao C, et al., Hyaluronan (HA) fragments induce chemokine gene expression in alveolar macrophages. The role of HA size and CD44, Journal of Clinical Investigation, 1996;98(10):2403.
26. Oertli B, Fan X, Wüthrich RP., Characterization of CD44-mediated hyaluronan binding by renal tubular epithelial cells, Nephrology Dialysis Transplantation, 1998;13(2):271.
27. Chen WYJ, Abatangelo G., Functions of hyaluronan in wound repair, Wound Repair and Regeneration, 1999;7(2):79-89.
28. Lee JY, Spicer AP., Hyaluronan: a multifunctional, megaDalton, stealth molecule, Current Opinion in Cell Biology, 2000;12(5):581-6.
29. Cowman MK, Matsuoka S., Experimental approaches to hyaluronan structure, Carbohydrate research, 2005;340(5):791-809.
30. Stern R, Kogan G, Jedrzejas MJ, Soltés L., The many ways to cleave hyaluronan, Biotechnology advances, 2007;25(6):537-57.
31. Šoltés L, Mendichi R, Kogan G, Schiller J, Stankovska M, Arnhold J., Degradative action of reactive oxygen species on hyaluronan, Biomacromolecules, 2006;7(3):659-68.
32. Arrich J, Piribauer F, Mad P, Schmid D, Klaushofer K, Müllner M., Intra-articular hyaluronic acid for the treatment of osteoarthritis of the knee: systematic review and meta-analysis, Canadian Medical Association Journal, 2005;172(8):1039.
33. Goldberg V, Buckwalter J., Hyaluronans in the treatment of osteoarthritis of the knee: evidence for disease-modifying activity, Osteoarthritis and cartilage, 2005;13(3):216-24.
34. Migliore A, Granata M., Intra-articular use of hyaluronic acid in the treatment of osteoarthritis, Clinical interventions in aging, 2008;3(2):365.
35. Allison DD, Grande-Allen KJ., Hyaluronan: a powerful tissue engineering tool, Tissue Engineering, 2006;12(8):2131-40.
36. Jiang D, Liang J, Noble PW., Hyaluronan in tissue injury and repair, Annu Rev Cell Dev Biol, 2007;23:435-61.
37. Tomihata K, Ikada Y., Crosslinking of hyaluronic acid with water soluble carbodiimide, Journal of biomedical materials research, 1997;37(2):243-51.
38. Vercruysse KP, Marecak DM, Marecek JF, Prestwich GD., Synthesis and in vitro degradation of new polyvalent hydrazide cross-linked hydrogels of hyaluronic acid, Bioconjugate chemistry, 1997;8(5):686-94.
39. Luo Y, Kirker KR, Prestwich GD., Cross-linked hyaluronic acid hydrogel films: new biomaterials for drug delivery, Journal of controlled release, 2000;69(1):169-84.
40. Liu Y, Zheng Shu X, Prestwich GD., Biocompatibility and stability of disulfide-crosslinked hyaluronan films, Biomaterials, 2005;26(23):4737-46.
41. Baier Leach J, Bivens KA, Patrick Jr CW, Schmidt CE., Photocrosslinked hyaluronic acid hydrogels: natural, biodegradable tissue engineering scaffolds, Biotechnology and bioengineering, 2003;82(5):578-89.
42. Burdick JA, Chung C, Jia X, Randolph MA, Langer R., Controlled degradation and mechanical behavior of photopolymerized hyaluronic acid networks, Biomacromolecules, 2005;6(1):386-91.
43. Cen L, Neoh K, Li Y, Kang E., Assessment of in vitro bioactivity of hyaluronic acid and sulfated hyaluronic acid functionalized electroactive polymer, Biomacromolecules, 2004;5(6):2238-46.
44. Collier JH, Camp JP, Hudson TW, Schmidt CE., Synthesis and characterization of polypyrrole–hyaluronic acid composite biomaterials for tissue engineering applications, Journal of biomedical materials research, 2000;50(4):574-84.
45. Aigner J, Tegeler J, Hutzler P, Campoccia D, Pavesio A, Hammer C, et al., Cartilage tissue engineering with novel nonwoven structured biomaterial based on hyaluronic acid benzyl ester, Journal of biomedical materials research, 1998;42(2):172-81.

46. Ramamurthi A, Vesely I., Evaluation of the matrix-synthesis potential of crosslinked hyaluronan gels for tissue engineering of aortic heart valves, Biomaterials, 2005;26(9):999-1010.
47. Ibrahim S, Kang QK, Ramamurthi A., The impact of hyaluronic acid oligomer content on physical, mechanical, and biologic properties of divinyl sulfone crosslinked hyaluronic acid hydrogels, Journal of Biomedical Materials Research Part A., 2010;94(2):355-70.
48. Zheng Shu X, Liu Y, Palumbo FS, Luo Y, Prestwich GD., In situ crosslinkable hyaluronan hydrogels for tissue engineering, Biomaterials, 2004;25(7-8):1339-48.
49. Yeo Y, Highley CB, Bellas E, Ito T, Marini R, Langer R, et al., In situ cross-linkable hyaluronic acid hydrogels prevent post-operative abdominal adhesions in a rabbit model, Biomaterials, 2006;27(27):4698-705.
50. Yeo Y, Ito T, Bellas E, Highley CB, Marini R, Kohane DS., In situ cross-linkable hyaluronan hydrogels containing polymeric nanoparticles for preventing postsurgical adhesions, Annals of surgery, 2007;245(5):819.
51. Tezel A, Fredrickson GH., The science of hyaluronic acid dermal fillers, Journal of Cosmetic and Laser Therapy, 2008;10(1):35-42.
52. Sadick NS, Karcher C, Palmisano L., Cosmetic dermatology of the aging face, Clinics in Dermatology, 2009;27(3):S3-S12.
53. Fisher GJ, Varani J, Voorhees JJ., Looking older: fibroblast collapse and therapeutic implications, Archives of dermatology, 2008;144(5):666.
54. Sánchez-Carpintero I, Candelas D, Ruiz-Rodríguez R., Dermal Fillers: Types, Indications, and Complications, Actas Dermo-Sifiliográficas (English Edition), 2010;101(5):381-93.
55. Christensen LH., Host tissue interaction, fate, and risks of degradable and nondegradable gel fillers, Dermatologic Surgery, 2009;35:1612-9.
56. Andre P., New trends in face rejuvenation by hyaluronic acid injections, Journal of Cosmetic Dermatology, 2008;7(4):251-8.
57. Brandt FS, Cazzaniga A., Hyaluronic acid gel fillers in the management of facial aging, Clinical interventions in aging, 2008;3(1):153.
58. Gold MH., Use of hyaluronic acid fillers for the treatment of the aging face, Clinical interventions in aging, 2007;2(3):369.
59. Buck I, Donald W, Alam M, Kim J., Injectable fillers for facial rejuvenation: a review, Journal of Plastic, Reconstructive & Aesthetic Surgery, 2009;62(1):11-8.
60. Monheit GD, Prather CL., Hyaluronic acid fillers for the male patient, Dermatologic therapy, 2007;20(6):394-406.
61. KABLIK J, MONHEIT GD, YU L, CHANG G, GERSHKOVICH J., Comparative physical properties of hyaluronic acid dermal fillers, Dermatologic Surgery, 2009;35:302-12.
62. Moreland LW., Intra-articular hyaluronan (hyaluronic acid) and hylans for the treatment of osteoarthritis: mechanisms of action, Arthritis Research and Therapy, 2003;5(2):54-67.
63. Yaszemski MJ., Tissue engineering and novel delivery systems,2003, CRC Press.
64. Conrad BP., The effects of glucosamine and chondroitin on the viscosity of synovial fluid in patients with osteoarthritis, 2001, Citeseer.
65. Altman R, Moskowitz R., Intraarticular sodium hyaluronate (Hyalgan) in the treatment of patients with osteoarthritis of the knee: a randomized clinical trial. Hyalgan Study Group, The Journal of rheumatology, 1998;25(11):2203.
66. Maheu E, Ayral X, Dougados M., A hyaluronan preparation (500-730 kDa) in the treatment of osteoarthritis: a review of clinical trials with Hyalgan, International journal of clinical practice, 2002;56(10):804.

67. Watterson JR, Esdaile JM., Viscosupplementation: therapeutic mechanisms and clinical potential in osteoarthritis of the knee, Journal of the American Academy of Orthopaedic Surgeons, 2000;8(5):277.
68. CARE FONP., Hyaluronic acid products for osteoarthritis of the knee, CPJ, 2007;140(3):195.
69. Fam H, Bryant J, Kontopoulou M., Rheological properties of synovial fluids, Biorheology, 2007;44(2):59-74.
70. Balazs EA, Denlinger JL., Viscosupplementation: A new concept in the treatment of osteoarthritis, The Journal of rheumatology Supplement, 1993;39:3.
71. Sun SF, Chou YJ, Hsu CW, Chen WL., Hyaluronic acid as a treatment for ankle osteoarthritis, Current reviews in musculoskeletal medicine, 2009;2(2):78-82.
72. Leopold SS, Warme WJ, Pettis PD, Shott S., Increased frequency of acute local reaction to intra-articular hylan GF-20 (synvisc) in patients receiving more than one course of treatment, The Journal of bone and joint surgery American volume, 2002;84(9):1619.
73. Kotevoglu N, Iy bozkurt PC, H z O, Toktas H, Kuran B., A prospective randomised controlled clinical trial comparing the efficacy of different molecular weight hyaluronan solutions in the treatment of knee osteoarthritis, Rheumatology international, 2006;26(4):325-30.
74. Cegnar M, KERC J., Self-assembled Polyelectrolyte Nanocomplexes of Alginate, Chitosan and Ovalbumin, Acta chimica slovenica, 2010;57(2):431-41.
75. Kamiya N, Klibanov AM., Controling the rate of protein release from polyelectrolyte complexes, Biotechnology and bioengineering, 2003;82(5):590-4.
76. Hu Z, Xia X, Tang L., Process for synthesizing oil and surfactant-free hyaluronic acid nanoparticles and microparticles, 2004, US Patent App. 20,060/040,892.

Chapter 2

Fabrication of hyaluronic acid nanoparticles

Chapter 2: Fabrication of hyaluronic acid nanoparticles

2.1. Introduction

Polymer nanotechnology has emerged as an important tool to successfully develop and modify biomaterials for drug delivery and tissue engineering. Methods have been developed to modify surface features and core components of nanoparticles for many applications (1). For instance, conjugation and optimization of targeting moieties to the surface of nanoparticles has been introduced to enhance targeted delivery of therapeutic agents to cells (2-6). Moreover, research studies have been developed to modify the surface of nanoparticles and fabricate biocompatible scaffold constructs for tissue engineering applications (7-9). In both cases, synthetic biopolymers such as polylactic acid (PLA), Poly(lactic-co-glycolic acid) (PLGA), poly(ε-caprolactone) and natural polymers such as chitosan, alginate, and hyaluronic acid have been explored (1). Moreover, polymers including dextran, poloxamer (Pluronic®) and poly(vinyl alcohol) (PVA) have been used as colloid stabilizers (1). Due to discrete properties of polymers and varied application of nanoparticles, multiple fabrication methods have been developed. However, continuous development of novel nanoparticle fabrication methods has always been required.

One of the natural polymers used for nanoparticle fabrication is hyaluronic acid (HA). Several methods have been proposed to fabricate HA nanoparticles. Electrostatic interactions with positively charged polymers such as chitosan or biological components such as proteins have been shown to form nanoparticles. Changing suspension conditions such as pH and ionic strength can dissociate the polyelectrolyte systems. Therefore, these

types of nanoparticles may only be stable under specific conditions in which the particles are formed. Studies have utilized electrostatic interactions to synthesize nanoparticles via complexation of HA with cationic polymers and therapeutic agents for delivery of anti-tumor drugs, treatment of asthma, and active tumor targeting (10-14). Chemical crosslinking has also been suggested to fabricate hydrophobic core-hydrophilic shell HA nanoparticles (15). Unlike electrostatic interactions, structurally stable HA nanoparticles can be synthesized via chemical crosslinking techniques. Not many reports are available for HA nanoparticle fabrication using chemical crosslinking. Techniques including water-in-oil-emulsion processes, spray drying, and solvent evaporation have also been reported to make micron-scale HA particles (16); however, these studies showed that completely removing oil and surfactant from the HA particles is difficult. Controlling the size distribution of particles by spray drying can also be difficult (17). Therefore, the development of HA nanoparticle fabrication methods which produce relatively uniform and stable colloids without the use of oil and surfactant is desirable (17).

A technique free from oil and surfactant by Hu et al. was used to fabricate HA nanoparticles (17). Chemical crosslinking based on carbodiimide chemistry was used to synthesize nanoparticles from HA polymer. Besides hyaluronic acid, chondroitin sulfate (CS), another naturally occurring glycosaminoglycan (GAG), was also selected to make nanoparticles in this study. Dynamic light scattering was employed to evaluate the effect of polymer type (hyaluronic acid and chondroitin sulfate), polymer concentration, HA molecular weight, reaction time, and the ratio between polymer to crosslinker on the size and charge of nanoparticles. Then, cryo-transmission electron microscopy was used to understand the morphology of nanoparticles. Fourier transform infrared spectroscopy

(FTIR) was also employed to confirm the crosslinking reaction. Nanoparticles synthesized in this chapter were used in chapters three and four to understand the possibility of colloidal gel fabrication and the effect of nanoparticles on the properties of HA suspensions.

2.2. Materials and Methods

2.2.1. Materials

Polymers of hyaluronic acid (HA) sodium salt manufactured using an extremely efficient microbial fermentation process (HA with different molecular weights of 17 kDa, 741 kDa, and 1500 kDa) were purchased from Lifecore Biomedical (Chaska, Minnesota). 1-Ethyl-3-[3-dimethylaminopropyl]carbodiimide hydrochloride (EDC) was purchased from Thermo Scientific (Rockford, Illinois). Acetone was obtained from Fisher Scientific (Fair Lawn, New Jersey). Chondroitin sulfate sodium salt from bovine cartilage (Mw ~ 30 kDa), adipic acid dihydrazide, and trinitrobenzene sulfonic acid (TNBS) (~1 M in H_2O) were purchased from Sigma-Aldrich (St. Louis, Missouri). Dialysis membrane (Regenerated Cellulose (RC), MWCO 50,000) was obtained from Spectrum Laboratory Products Inc. (Rancho Dominguez, CA, USA).

2.2.2. Methods

2.2.2.1. Nanoparticle fabrication method

Nanoparticles were fabricated by adapting a technique described by Hu et al. (17). In this method, nanoparticles were synthesized based on crosslinking polymer chains through their carboxyl groups via carbodiimide chemistry. Briefly, aqueous solution of polymer (HA or CS) was prepared by mixing polymer in deionized water (2.5 mg/mL, 80 mL) in a 500 mL round flask. Then, 136 mL acetone was added to the flask and stirred for 15 minutes (500 rpm) to make sure all the components in the solution were well dissolved. To avoid acetone evaporation, the flask was sealed properly. EDC (80 mg) and adipic acid dihydrazide (40 mg) were dissolved in 2 mL of deionized water and added to the flask. After mixing the solution for 30 minutes, another 131 mL acetone was added to the solution and stirring was continued for another 3 hours (Final HA concentration ~ 0.57 mg/mL). Then, the reaction was stopped by dialysis of the solution against deionized water using dialysis membrane (Regenerated Cellulose (RC), MWCO 50,000). Finally, the nanoparticles were freeze dried and dry powder was stored at -20 °C (Figure 2-1) (17).

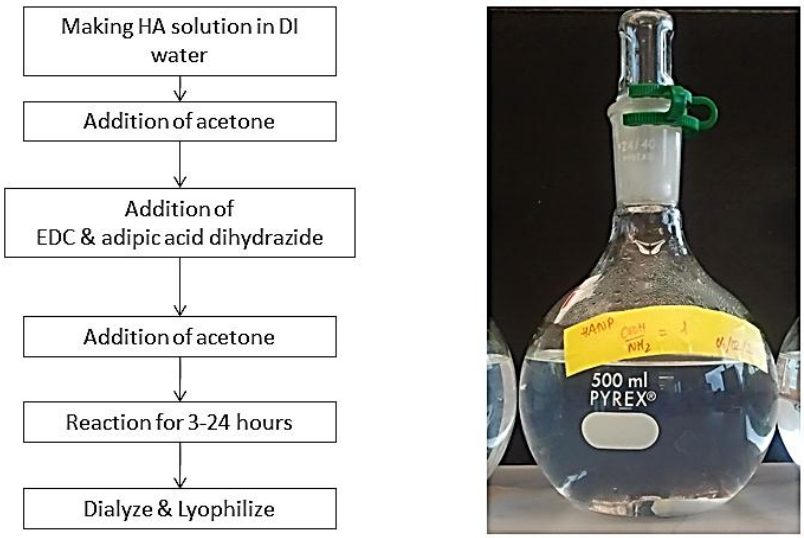

Figure (2-1) (A) Particle fabrication steps. (B) Before dialyzing, light blue color of the solution indicates formation of nanoparticles.

EDC activates carboxyl groups available on HA (or CS) and provides reactive intermediates (O-acylisourea derivatives, extremely short-lived) which react with two primary amines of adipic acid dihydrazide forming a peptide bond and resulting in the neighboring HA (or CS) chains being chemically crosslinked (Figure 2-2). With the first addition of acetone, there were no nanoparticles formed in a control experiment. After the second addition of acetone, the volume ratio of acetone/water reached to approximately 269/80 (the ratio range to form HA (or CS) nanoparticles is between 200/80 to 300/80) (17). This acetone/water ratio was reported to break the strong hydrogen bonding between HA (or CS) chains and HA-water molecules (or CS-water molecules) to release carboxyl groups for the crosslinking reaction. After the consumption of carboxyl groups by adipic acid dihydrazide, the crosslinked HA (or CS) polymer chains become less

soluble (hydrophilic) and were suggested to transform from coils to globules the resulting solution turns from clear to light blue, indicating nanoparticle formation (Figure 2-1) (17).

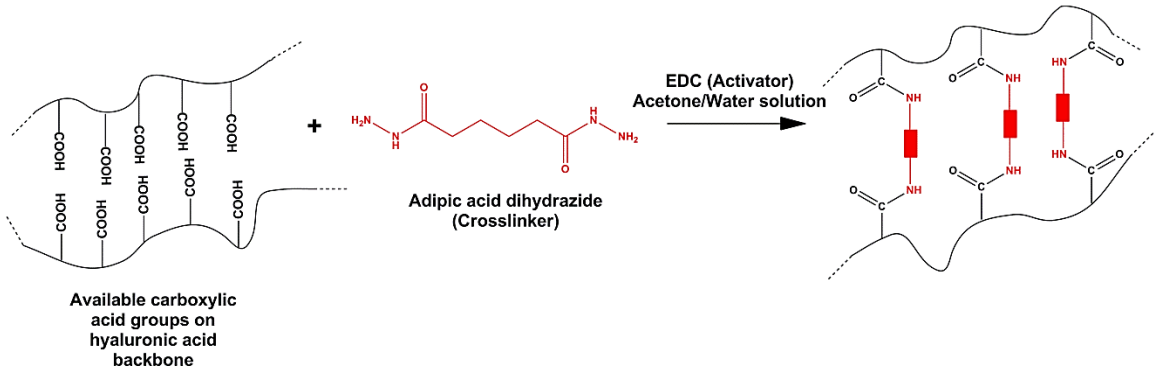

Figure (2-2) Application of carbodiimide chemistry for HA (or CS) nanoparticle fabrication. EDC activates carboxyl groups available on HA and provides reactive intermediates which react with two primary amines of adipic acid dihydrazide forming peptide bonds and resulting in the neighboring HA chains being chemically crosslinked.

2.2.2.2. Particle size and zeta potential characterization

Particle size and zeta potential were measured using a ZetaPALS dynamic light scattering instrument (Brookhaven, USA) after dispersion of freeze dried nanoparticles in deionized water (2 mg/mL). A cryo-transmission electron microscope (FEI field emission transmission electron microscope, Tecnai™ G2 at 200 kV) was employed for morphological characterization. Cryo-TEM samples were prepared using a Vitrobot™ (FEI), a PC-controlled robot for sample preparation. Substratek™ grids with 2-3 nm platinum coating on 400 square mesh gold grids were used (Ted Pella Inc., California) for sample preparation. First, nanoparticles were dispersed in deionized water at 2 mg/mL

concentration. Then, 3 μl of nanoparticle suspension was placed on the grid, blotted to reduce film thickness (3 seconds blot time), and vitrified in liquid ethane. Finally, the grid was transferred to liquid nitrogen for storage and imaging was performed after placing the prepared grid into a cryo sample holder filled with liquid nitrogen.

2.2.2.3. Characterization of bond formation via FTIR

To confirm peptide bond formation between HA carboxyl groups and adipic acid dihydrazide amine groups, a Spectrum 100 FTIR Spectrometer was used (PerkinElmer, Inc., Massachusetts). The FTIR spectra for the starting polymer and fabricated nanoparticles were compared. Adipic acid dihydrazide was also used to identify its related peaks.

2.2.2.4. Evaluation of crosslinker consumption

Analysis of fabricated nanoparticles with trinitrobenzene sulfonic acid (TNBS) allows quantification unreacted adipic acid dihydrazide. TNBS is known to react to amines, hydrazines, and hydrazides creating a stable trinitrophenyl complex. The trinitrophenyl complex of adipic dihydrazide has maximum absorbance at λ=334 nm, which can be detected via spectrophotometry (18-20).

Briefly, nanoparticles made from 17 kDa HA were dispersed in deionized water at 5 mg/mL concentration. A 17 kDa HA polymer solution at the same concentration was also prepared as a negative control sample. Adipic acid dihydrazide (0.833 mg/mL) was also added to separate nanoparticle suspension and polymer solution (5 mg/mL) to make

positive controls. To one mL of nanoparticle suspension, negative control, or positive controls, 5 µL TNBS solution was added. Then, the samples were incubated at 37 °C for one hour to let TNBS react with primary amines of adipic acid dihyadrazide resulting in trinitrophenyl complex formation. Finally, 100 µL of each sample was transferred into three wells of a 96-well cell culture plate and the absorbance of trinitrophenyl complex of adipic acid dihydrazide was measured at λ=334 nm using a microtiter plate reader (SpectraMax, M25, Molecular Devices Corp., CA). HA nanoparticle suspension and polymer solution (without TNBS) was also used to quantify the absorbance of nanoparticles at a similar wavelength.

2.2.2.5. Statistical analysis

Statistical analysis was performed using one-way analysis of variance (ANOVA). To evaluate the significance of differences, Newman–Keuls was used as a post-hoc test. A value of $p<0.05$ was accepted as significant in all cases.

2.3. Results and Discussion

2.3.1. Nanoparticle fabrication and the effect of process parameters on size and charge of the particles

Hyaluronic acid and chondroitin sulfate nanoparticles were successfully fabricated. It appears the fabrication of chondroitin sulfate nanoparticles and nanoparticles made from different molecular weights of HA has not been reported

previously. This technique could enable fabrication of nanoparticles from other polymers if the carobodiimide chemistry is transferable.

The effect of polymer concentration (0.28 mg/mL, 0.57 mg/mL, and 2.28 mg/mL) on the size and charge of HA (17 kDa) and CS nanoparticles was evaluated (Table 2-1).

Table (2-1) Effect of polymer concentration on size and charge of HA and CS nanoparticles. Polydispersity values were less than 0.22. Data represent the mean ± SD (n=3).

Polymer concentration (mg/mL)	Hyaluronic acid (17 kDa)		Chondroitin sulfate	
	Particle size (nm)	Zeta potential (mV)	Particle size (nm)	Zeta potential (mV)
0.28	167±15.5	-31±1.1	177±3.1*	-50±0.3
0.57	188±23.9*	-32±2.9	282±1.1	-52±1
2.28	564±27.2**	-36±0.7	449±2.1**	-49±0.1

* $p<0.005$ comparing 0.57 mg/mL to 0.28 mg/mL (HA data) and comparing 0.28 mg/mL to 0.57 mg/mL (CS data).
** $p<0.005$ comparing 2.28 mg/mL to 0.28 mg/mL (HA data) and comparing 2.28 mg/mL to 0.57 mg/mL (CS data).

Increasing polymer concentration increased particle size for both hyaluronic acid (HA Mw = 17 kDa) and chondroitin sulfate (CS Mw ~ 30 kDa). The size of HA nanoparticles at 2.28 mg/mL polymer concentration was significantly greater than the size of the nanoparticles at 0.28 mg/mL and 0.57 mg/mL polymer concentration. CS nanoparticles at 0.57 mg/mL polymer concentration were significantly larger than CS nanoparticles at 0.28 mg/mL polymer concentration. The data suggested that increasing polymer concentration increases particle size. This increase was shown to be independent of polymer type and might be due to more intermolecular crosslinking at higher concentrations resulting in fabrication of larger particles. CS nanoparticles showed greater negative charge values compared to HA nanoparticles. This is likely be due to the

presence of functional groups available on CS and ionization of these groups in suspension resulting in more negative charge for CS nanoparticles. Finally, these results indicated that the charge of the nanoparticles were not significantly different at different polymer concentrations.

Molecular weight of HA used for nanoparticle fabrication influenced the size of the nanoparticles. HA with three different molecular weights (17 kDa, 741 kDa, and 1500 kDa) was used to evaluate the effect of polymer molecular weight on particle size and charge (Table 2-2).

Table (2-2) Effect of HA molecular weight on size and charge of HA nanoparticles. Polydispersity values were less than 0.21. Data represent the mean ± SD (n=3).

HA molecular weight	Particle size (nm)	Zeta potential (mV)
17 kDa	188±23.9*	-32±2.9
741 kDa	78±0.7**	-21±0.5
1500 kDa	87±2.5	-26±0.9

* and ** $p<0.005$ comparing to 1500 kDa HA.

Nanoparticles made from 17 kDa HA were larger than nanoparticles made from 741 kDa HA. Nanoparticles made from 1500 kDa HA were larger than the nanoparticles made from 741 kDa HA but they were significantly smaller than the nanoparticles made from 17 kDa. The zeta potential of the nanoparticles was not dependent on the HA molecular weight and negative charge was observed for all the HA nanoparticles (Table 2-2). Due to the short length of 17 kDa HA, the chance of intramolecular crosslinking during the fabrication of nanoparticles may be less than the chance of intermolecular crosslinking. On the other hand, the chance of intramolecular crosslinking of 1500 kDa HA may be greater due to its long polymer chain length, more coiled structure, and

greater self-association compared to 17 kDa HA (Figure 2-3). This may provide a packed structure for nanoparticles made from 1500 kDa HA also resulting in smaller particle size compared to nanoparticles made from 17 kDa HA. In addition, more "dangling" chains may be available on the nanoparticles made from 17 kDa HA due to the greater chance of intermolecular crosslinking compared to nanoparticles made from 1500 kDa (Figure 2-3). The presence of dangling chains on the nanoparticles may affect particle-particle and particle-polymer interactions which will be discussed in chapters three and four.

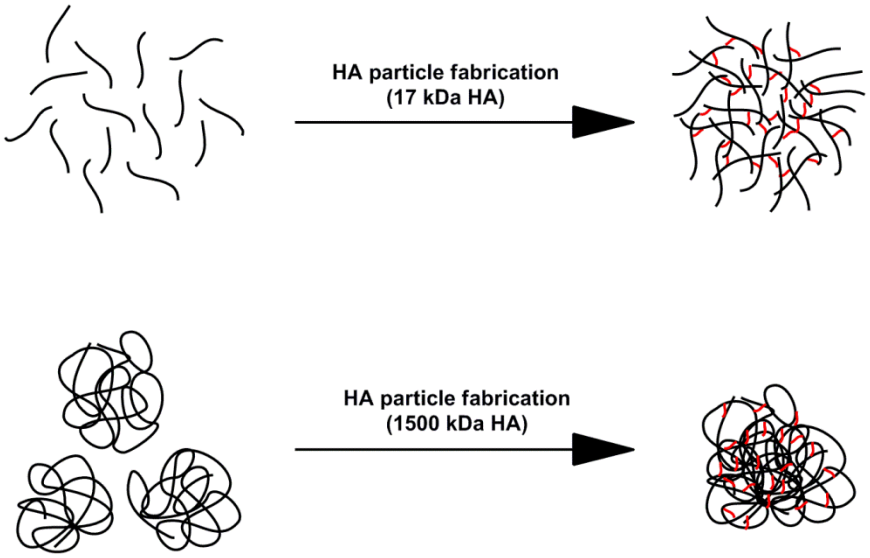

Figure (2-3) Particle formation and the effect of HA Mw on nanoparticles.

The effect of process parameters in this nanoparticle fabrication method including reaction time and the molar reactive site ratio (-COOH:-NH_2) were also evaluated (Table 2-3). HA with 17 kDa molecular weight was used for this experiment. Three different reaction times, 3, 10, and 24 hours were selected for nanoparticle fabrication. Three different molar ratio reactive sites (-COOH:-NH_2), 1:2 (excess of primary amine groups),

1:1 (equal molar of carboxyl and primary amine groups), and 2:1 (excess of carboxyl groups) were theoretically calculated for the experiment (Table 2-3).

Increasing reaction time in the formulation with a 1:2 reactive site ratio increased particle size. Normally, the carbodiimide reaction is near complete in two hours (21-23). Therefore, the increase in particle size may not be the result of further crosslinking over time. The presence of larger nanoparticles in this formulation at longer reaction times may have been caused by aggregation of nanoparticles. Perhaps this is supported by the lack of change of particle charge at different reaction times. Nanoparticles with a 1:2 reactive site ratio had the largest particle size at all reaction times. That might be due to the molar excess of crosslinker resulting in a higher probability of polymer-nanoparticle or nanoparticle-nanoparticle reaction (Table 2-3).

This study also suggested that the reactive site ratio influenced zeta potential in all reaction times. Increasing the relative amount of primary amine groups in the formulation decreased particle charge. The greater chance for crosslinking at higher molarities of primary amine groups appeared to occupy carboxyl groups and decrease zeta potential resulting in less negative charge for nanoparticles (Table 2-3).

Table (2-3) Effect of reaction time and molar reactive site ratio (-COOH:-NH_2) on size and charge of HA nanoparticles. Polydispersity values were less than 0.31. Data represent the mean ± SD (n=3).

Reaction time (hours)	**Molar reactive site ratio (-COOH:-NH_2)**					
	1:2		**1:1**		**2:1**	
	Particle size (nm)	**Zeta potential (mV)**	**Particle size (nm)**	**Zeta potential (mV)**	**Particle size (nm)**	**Zeta potential (mV)**
3	298±7.2	-22.33±1.2	188±23.9	-32±2.9	239±10.1	-41±0.02
10	350±3.8*	-27.41±1.1	209±1.3*	-33.29±1.1	225±9.3*	-38±1.3
24	501±1.9**	-19.3±0.6l	341±0.3	-36.28±1.0	278±7.8	-41±0.2

* $p<0.005$ comparing 10 hours data to 3 hours data.
** $p<0.005$ comparing 24 hours data to 3 hours data.

2.3.2. Cryo-TEM imaging

Cryo-transmission electron microscopy was employed to investigate the morphology of HA nanoparticles made from 17 kDa and 1500 kDa HA at 0.57 mg/mL polymer concentration, 1:1 molar reactive site ratio, and three hours reaction time. The images suggested spherical shape for HA nanoparticles made from both 17 kDa and 1500 kDa HA (Figure 4-2).

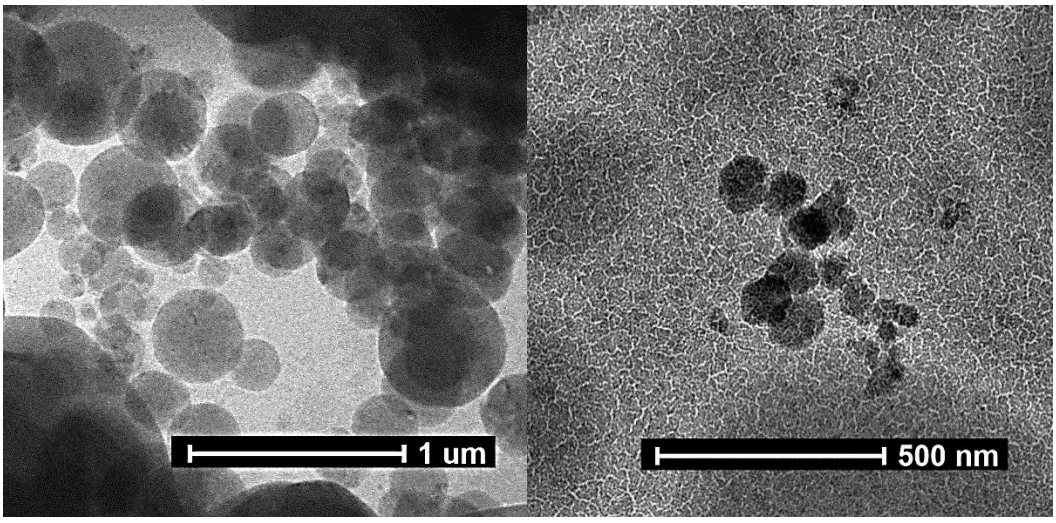

Figure (2-4) Cryo-transmission electron micrographs of hyaluronic acid nanoparticles. Left: nanoparticles made from 17 kDa HA, right: nanoparticles made from 1500 kDa HA.

2.3.3. Characterization of bond formation via FTIR

To confirm peptide bond formation between HA carboxyl groups and adipic acid dihydrazide primary amine groups, Fourier transform infrared spectroscopy (FTIR) was employed. The FTIR spectra for the HA nanoparticles (Figure 2-5) showed the appearance of a new peak corresponding to the presence of adipic acid dihydrazide (N-N bond) (around 1635 cm^{-1}). This peak appearance was also observed in FTIR spectra of CS nanoparticles (Figure 2-5). The presence of these peaks in the FTIR spectrum after purification of nanoparticles confirmed the carbodiimide reaction and peptide bond formation.

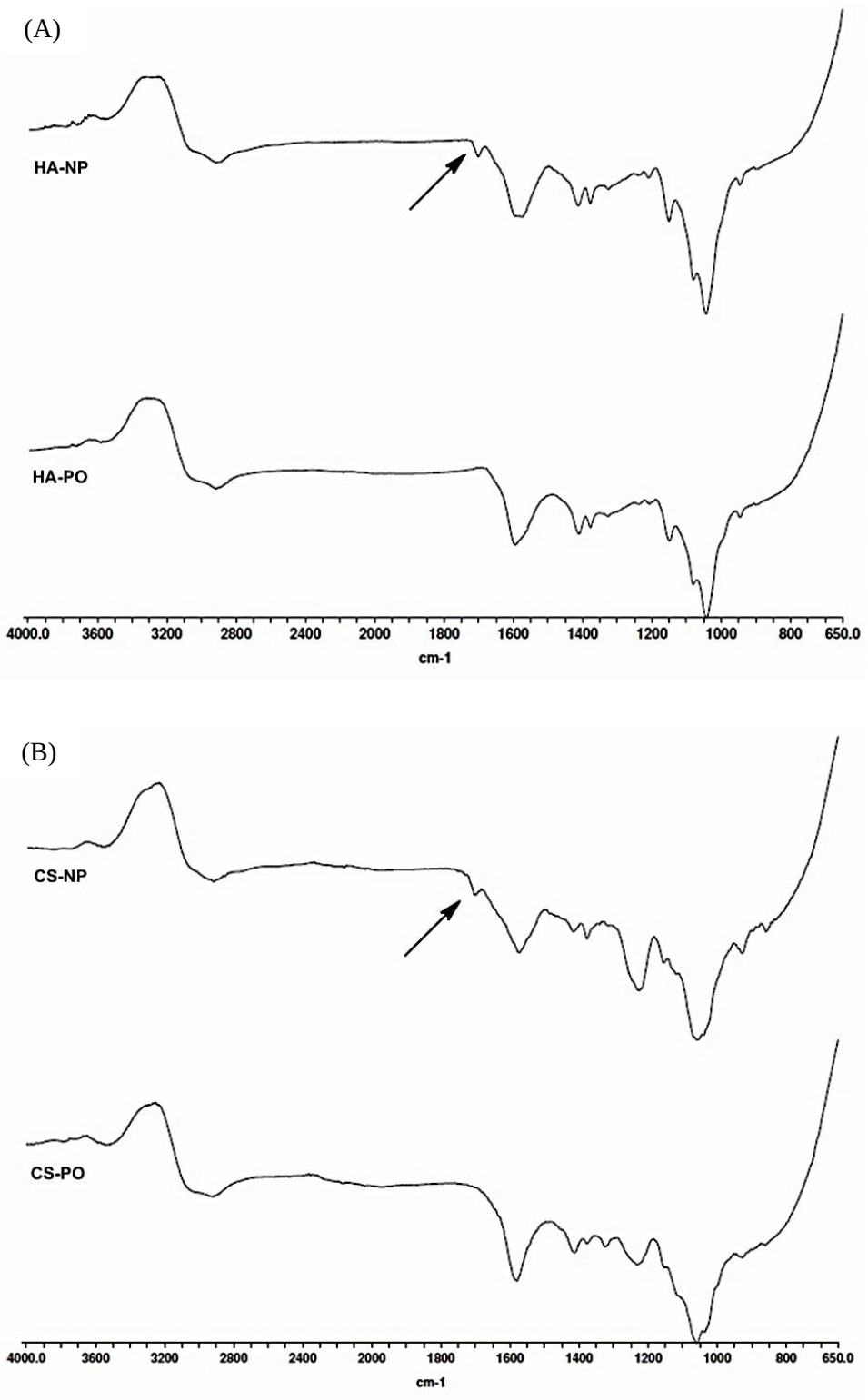

Figure (2-5) (A) FTIR spectra of 17 kDa HA polymer (HA-PO) and nanoparticles made from 17 kDa HA (HA-NP). (B) FTIR spectra of CS polymer (CS-PO) and CS nanoparticles (CS-NP).

2.3.4. Evaluation of crosslinker consumption

A TNBS assay was also used to determine the availability of unreacted primary amine groups on the crosslinker after purifying nanoparticles. HA nanoparticles made from 17 kDa HA at 0.57 mg/mL polymer concentration, 1:1 molar reactive site ratio, and three hours reaction time were employed for this experiment. HA polymer was also used as a negative control to compare with the nanoparticles. The TNBS assay revealed that the unreacted primary amine groups on crosslinker were not available in the nanoparticle suspension after purification due to similar optical density measured at 334 nm for nanoparticle sample compared to negative control sample. Therefore, no subsequent side reactions would occur in the application of HA nanoparticles in colloidal systems, due to elimination of unreacted crosslinker from nanoparticles.

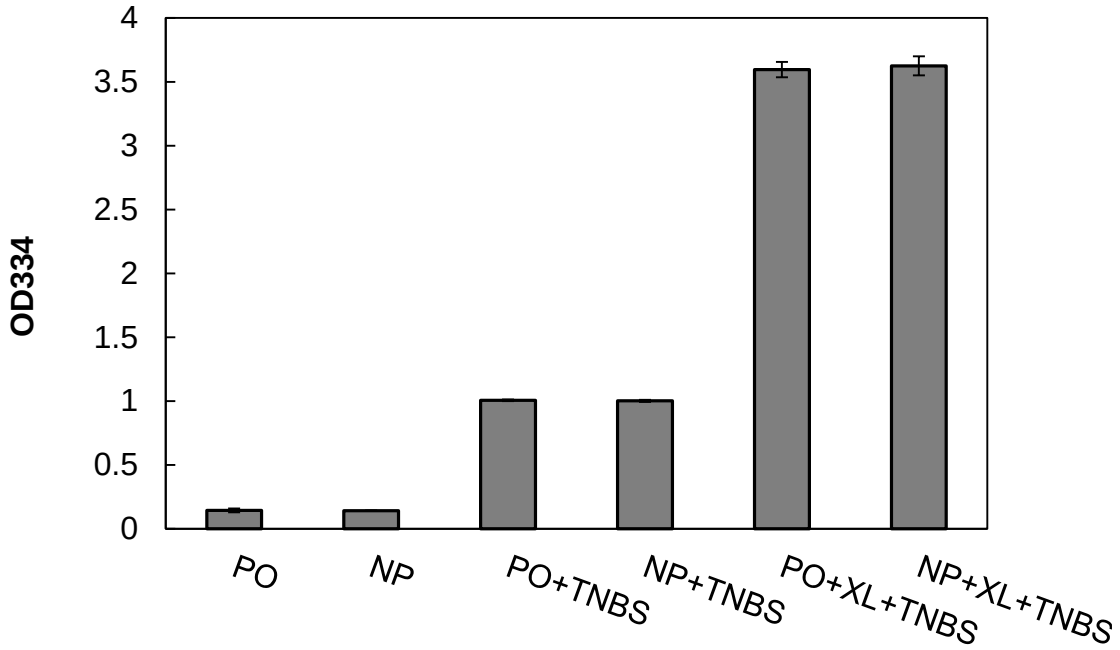

Figure (2-6) Using the TNBS assay as a probe to identify the availability of unreacted primary amine groups on crosslinker (PO=Polymer, NP=Nanoparticles, and XL=crosslinker). Data represent the mean ± SD (n=3).

2.4. Conclusion

In this chapter, a technique adapted from Hu et al. was used to fabricate nanoparticles. This method was able to successfully synthesize nanoparticles from both hyaluronic acid and chondroitin sulfate using carbodiimide chemistry. Previously, this method has not been employed to fabricate nanoparticles from chondroitin sulfate or from different molecular weights of hyaluronic acid. It was also observed that nanoparticles made from chondroitin sulfate had a more negative charge compared to nanoparticles made from 17 kDa HA. The size and charge of nanoparticles was affected by polymer concentration, polymer molecular weight, reaction time, and the polymer to crosslinker ratio. Increasing polymer concentration increased the particle size; however, HA with higher molecular weights led to smaller particles, presumably with less "dangling" chains. Moreover, FTIR data also suggested the formation of peptide bonds resulting in crosslinking of HA polymer chains via adipic acid dihydrazide. Nanoparticles fabricated at 0.57 mg/mL polymer concentration, 1:1 molar reactive site ratio, and three hours reaction time were used in chapters three and four to investigate the possibility of colloidal gel fabrication and the effect of nanoparticles on the properties of HA suspensions.

2.4. References

1. Vauthier C, Bouchemal K., Methods for the preparation and manufacture of polymeric nanoparticles, Pharmaceutical research, 2009;26(5):1025-58.
2. Fakhari A, Baoum A, Siahaan TJ, Le KB, Berkland C., Controlling ligand surface density optimizes nanoparticle binding to ICAM 1, Journal of pharmaceutical sciences. 2010.
3. Baoum A, Xie SX, Fakhari A, Berkland C., "Soft" Calcium Crosslinks Enable Highly Efficient Gene Transfection Using TAT Peptide, Pharmaceutical research, 2009;26(12):2619-29.
4. Chittasupho C, Manikwar P, Krise JP, Siahaan TJ, Berkland C., cIBR effectively targets nanoparticles to LFA-1 on acute lymphoblastic T cells, Molecular pharmaceutics, 2009;7(1):146-55.
5. Chittasupho C, Xie SX, Baoum A, Yakovleva T, Siahaan TJ, Berkland CJ., ICAM-1 targeting of doxorubicin-loaded PLGA nanoparticles to lung epithelial cells, European journal of pharmaceutical sciences, 2009;37(2):141-50.
6. Zhang N, Chittasupho C, Duangrat C, Siahaan TJ, Berkland C., PLGA Nanoparticle- Peptide Conjugate Effectively Targets Intercellular Cell-Adhesion Molecule-1, Bioconjugate chemistry, 2007;19(1):145-52.
7. Wang Q, Jamal S, Detamore MS, Berkland C., PLGA chitosan/PLGA alginate nanoparticle blends as biodegradable colloidal gels for seeding human umbilical cord mesenchymal stem cells, Journal of Biomedical Materials Research Part A., 2011.
8. Wang Q, Wang J, Lu Q, Detamore MS, Berkland C., Injectable PLGA based colloidal gels for zero-order dexamethasone release in cranial defects, Biomaterials, 2010;31(18):4980-6.
9. Wang Q, Wang L, Detamore MS, Berkland C., Biodegradable colloidal gels as moldable tissue engineering scaffolds, Advanced Materials, 2008;20(2):236-9.
10. Jeong YI, Kim ST, Jin SG, Ryu HH, Jin YH, Jung TY, et al., Cisplatin incorporated hyaluronic acid nanoparticles based on ion complex formation, Journal of pharmaceutical sciences, 2008;97(3):1268-76.
11. Han SY, Han HS, Lee SC, Kang YM, Kim IS, Park JH., Mineralized hyaluronic acid nanoparticles as a robust drug carrier, J Mater Chem, 2011;21(22):7996-8001.
12. Choi KY, Chung H, Min KH, Yoon HY, Kim K, Park JH, et al., Self-assembled hyaluronic acid nanoparticles for active tumor targeting, Biomaterials, 2010;31(1):106-14.
13. Liu Y, Sun J, Cao W, Yang J, Lian H, Li X, et al., Dual targeting folate-conjugated hyaluronic acid polymeric micelles for paclitaxel delivery, International journal of pharmaceutics, 2011.
14. Cho HJ, Yoon HY, Koo H, Ko SH, Shim JS, Lee JH, et al., Self-assembled nanoparticles based on hyaluronic acid-ceramide (HA-CE) and Pluronic® for tumor-targeted delivery of docetaxel, Biomaterials, 2011.
15. Yang X, Kootala S, Hilborn J, Ossipov DA., Preparation of hyaluronic acid nanoparticles via hydrophobic association assisted chemical cross-linking—an orthogonal modular approach, Soft Matter, 2011.
16. Kyyronen K, Hume L, Benedetti L, Urtti A, Topp E, Stella V., Methylprednisolone esters of hyaluronic acid in ophthalmic drug delivery: in vitro and in vivo release studies, International journal of pharmaceutics, 1992;80(1-3):161-9.
17. Hu Z, Xia X, Tang L., Process for synthesizing oil and surfactant-free hyaluronic acid nanoparticles and microparticles, 2004, US Patent App. 20,060/040,892.
18. Bouhadir KH, Hausman DS, Mooney DJ., Synthesis of cross-linked poly (aldehyde guluronate) hydrogels, Polymer, 1999;40(12):3575-84.
19. Lee KY, Bouhadir KH, Mooney DJ., Degradation behavior of covalently cross-linked poly (aldehyde guluronate) hydrogels, Macromolecules, 2000;33(1):97-101.

20. Yang TF, Chen CN, Chen MC, Lai CH, Liang HF, Sung HW., Shell-crosslinked Pluronic L121 micelles as a drug delivery vehicle, Biomaterials, 2007;28(4):725-34.
21. Izdebski J, Kunce D., Evaluation of carbodiimides using a competition method, Journal of Peptide Science, 1997;3(2):141-4.
22. Gauthier MA, Klok HA., Peptide/protein–polymer conjugates: synthetic strategies and design concepts, Chem Commun, 2008(23):2591-611.
23. Yang H, Lopina ST., Penicillin V-conjugated PEG-PAMAM star polymers, Journal of Biomaterials Science, Polymer Edition, 2003;14(10):1043-56.

Chapter 3

Application of hyaluronic acid nanoparticles for colloidal gel fabrication

Chapter 3: Application of hyaluronic acid nanoparticles for colloidal gel fabrication

3.1. Introduction

Colloidal gels are materials made from particles that interact to form three-dimensional (3-D) networks. Such materials have been suggested as tissue engineering scaffolds, drug delivery systems, and biosensors (1, 2). Interparticle interactions including electrostatic interactions, van der Waals forces, and steric hindrance enable the internal cohesion of colloidal gels. Applying shear force can disrupt these interactions allowing the colloidal gels to flow (1-3). To stabilize the structure of colloid-containing materials, chemical reactions such as *in situ* crosslinking have been reported, although the application of these reactions are limited due to toxicity (4). Advanced techniques need to be developed to stabilize the mechanical properties or to enhance dynamic properties of colloidal gels while maintaining compatibility with tissues.

The fabrication of moldable colloidal gels has already been reported for tissue engineering applications, but few reports utilize nanoparticles made from biomaterials commonly used as tissue engineering scaffolds (2, 5, 6). Application of poly(*D*,*L*-lactic-co-glycolic acid) (PLGA) nanoparticles for colloidal gel fabrication was proposed by Wang et al. (2, 7). Oppositely charged PLGA nanoparticles formed a cohesive colloidal gel through electrostatic interactions between nanoparticles resulting in a moldable 3-D network. The colloidal gel could flow by applying shear force as a result of the disruption of inter-particle electrostatic interactions. The cohesive property of the colloidal gels was

showed to be recoverable after removal of the external shear force. This reversible property facilitates injection for drug delivery or tissue engineering (1, 2, 7, 8).

Here, a novel colloidal gel based on glycosaminoglycan (GAG) nanoparticles (hyaluronic acid or chondroitin sulfate nanoparticles) was explored as a means to form stable 3-D networks. As an alternative to inter-particle electrostatic interactions, other properties of polymers such as physical entanglement may occur between 'self-associating' polymeric nanoparticles. Several characterization methods were employed to evaluate physical, mechanical, and rheological properties of colloidal gels composed of high concentrations of HA nanoparticles.

3.2. Materials and Methods

3.2.1. Materials

Hyaluronic acid and chondroitin sulfate nanoparticles synthesized as in chapter two (section 2.2.2.1) at 0.57 mg/mL polymer concentration, 1:1 molar reactive site ratio, and three hours reaction time were used to make colloidal gel systems. Nanoparticles made from 17 kDa HA, 1500 kDa HA, and ~ 30 kDa CS were selected to investigate the effect of HA molecular weight and type of GAG on the potency of colloidal gel formation. HA (17 kDa and 1500 kDa) manufactured using an extremely efficient microbial fermentation process (Lifecore Biomedical, Chaska, Minnesota) and CS (~ 30 kDa) polymers from bovine cartilage (Sigma-Aldrich, St. Louis, Missouri) were used to make controls. 1-Ethyl-3-[3-dimethylaminopropyl]carbodiimide hydrochloride (EDC) was purchased from Thermo Scientific (Rockford, Illinois). Adipic acid dihydrazide was purchased from Sigma-Aldrich (St. Louis, Missouri).

3.2.2. Methods

3.2.2.1. Fabrication of colloidal gel

Colloidal systems were formed by mixing nanoparticles with deionized water at different concentrations. All experiments were performed in triplicate. First, dried nanoparticles (HA or CS) were removed from a freezer and equilibrated at room temperature. Nanoparticles were weighed and transferred to different microtubes at concentrations from 1.4% w/v up to 60% w/v in deionized water. The mixture was transferred to cylindrical molds (5 mm diameter and ~ 1.8 mm height) and left for at least

five hours. Polymers of HA (17 kDa and 1500 kDa) and CS (~ 30kDa) were used as negative controls at similar concentrations to investigate the possible formation of physically entangled gels in polymer solutions. Positive controls were also formed by adding ECD and adipic acid dihydrazide (with similar molarity used in nanoparticle fabrication) to 17 kDa HA polymer solutions at 15%, 30%, and 45% w/v. Positive controls were also used to investigate the possibility of gel formation with carbodiimide chemistry at similar colloidal gel concentrations.

3.2.2.2. Characterization of colloidal gels via FTIR

A Spectrum 100 FTIR Spectrometer (PerkinElmer, Inc., Massachusetts) was employed to confirm that no chemical side reaction took place during colloidal gel fabrication. The FTIR spectra of the starting polymer, nanoparticles, and colloidal gel were compared.

3.2.2.3. Swelling experiment

To investigate the swelling behavior and stability of colloidal gels, a swelling experiment was carried out as previously described (9-11). All experiments were performed in triplicate. Briefly, colloidal gels at 15%, 30%, and, 45% w/v nanoparticle concentrations made from 17 kDa HA nanoparticles were placed into an excess of water or 0.1 M PBS for at least 6 hours. The equilibrated colloidal gel samples were weighed and placed into a desiccator chamber. After 48 hours, the dried colloidal gels were weighed again and the swelling ratio of colloidal gels was calculated according to

Equation (1) where W_S (mg) is the swollen weight and W_D (mg) is the dry weight of colloidal gels (9-11):

$$Swelling\ ratio = \frac{(W_S - W_D)}{W_D} \qquad Eq.(1)$$

3.2.2.4. Compression testing and mechanical analysis

Compression testing was performed to investigate the mechanical properties of samples after fabrication, after swelling in water, and after swelling in 0.1 M PBS. Colloidal gels made from 17 kDa HA nanoparticles at 15%, 30%, and 45% w/v were used in this experiment. First, samples were placed on a glass slide and the dimensions of the cylindrical colloidal gels were determined with calipers using a microscope (Nikon TS100F). Since the dimensions of samples changed after swelling in water and 0.1 M PBS, samples were initially punched to a diameter of approximately 5 mm. Then, a uniaxial compression test using a RSA-III dynamic mechanical analyzer (TA Instruments, Delaware) was performed. Sample height was directly measured from the instrument. Mineral oil was used to lubricate both compression plates to reduce any sample-plate adhesion and prevent sample drying during the test. Compression testing was performed at a rate of 0.005 mm/s to obtain a stress-strain curve. The results were then analyzed according to the neo-Hookean model for an ideal elastomer in which the slope of the stress-strain fraction curve (λ-$1/\lambda^2$, where $\lambda=L/L_o$) yields a straight line with a slope equal to the shear modulus (9). Young's modulus, the slope of the stress-strain curve, was also estimated based on the linear portion of the stress-strain fraction curve. If

the initial region was not a straight line, that region was not considered in calculations. Toughness of samples, the absorbed energy, was finally calculated by numerical integration of the stress-strain curve (9). All experiments were performed in triplicate.

3.2.2.5. Effect of pH and ionic strength on mechanical properties of HA colloidal gel

Studies have shown that pH and ionic strength are two important factors that must be considered for injected formulation (12-14). Moreover, the influence of these factors on HA structure and hydrodynamic radius was briefly discussed in chapter one (15). To investigate the effect of pH and ionic strength on the formation of HA colloidal gels and their mechanical properties, phosphate buffer (phosphate buffer concentration=10 mM) was made at three different pH values (pH=6, 7.4, and 8). This range covers the reported local pH tolerance for subcutanous injection (12-14). Sodium phosphate was chosen as buffer at pH=6 since other buffers such as citrate are known to be painful for injection (12). Usually, an isotonic solution containing 150 mM salt was reported for injection (12, 14). In order to explore an ionic strength range similar to isotonic solution, three different ionic strengths (100 mM, 150mM, and 200 mM) were selected for the buffer formulations. The buffers were prepared by mixing sodium phosphate salt and sodium chloride salt in deionized water at the desired pH and ionic strength.

3.2.2.6. Viscoelasticity of HA colloidal gel after fabrication

In order to investigate the viscoelasticity of HA colloidal gels, dynamic oscillatory rheological measurements were performed using an AR 2000 rheometer (TA Instruments, Delaware) equipped with a 2°, 20 mm diameter cone-plate geometry at a controlled temperature of 25 °C. HA colloidal gel samples were prepared by mixing nanoparticles (made from 17 kDa HA) at different concentrations (5%, 15%, 30%, 45% w/v) in deionized water. 17 kDa HA polymer was also dissolved in deionized water at 45% w/v concentration as negative control. First, strain sweep experiments were performed to determine the linear viscoelastic regime, where the rheological properties are not strain dependent. Then, the viscoelastic properties of colloidal gels were evaluated using a frequency sweep from 0.1 to 10 Hz at 1% strain, which was in the linear viscoelastic region. This range includes the physiological frequencies of the knee, ranging from 0.5 Hz (walk) to 3 Hz (running) (16-19). All experiments were performed in triplicate.

In the oscillatory experiment, a sinusoidal shear strain was applied to the samples accordingly to:

$$\gamma = \gamma_{\circ} \sin(\omega t) \qquad Eq.(2)$$

where $\gamma_{\circ}$ is the shear strain amplitude, ω is the oscillation frequency and t is the time. The mechanical response, expressed as the shear stress (τ) of viscoelastic materials, ranges from an ideal pure elastic solid (follows Hooke's law) and an ideal pure viscous

fluid (follows Newton's law) (16). If viscoelastic, the mechanical response is out of phase by δ from *Eq. (5)* with respect to the imposed deformation as stated by:

$$\tau = G'(\omega)\gamma_{\circ}\sin(\omega t) + G''(\omega)\gamma_{\circ}\cos(\omega t) \qquad Eq.(3)$$

where $G'(\omega)$ is the shear elastic modulus giving information about elasticity or the energy stored in the material during deformation and $G''(\omega)$ is the shear viscous modulus which describes the viscous characteristic or the energy scattered as heat (16).

The combined viscous and elastic behavior is defined by the absolute value of complex shear modulus G^* (16):

$$G^*(\omega) = \sqrt{G'^2 + G''^2} \qquad Eq.(4)$$

The ratio between the viscous modulus and the elastic modulus is defined by the loss tangent (tan delta):

$$\tan\delta = \frac{G''}{G'} \qquad Eq.(5)$$

The loss tangent is the ratio of the energy lost to the energy stored in the cyclic deformation (16-18).

3.2.2.7. Viscosity of HA colloidal gel

The viscosity of the different formulations was determined using an AR 2000 rheometer (TA Instruments, Delaware) equipped with a 2°, 20 mm diameter cone-plate at 25 °C. HA nanoparticles (made from 17 kDa HA) were mixed with deionized water at different concentrations (5%, 15%, 30%, 45% w/v). Shear stress and viscosity of the samples were measured over a shear rate sweep of 0.01-100 s^{-1}. 17 kDa HA polymer was also dissolved in deionized water at 45% w/v concentration as a negative control. All experiments were performed in triplicate.

3.2.2.8. HA colloidal gel recovery

3.2.2.8.1. Mechanical dynamics and recovery

To characterize recovery and the dynamic behavior of HA colloidal gels, compression testing was performed as described in section 3.2.2.4. Two sets of samples (after fabrication and swollen in 0.1 M PBS) were prepared for this experiment. After fabrication of colloidal gels at different nanoparticle concentrations (15%, 30%, and 45% w/v), one set of samples was swollen in 0.1 M PBS solution for at least 24 hours. Each sample was punched to a diameter of approximately 5 mm. After loading each sample, five preconditioning compression cycles at 6% strain were applied to initiate the recovery experiment. Then, a compression at 30% strain (0.005 mm/s) was applied. After squeezing the sample, compression force was removed and the sample was allowed to relax for five minutes. Meanwhile, the sample was hydrated with deionized water to prevent dryness. Finally, another compression at 30% strain (0.001 mm/s) was applied.

The mechanical recovery and dynamic property of samples were identified by comparing the recovered height of the samples after the second compression to the height of the samples before the first compression. Normal stress-gap curves were generated and used to identify the recovery. All experiments were performed in triplicate.

3.2.2.8.2. Rheological recovery

To evaluate the rheological recovery of colloidal gels, the viscosity was measured as in section 3.2.2.7. Samples at 15% w/v nanoparticle concentration in deionized water were prepared for this experiment. Then, the colloidal gel was loaded under the rheometer and three cycles of shear rate sweeps (0.01-100 s^{-1}) with a one minute delay between each cycle were applied to the samples. The changes in shear stress and viscosity over shear rate sweep after each run was evaluated. All experiments were performed in triplicate.

3.2.2.8.3. Physical recovery

To evaluate the physical recovery of the colloidal gel, samples at 30% w/v nanoparticle concentration in deionized water were prepared. The samples were swollen in water for at least 24 hours. Then, the swollen samples were completely crushed and dried in a desiccator for at least 48 hours. Finally, dried samples were weighed and again the colloidal gel samples at 30% w/v were remade. The physical recovery of the samples was evaluated by visual observation. All experiments were performed in triplicate.

3.2.2.9. Statistical analysis

Statistical analysis was performed by one-way analysis of variance (ANOVA). To evaluate the significance of differences, Newman–Keuls was used as a post-hoc test. A value of $p<0.05$ was accepted as significant in all cases.

3.3. Results

3.3.1. Fabrication of colloidal gel

Colloidal gels were formed by mixing nanoparticles with deionized water at different concentrations. Samples were made from 17 kDa and 1500 kDa HA (Figure 3-1). These nanoparticles were assumed to have different structural properties. 17 kDa HA nanoparticles were suspected to have a more 'hairy' structure with dangling chains compared to 1500 kDa HA nanoparticles. Colloidal gels with a stable 3-D structure formed at 15%, 30%, and 45% w/v when nanoparticles made from 17 kDa HA were used. Colloidal gels could also hold their structure upon swelling in deionized water. At 5% w/v nanoparticle concentration, the mixture could not form a stable 3-D structure; however, a viscous suspension of HA nanoparticles was obtained (Figure 3-1, B). That might be because of the physical entanglement between dangling chains of nanoparticles. On the other hand, 17 kDa HA polymer solutions at 5%, 15%, 30%, and 45% were liquid and a 3-D network was not evident (Figure 3-1, A). Even positive controls using EDC and adipic acid dihydrazide with hyaluronic acid resulted in no gel formation at similar concentrations. Positive controls were made by activating carboxyl groups of 17 kDa HA via EDC and trying to crosslink them via adipic acid dihydrazide in deionized water (but

without acetone in this case) at similar concentrations to colloidal gel formulations (Figure 3-1, C).

Mixing nanoparticles fabricated from 1500 kDa HA at 1.4%, 5%, 10%, 15%, 30%, and 45% w/v concentrations did not form any stable colloidal gel network (Figure 3-1, E). At lower concentrations (1.4%, 5%, 10%, and 15% w/v), formation of a low viscosity nanoparticle suspension was observed; however, at 30% and 45% w/v nanoparticle concentrations, paste-like materials were obtained (Figure 3-1, E and F). Mixing 1500 kDa HA polymer with deionized water at 1.4% w/v resulted in formation of a viscous polymer solution however at 5%, 10%, and 15% w/v polymer concentrations, 3-D gels formed (Figure 3-1, D). These gels, however, could be dissolved while swelling in deionized water.

Results showed that at 15%, 30%, and 45% w/v nanoparticle concentrations (17 kDa HA nanoparticles), colloidal gels with stable 3-D structure were formed. In contrast, paste-like materials were formed in the samples made from 1500 kDa HA nanoparticles at similar concentrations. Formation of stable colloidal gels in the samples made from 17 kDa HA nanoparticles may be due to physical entanglement of the dangling chains available on the surface of 17 kDa HA nanoparticles. On the other hand, the absence of these dangling chains on the nanoparticles made from 1500 kDa HA negated physical entanglement and yielded weak paste-like materials (Figure 3-2).

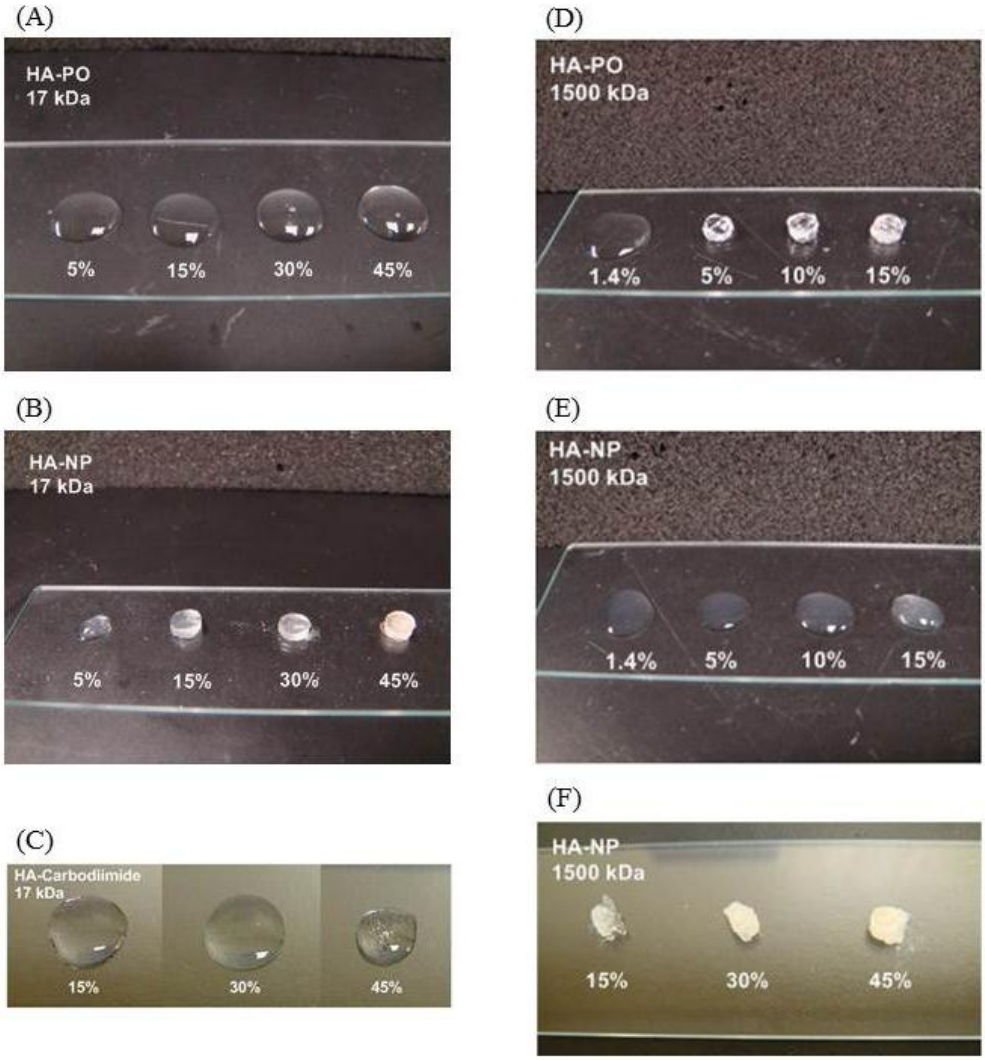

Figure (3-1) (A) 17 kDa HA polymer solutions (HA-PO) at different concentrations (5%, 15%, 30%, and 45% w/v). (B) Colloidal gels (HA-NP) formed at different HA (17 kDa) nanoparticles concentrations (15%, 30%, and 45% w/v). (C) Carbodiimide chemistry also did not form stable gel at different HA (17 kDa) concentrations. (D) 1500 kDa polymer solutions (HA-PO) at different concentrations (1.4%, 5%, 10, 15% w/v). (E) Nanoparticle suspensions (HA-NP) formed at different HA (1500 kDa) nanoparticles concentrations (1.4%, 5%, 10, 15% w/v). (F) Formation of paste-like materials was observed at 30% and 45% w/v HA (1500 kDa) nanoparticle concentrations.

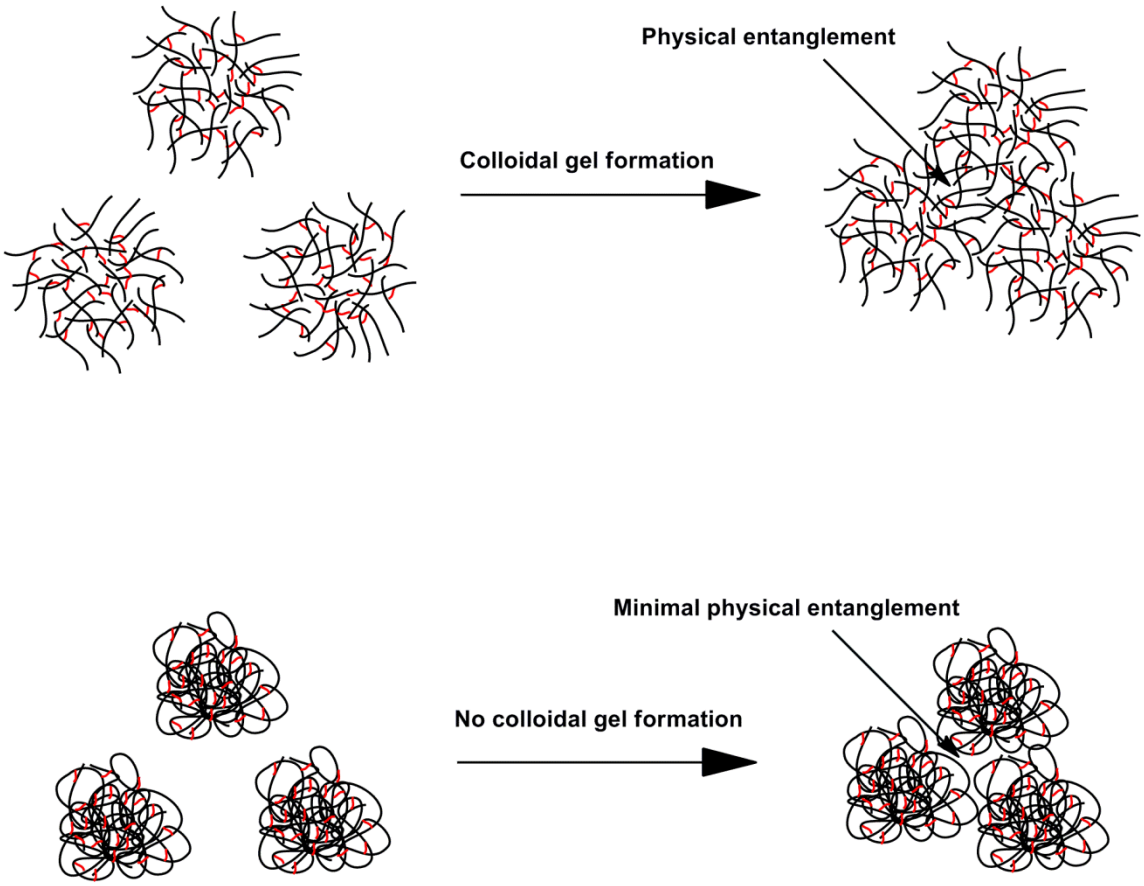

Figure (3-2) (Top) Physical entanglement due to the presence of dangling chains on the surface of 17 kDa HA nanoparticles may facilitate formation of stable colloidal gel networks. (Bottom) Due to the absence of dangling chains on 1500 kDa HA nanoparticles, physical entanglement and formation of stable colloidal gel networks did not occur.

Chondroitin sulfate (CS) (~ 30 kDa) nanoparticles were also tested; however, a stable 3-D structure network did not form even at high concentration of CS nanoparticles (60% w/v). Mixing CS nanoparticles with deionized water only formed colloidal suspensions. This might be due to the absence of physical properties such as entanglement and self-association of CS polymer chains compared to hyaluronic acid (Figure 3-3).

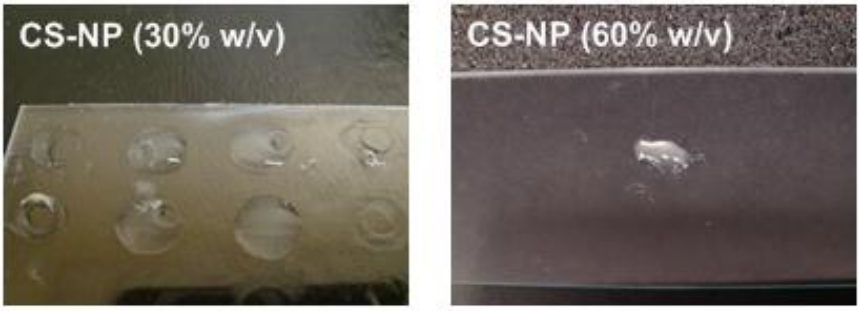

Figure (3-3) Colloidal gel networks did not form when using chondroitin sulfate nanoparticles even at 60% w/v concentration.

3.3.2. Characterization of colloidal gels via FTIR

FTIR spectra of HA polymer, HA nanoparticles, and HA colloidal gel at 30% w/v nanoparticle concentration (17 kDa HA) showed that no chemical side reaction occurred during the colloidal gel fabrication process (Figure 3-4).

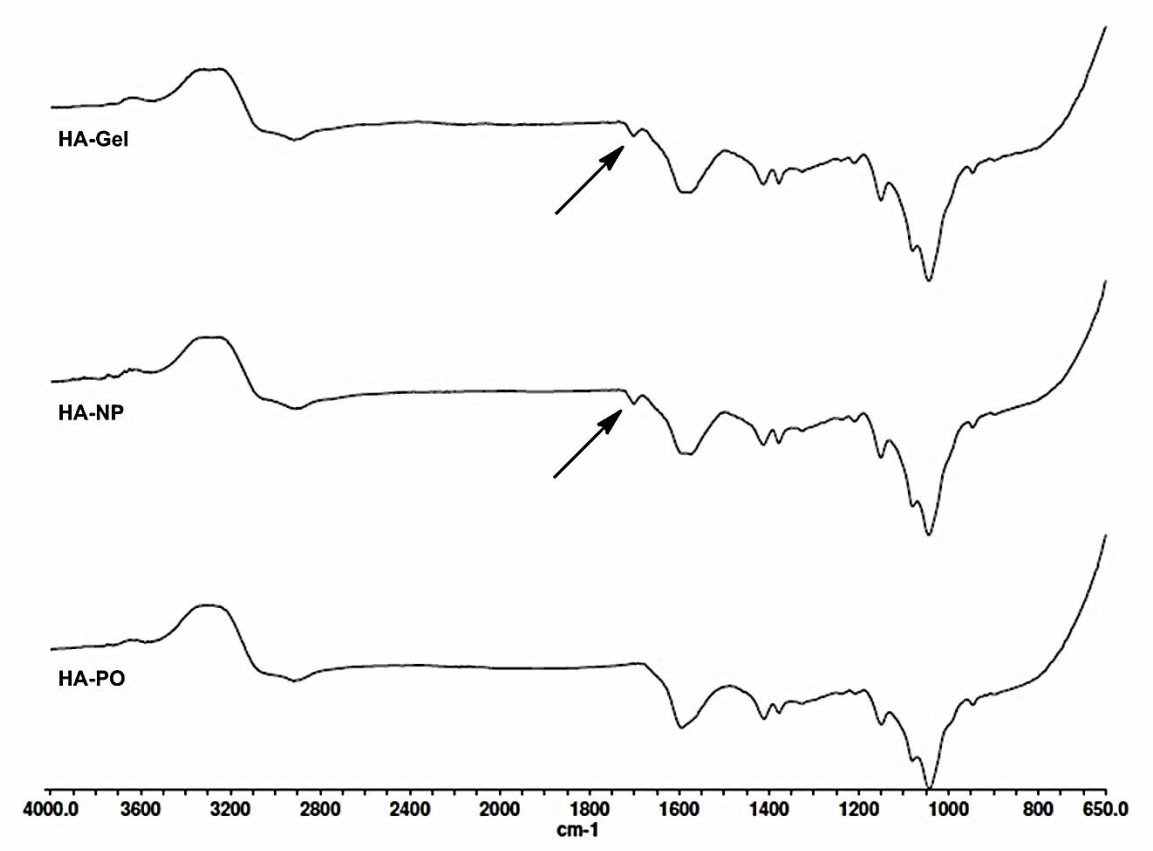

Figure (3-4) FTIR spectra of HA polymer (HA-PO), HA nanoparticles (HA-NP), and HA colloidal gel (HA-Gel) at 30% w/v concentration. The results indicated that chemical side reactions did not occur during colloidal gel formation (17 kDa HA).

3.3.3. Swelling experiment

The swelling ratio of HA colloidal gels at different nanoparticle (17 kDa HA) concentrations (15%, 30%, and 45% w/v) were measured at 6 and 24 hours (Figure 3-5 and Figure 3-6). The swelling ratio of samples swollen in deionized water was greater than the swelling ratio of samples swollen in 0.1 M PBS. The presence of salt in 0.1 M PBS solution may keep the HA structure more coiled with a lower hydrodynamic radius resulting in less swelling of nanoparticles (15). Increasing nanoparticle concentration decreased the swelling ratio for the samples swollen in both water and 0.1 M PBS. More

physical entanglement between nanoparticles was expected at higher concentrations. Finally, HA colloidal gels swollen in water and 0.1 M PBS could hold their stable 3-D structures (Figure 3-7).

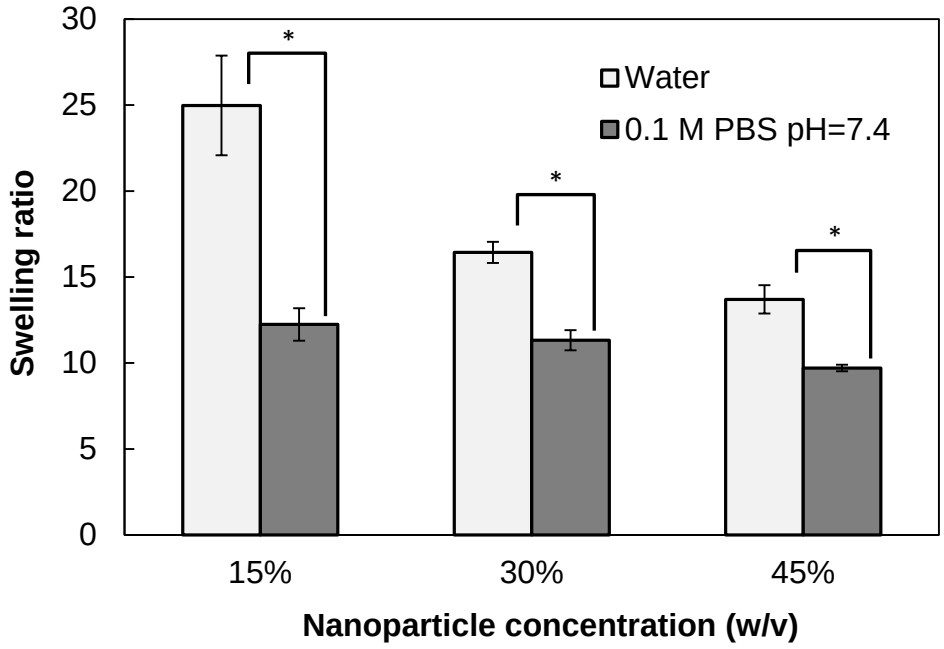

Figure (3-5) Swelling experiment on colloidal gels after 6 hours incubation. Samples with lower nanoparticle concentrations tended to swell more in both water and 0.1 M PBS. Samples tended to swell more in water at all concentrations. Data represent the mean ± SD (n=3). * indicates $p< 0.05$.

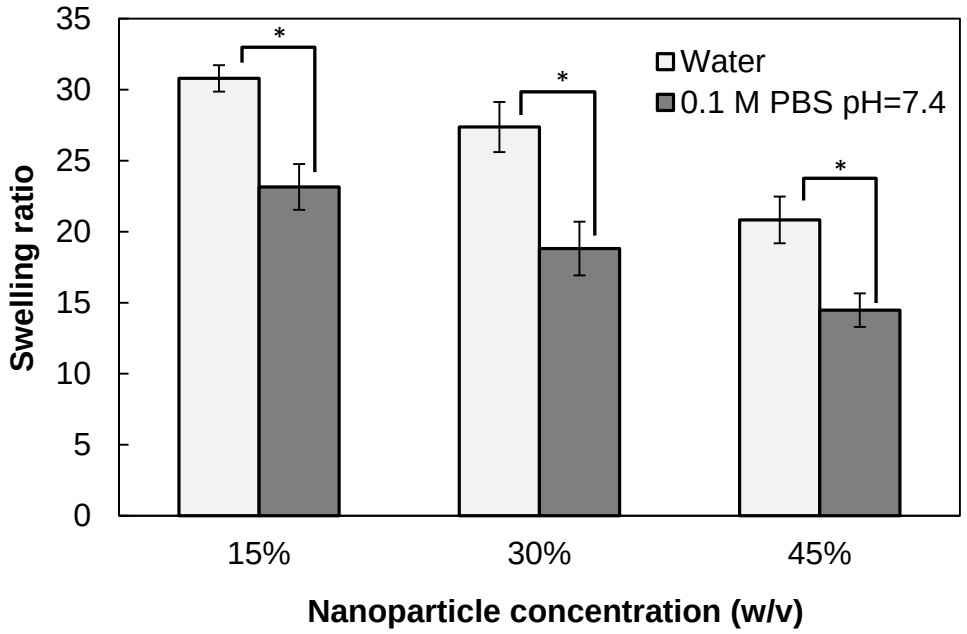

Figure (3-6) Swelling experiment on colloidal gels after 24 hours incubation. Samples with lower nanoparticle concentrations tended to swell more in both water and 0.1 M PBS. Samples tended to swell more in water at all concentrations. Swelling ratios were higher after 24 hours incubation than swelling ratios after 6 hours incubation. Data represent the mean ± SD (n=3). * indicates $p< 0.05$.

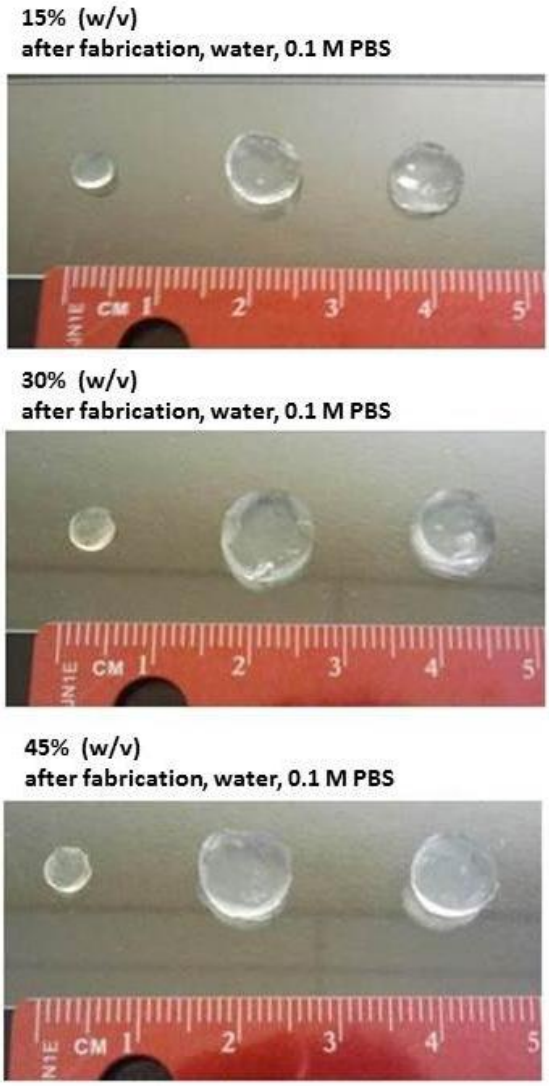

Figure (3-7) Samples after fabrication, swollen in deionized water, and in 0.1 M PBS.

3.3.4. Compression testing and mechanical analysis

Uniaxial compression testing was performed on colloidal gels at 15%, 30%, and 45% w/v nanoparticle concentrations (17 kDa HA) after fabrication, and after swelling in deionized water or 0.1 M PBS. Stress-strain curves collected for colloidal gels after fabrication suggested that the colloidal gels behave as soft materials without a failure point (Figures 3-8). Samples did not even break during compression testing up to 80% strain. After removing the force, samples could recover their initial shape over time (~ 5 minutes) before and after compression testing up to 80% strain (Figure 3-9).

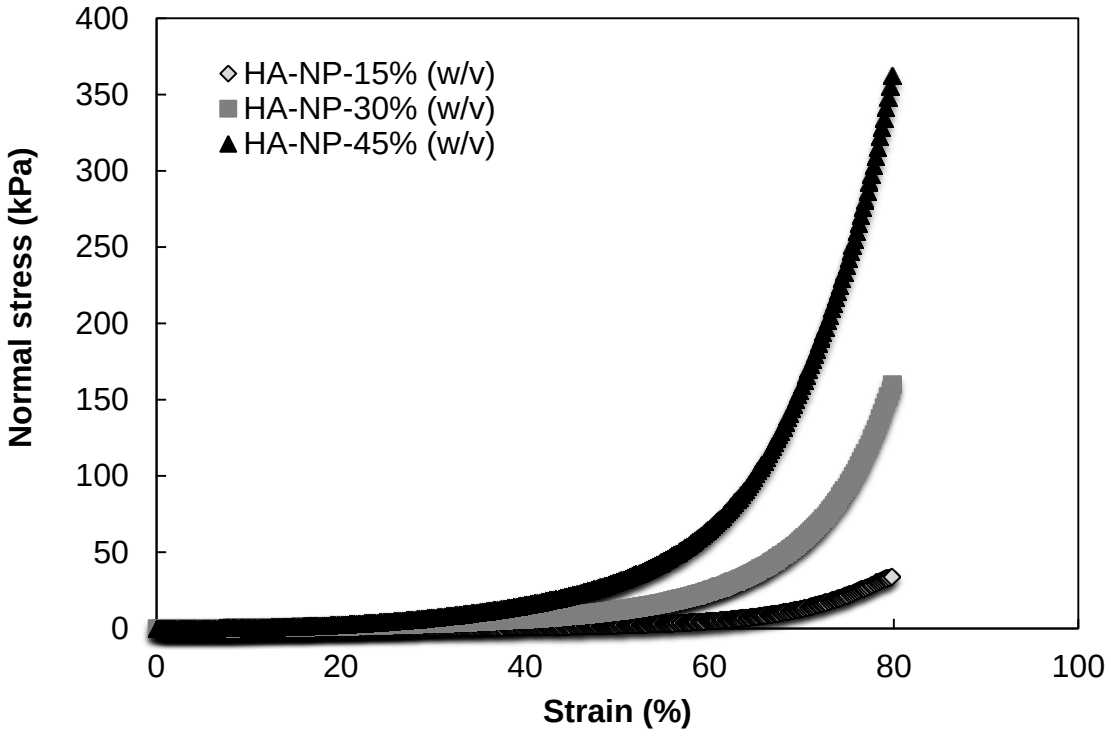

Figure (3-8) Compression testing up to 80% stain on colloidal gels after fabrication. A failure point was not observed.

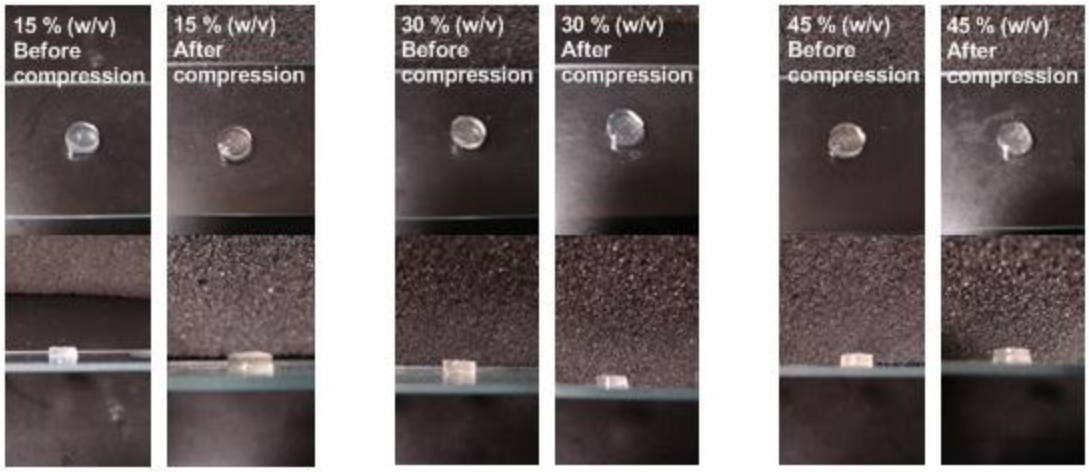

Figure (3-9) Colloidal gels before and after compression testing (80% strain, 0.005 mm/s). After removing the force, samples could recover their initial shape over time (~ 5 minutes).

In addition, stress-strain curves were collected for the samples swollen for 24 hours in deionized water (Figure 3-10). Samples at different nanoparticle concentrations broke with different stress and strain values (Table 3-1). Increasing nanoparticle concentration increased the slope of the curves indicating stiffer materials (higher E) (Figure 3-10 and Figure 3-12). Similar behavior was also observed for the samples swollen in 0.1 M PBS. Swollen samples failed at different stress strain values depending on the nanoparticle concentration (Table 3-1). Increasing nanoparticle concentration increased the stiffness (the slope of stress-strain curves, E) of the samples (Figure 3-11).

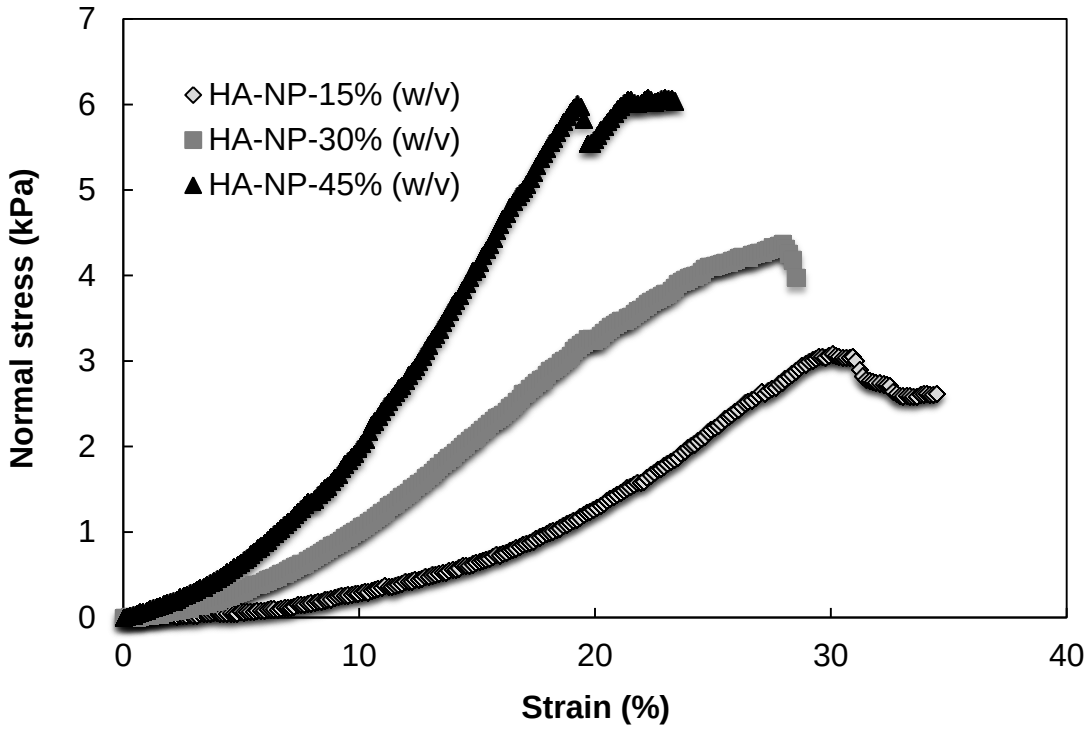

Figure (3-10) Uniaxial compression testing of colloidal gels after swelling in deionized water.

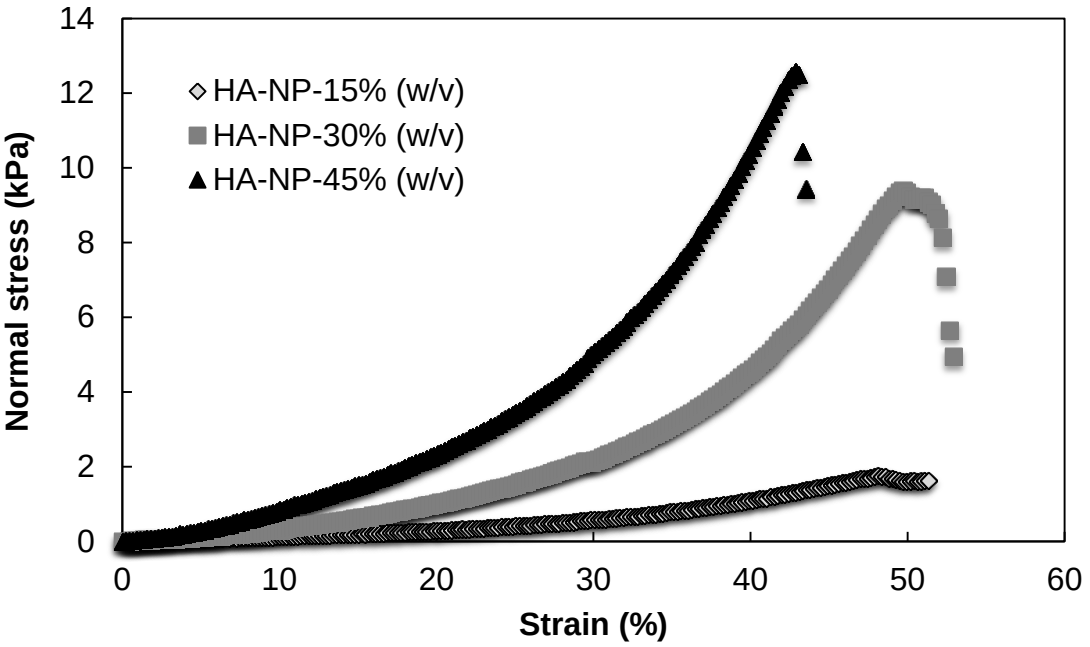

Figure (3-11) Uniaxial compression testing of colloidal gels after swelling in 0.1 M PBS.

Young's modulus (E) is defined as the initial slope of stress-strain curves indicating the stiffness of material. Young's modulus of colloidal gels was determined at different conditions (Figure 3-12). Increasing nanoparticle concentration increased Young's modulus. This increase was greater for the samples swollen in deionized water. Moreover, samples swollen in deionized water had the highest Young's modulus. Perhaps due to the decrease in chain entanglement in 0.1 M PBS due to ionic strength (15).

In addition, the Young's modulus of colloidal gel samples at 15%, 30% and 45% w/v were statistically different (Figure 3-12). Increasing nanoparticle concentration significantly increased the Young's modulus of the samples swollen in deionized water and 0.1 M PBS. Based on these results, Young's modulus is a concentration dependent factor of HA colloidal gels and that may be influenced by the environment of the samples (Figure 3-12).

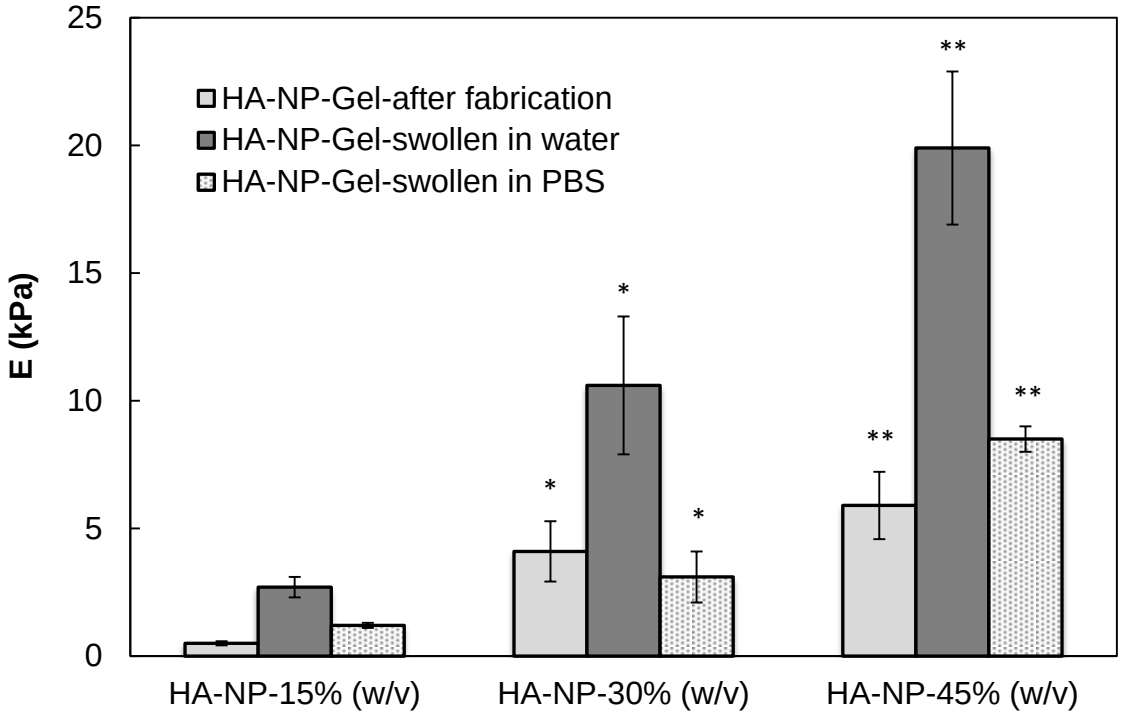

Figure (3-12) Calculated Young's modulus for colloidal gels at different conditions (after fabrication, swollen in deionized water, or swollen in 0.1 M PBS). Increasing nanoparticle concentration increased Young's modulus. Samples swollen in water had the highest modulus. Data represent the mean ± SD (n=3). * and ** $p<0.05$ as compared to HA-NP-15% w/v.

Based on the neo-Hookean model, the initial slope of the stress versus stain function curve (where the curve is linear) is identified as the shear modulus (G), the rigidity of material (9). The shear modulus of colloidal gels was determined at different conditions (Figure 3-13). Increasing nanoparticle concentration increased the shear modulus for all conditions; however, this increase was more pronounced in the samples after fabrication. Similar to Young's modulus, nanoparticle concentration and salt content influenced the shear modulus.

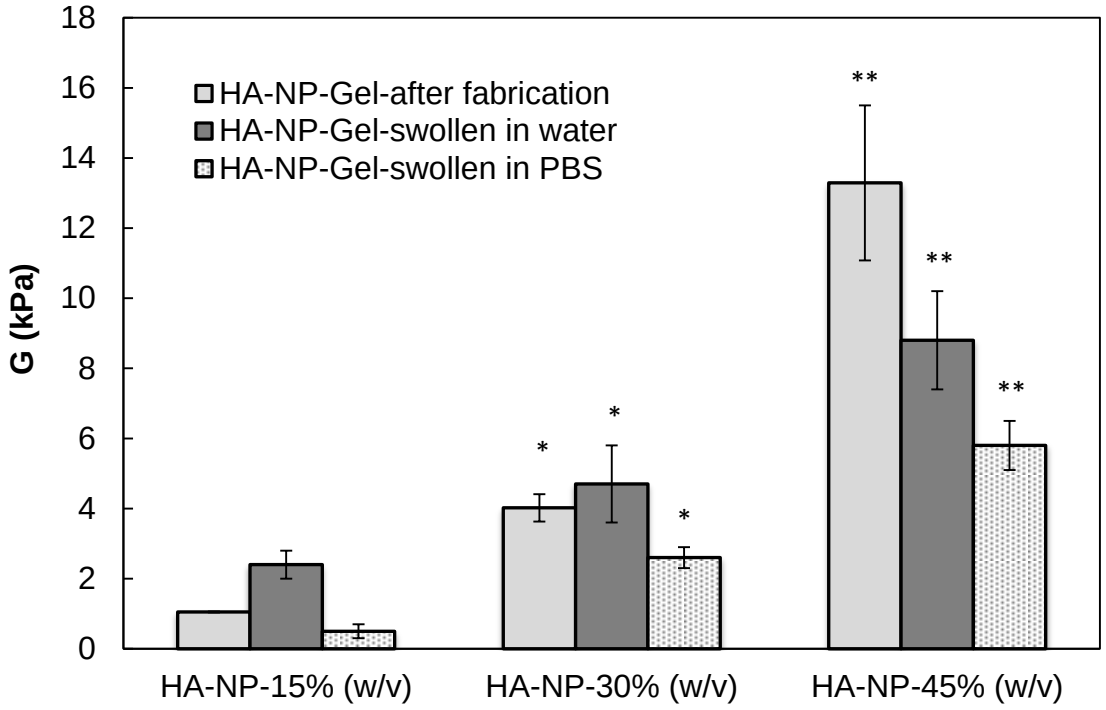

Figure (3-13) Calculated shear modulus for colloidal gels at different conditions (after fabrication, swollen in deionized water, or swollen in 0.1 M PBS). Increasing nanoparticle concentration increased shear modulus. Data represent the mean ± SD (n=3). * and ** p<0.05 as compared to HA-NP-15% w/v.

For incompressible materials (ideal elastomers) such as hydrogels, E was reported to be approximately equal to 3G ($E = 2(1 + \nu)G$, ν~1/2) (9). E/G values identify the relationship between the stiffness and rigidity of the material and E/G was calculated for colloidal gels at different conditions (Figure 3-14). Obviously, colloidal gels were elastomeric materials but did not behave as an ideal neo-Hookean elastomer. The data suggested that Young's modulus is less than 3G. Increasing nanoparticle concentration from 15% to 30% w/v increased E/G for the samples swollen in deionized water. In contrast, increasing nanoparticle concentration decreased E/G values for the samples

swollen in 0.1 M PBS at similar concentrations. The influence of nanoparticle concentration on E/G did not follow a similar pattern for all sample conditions.

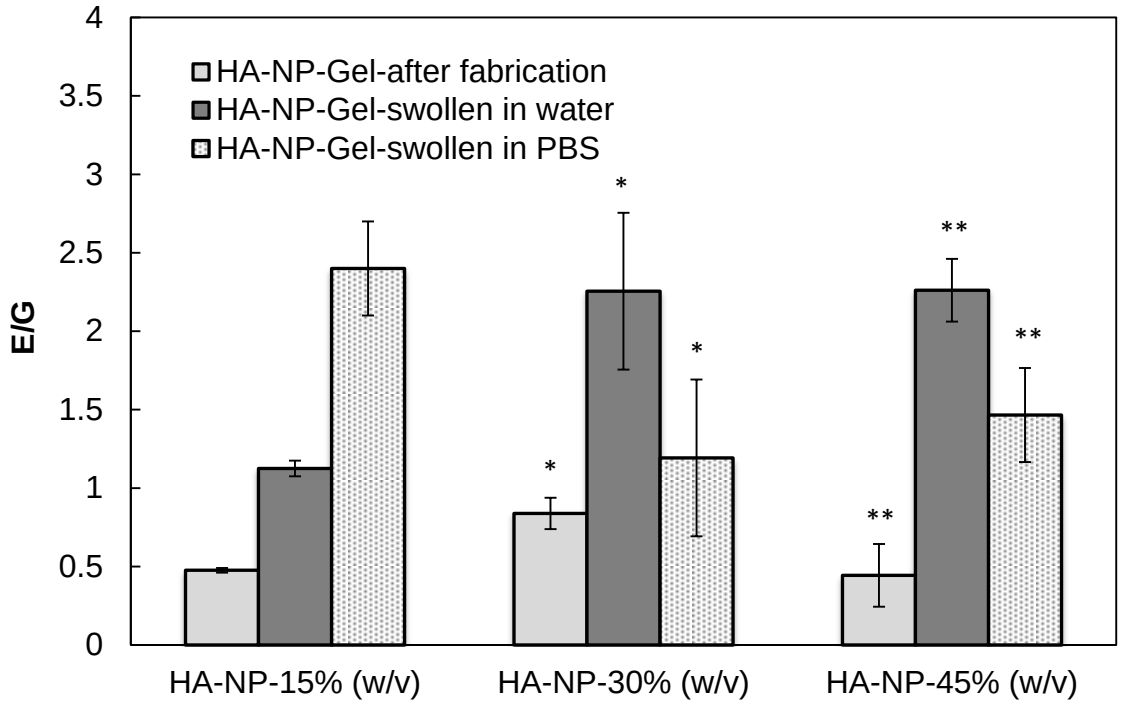

Figure (3-14) Calculated E/G for colloidal gel samples at different nanoparticle concentrations (after fabrication, swollen in deionized water, or swollen in 0.1 M PBS). Data represent the mean ± SD (n=3). * and ** $p<0.05$ as compared to HA-NP-15% w/v.

Compressive failure properties were determined for samples swollen in deionized water or 0.1 M PBS (Table 3-1). Failure strain of samples swollen in water was significantly lower than the failure strain of samples swollen in 0.1 M PBS at all nanoparticle concentrations. Increasing nanoparticle concentration, increased stress failure and toughness for samples swollen in deionized water or in 0.1 M PBS. The toughness of samples swollen in deionized water was statistically different from the toughness of samples swollen in 0.1 M PBS at all concentrations (Table 3-1). It could be

concluded that the increase of failure stress and toughness might be due to greater physical entanglement between nanoparticles at higher nanoparticle concentrations.

Table (3-1) Compressive failure properties of colloidal gels swollen in deionized water or 0.1 M PBS. Data represent the mean ± SD (n=3).

Gel formulation	Compressive failure properties					
	Swollen in water			Swollen in 0.1M PBS		
	Strain (%)	Stress (kPa)	Toughness (kJ/m^3)	Strain (%)	Stress (kPa)	Toughness (kJ/m^3)
HA-NP 15% (w/v)	30±2.1	3±0.16	0.3±0.032	53±3.4	1±0.7	0.5±0.082
HA-NP 30% (w/v)	26±3.4	5±1.6*	0.6±0.183	60±1.5	10±0.24	2.7±0.365*
HA-NP 45% (w/v)	21±1.4**	6±2.5**	0.6±0.234	48±2.6	16±4.6	3.3±0.667**

* and ** $p<0.05$ comparing to HA-NP 15% w/v.

3.3.5. Effect of pH and ionic strength on mechanical properties of HA colloidal gel

The stress-strain curves were determined for samples at 15% w/v nanoparticle concentration and different pH values (17 kDa HA) (Figure 3-15). Increasing pH influenced the behavior of material as was observed from the calculated Young's modulus and shear modulus which showed that the material become softer at higher pH values. Increasing pH at 150 mM salt concentration decreased both Young's modulus and shear modulus; however, this decrease was not significant for all the samples. Increasing pH can reduce the hydrodynamic radius of HA (15). Therefore, the physical entanglement between nanoparticles may decrease at higher pH values resulting in formation of softer materials. The highest values for Young's modulus and shear modulus occurred at pH=6.0 (Figure 3-16).

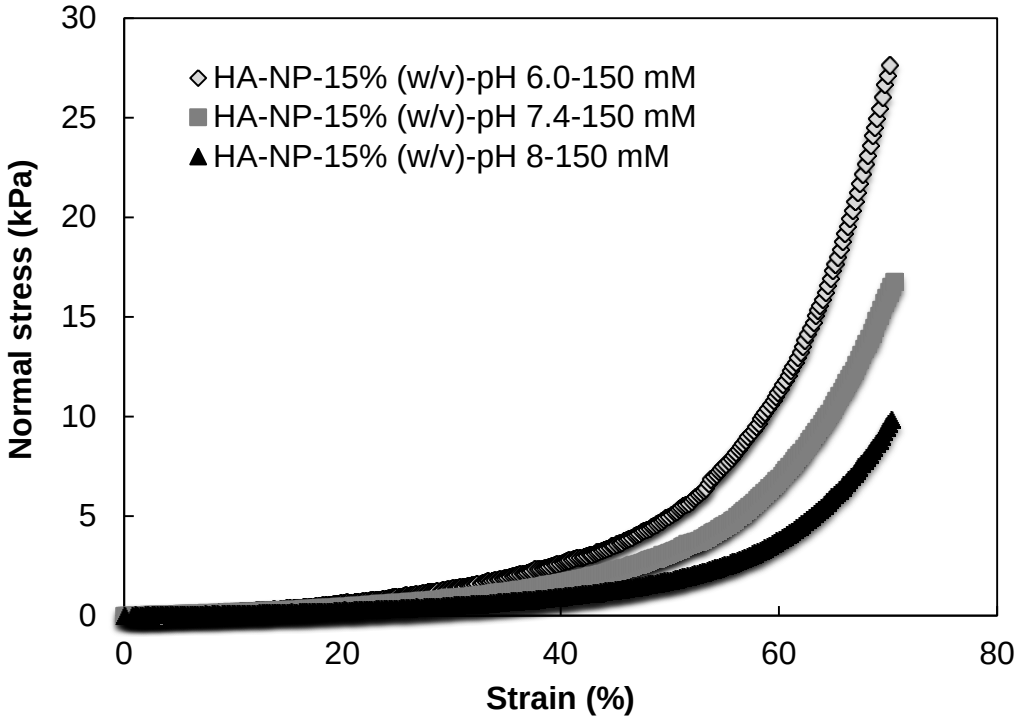

Figure (3-15) Compression testing up to 70% stain on colloidal gels after fabrication in phosphate buffer solutions at different pH values (6.0, 7.4, and 8) and constant ionic strength (150 mM). A failure point was not observed for the samples.

-

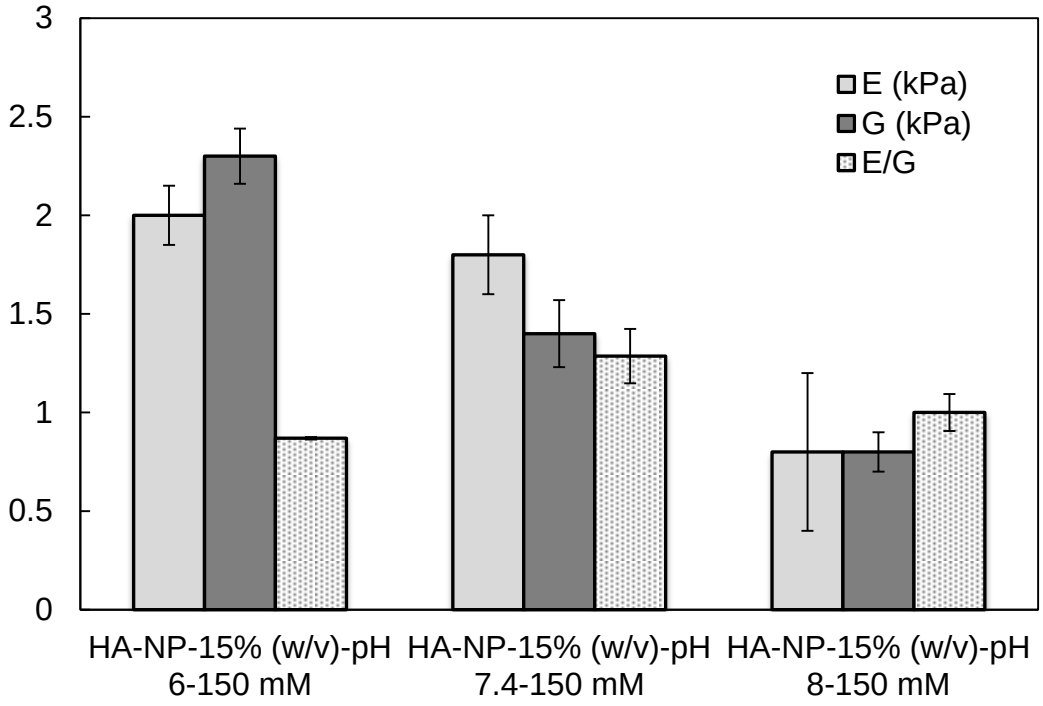

Figure (3-16) Calculated Young's modulus, shear modulus, and E/G for colloidal gels at different pH values and constant ionic strength (150 mM). Increasing pH decreased Young's modulus and shear modulus. Data represent the mean ± SD (n=3).

Changing the salt concentration at a constant pH of 7.4 also affected the mechanical properties of colloidal gels at 15% w/v nanoparticle concentration (17 kDa HA). Increasing salt concentration made colloidal gels softer (Figure 3-17). Young's modulus and shear modulus appeared greater at lower salt concentrations; however, the results were not statistically significant (Figure 3-18). The presence of salt in the formulations can influence the structure and reduce HA hydrodynamic radius (15). Therefore, this effect may also decrease physical entanglement between nanoparticles leading to a softer material (Figure 3-18).

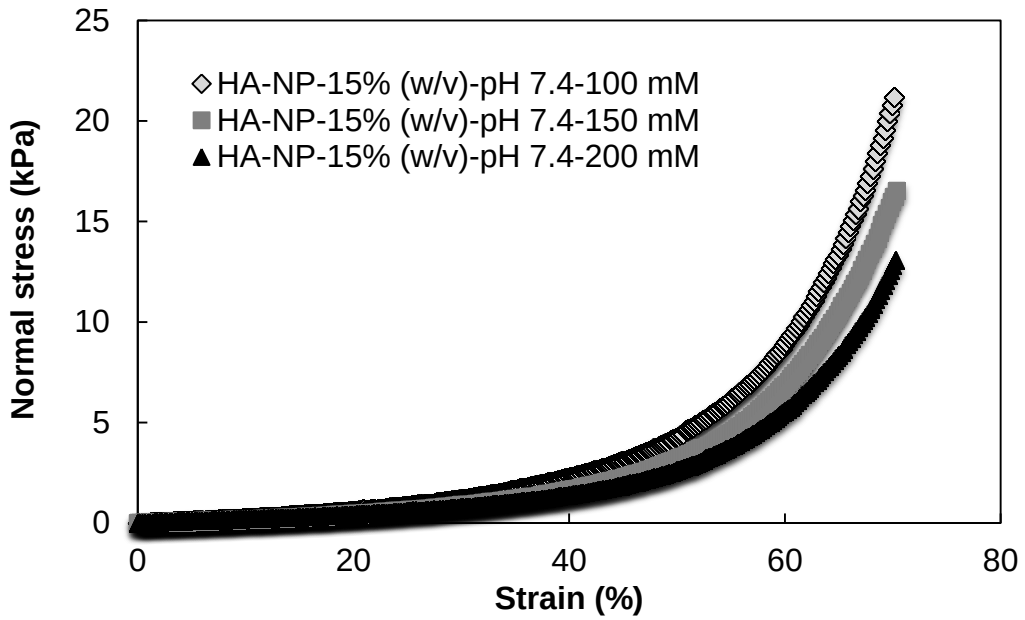

Figure (3-17) Compression testing up to 70% stain on colloidal gels in phosphate buffer solutions at different ionic strength values (100, 150, and 200 mM) and a pH of 7.4. A failure point was not observed for the samples.

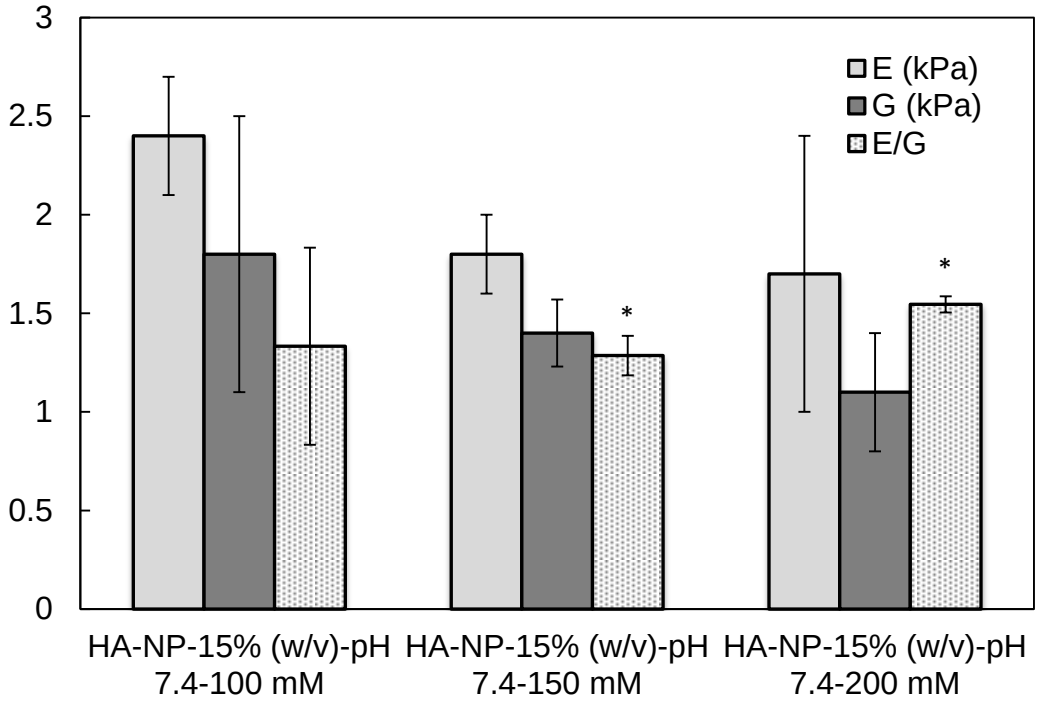

Figure (3-18) Calculated Young's modulus, shear modulus, and E/G for colloidal gels at different ionic strength values and constant pH of 7.4. Data represent the mean ± SD (n=3). * p<0.05 comparing to HA-NP-15% w/v-pH 7.4-100 mM.

3.3.6. Viscoelasticity of HA colloidal gel after fabrication

Viscoelastic properties were evaluated for HA colloidal gels using different nanoparticle concentrations. Nanoparticles made from 17 kDa HA were used to make colloidal gels at 5%, 15%, 30%, and 45% w/v. 17 kDa HA polymer at 45% w/v in deionized water was also used as a control. The changing elastic modulus (G') of colloidal gels was determined over a frequency range of 0.1-10 Hz (Figure 3-19). Increasing nanoparticle concentration increased the elastic modulus of colloidal gels. Samples at 5% w/v nanoparticle concentration had a similar elastic modulus compared to the 45% polymer solution. The elastic modulus of other colloidal samples was greater than the control.

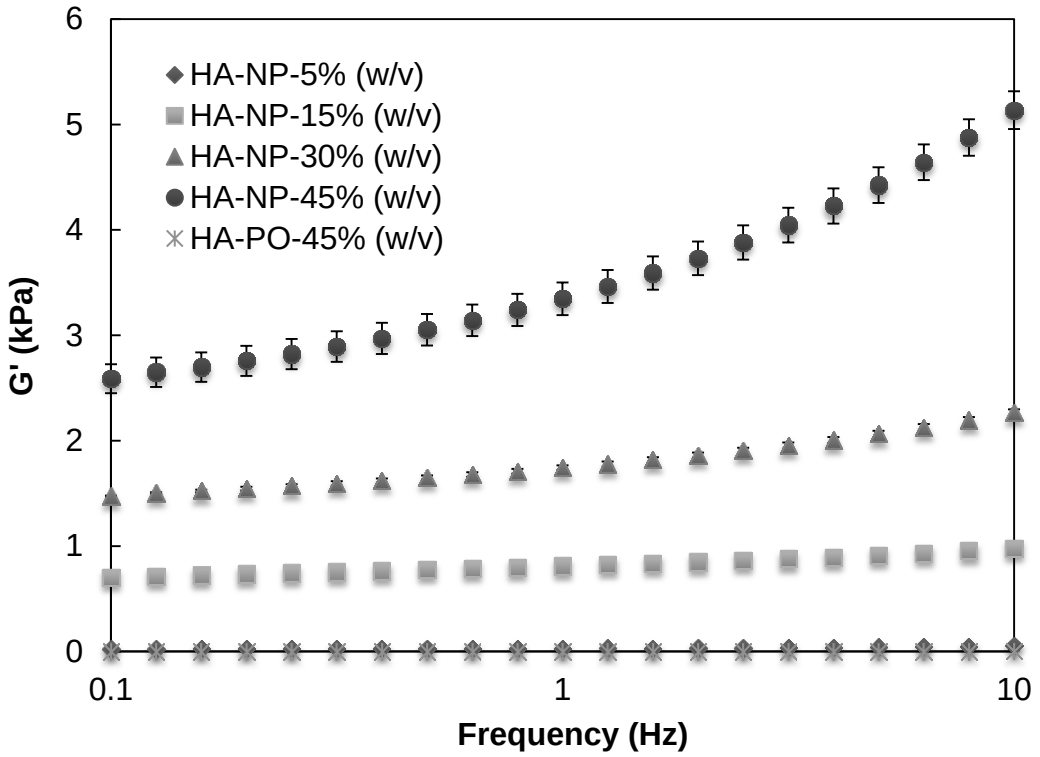

Figure (3-19) Viscoelasticity of colloidal gels: elastic modulus over frequency range. Increasing nanoparticle concentration increased elastic modulus. Data represent the mean ± SD (n=3).

Increasing nanoparticle concentration also increased the viscous modulus (G") of colloidal gels (Figure 3-20). Samples at 5% w/v nanoparticle concentration showed a similar viscous modulus compared to the 45% polymer solution. The viscous modulus of the other colloidal samples was greater than the control.

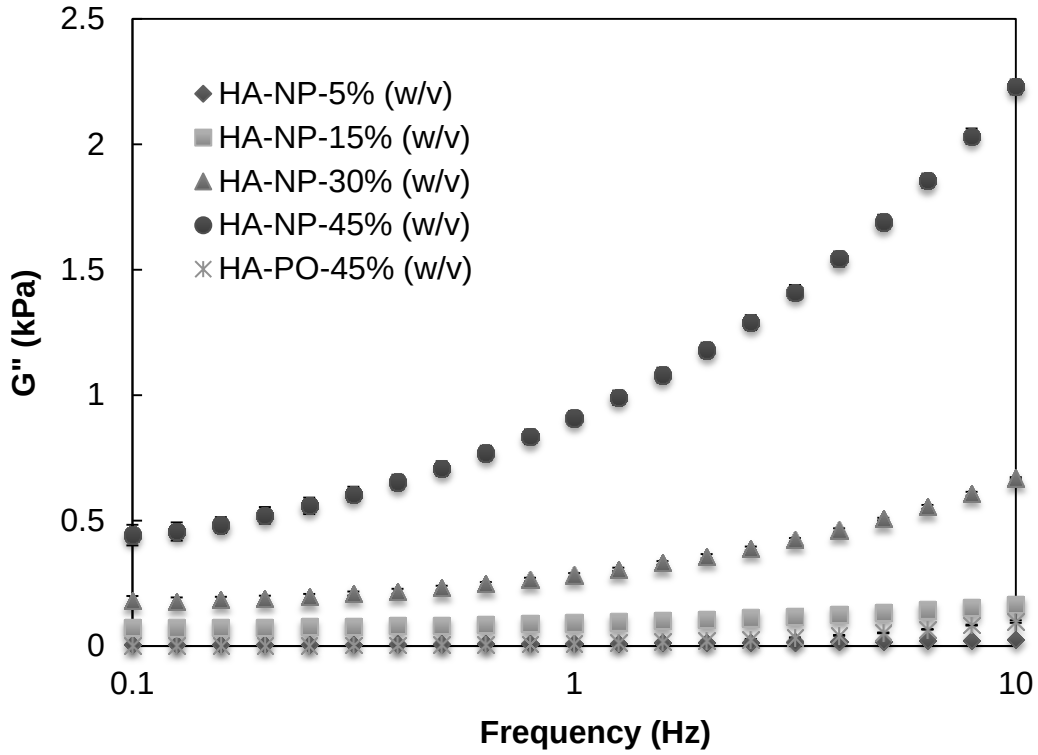

Figure (3-20) Viscoelasticity of colloidal gels: viscous modulus over frequency range. Increasing nanoparticle concentration increased viscous modulus. Data represent the mean ± SD (n=3).

The calculated complex modulus (G*) showed behavior similar to the elastic and loss moduli over frequency range (Figure 3-21). Samples at 5% w/v nanoparticle concentration had a similar complex modulus compared to 45% polymer solution.

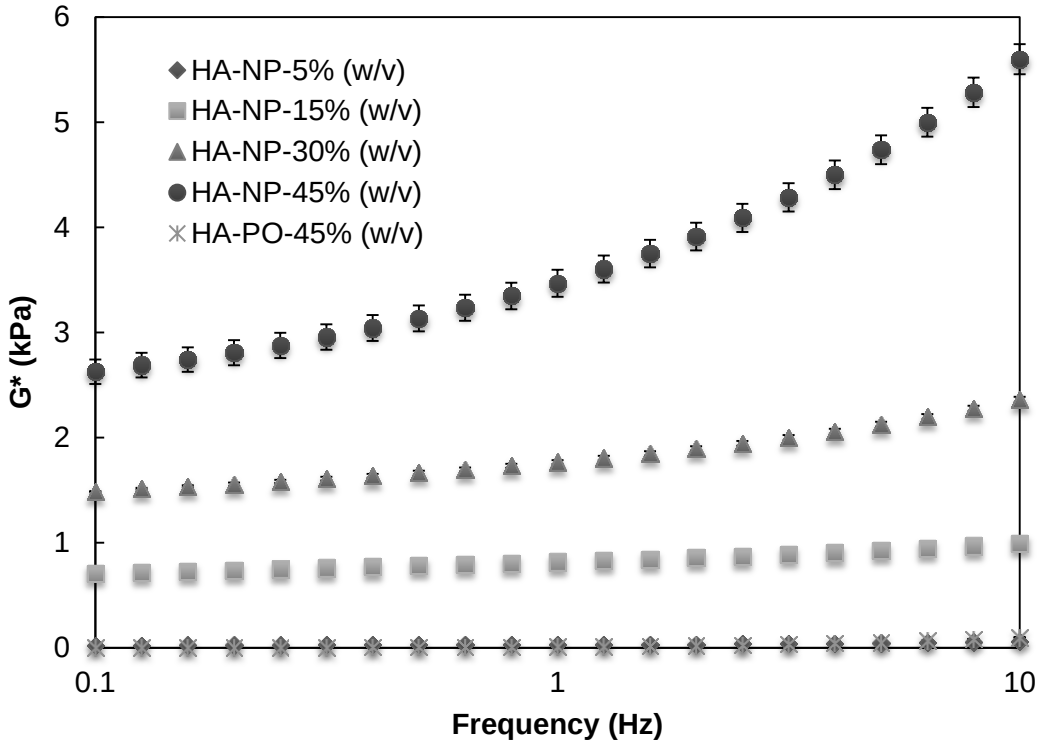

Figure (3-21) Viscoelasticity of colloidal gels: complex modulus over frequency range. Increasing nanoparticle concentration increased complex modulus. Data represent the mean ± SD (n=3).

Excluding data for the sample at 5% w/v concentration, tan delta was also increased by increasing the concentration of nanoparticles (Figure 3-22). Since a stable 3-D structure was not formed at 5% w/v, the calculated tan delta for this sample showed a different behavior compared to the rest of the samples.

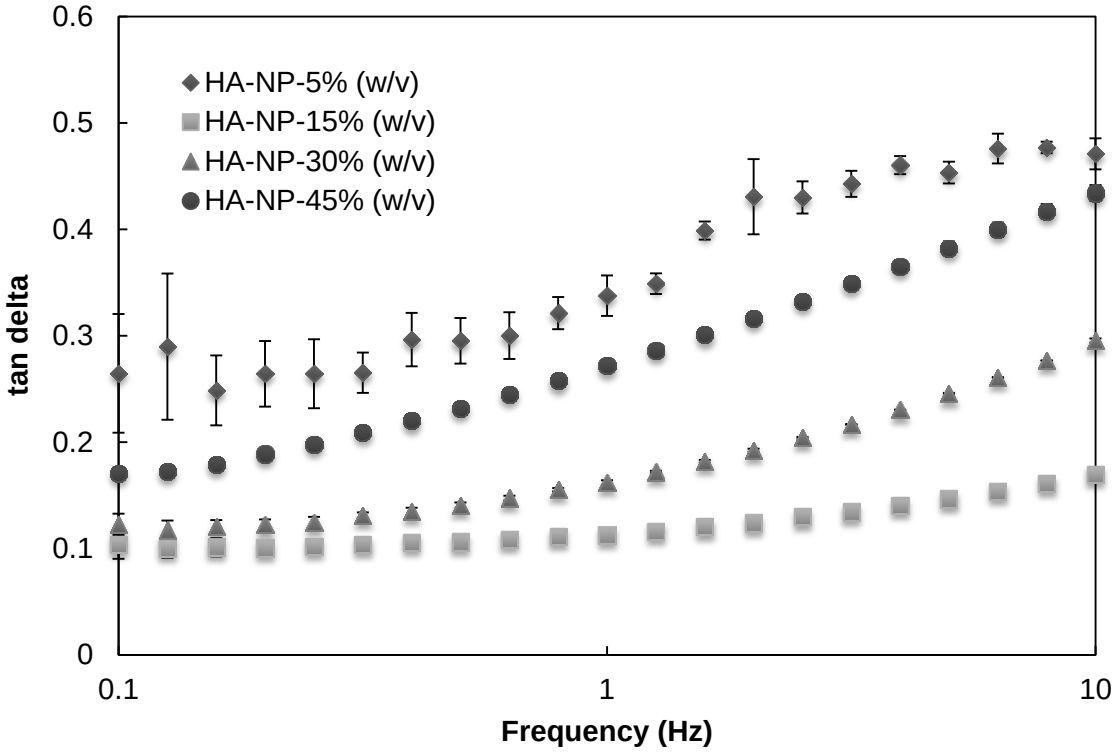

Figure (3-22) Viscoelasticity of colloidal gels: tan delta over frequency range. Data represent the mean ± SD (n=3).

3.3.7. Viscosity of HA colloidal gel

The viscosity of colloidal gels was measured at different nanoparticle concentrations in deionized water (Figure 3-23). Changes in viscosity over shear rate sweep are also presented (Figure 3-24). The 17 kDa HA polymer solution at 45% w/v concentration was used as a control to compare the behavior of colloidal gels with polymer solution.

Results showed that samples at 5% w/v behaved similar to the control since a colloidal gel network did not form at that concentration. By increasing nanoparticle concentration up to 15% w/v and higher, the behavior of the samples changed. A yield point was observed for the samples at 15%, 30%, and 45% w/v concentrations. In

addition to that, increasing nanoparticle concentration increased shear stress and viscosity of the samples. At lower shear rates, the viscosity of samples increased to a maximum (yield point) and then dropped by increasing shear rate. This yield point correlated to the yield stress point on shear stress-shear rate curves. Increases in the viscosity and shear stress up to the yield point might be due to the interlocking of dangling chains available on the surface of nanoparticles (Figure 3-24). After the yield point, nanoparticles may thus lower the shear stress and viscosity at higher shear rates. The colloidal gels shear thinned after the yield point, which indicated a "pseudo-plastic" material (Figure 3-24).

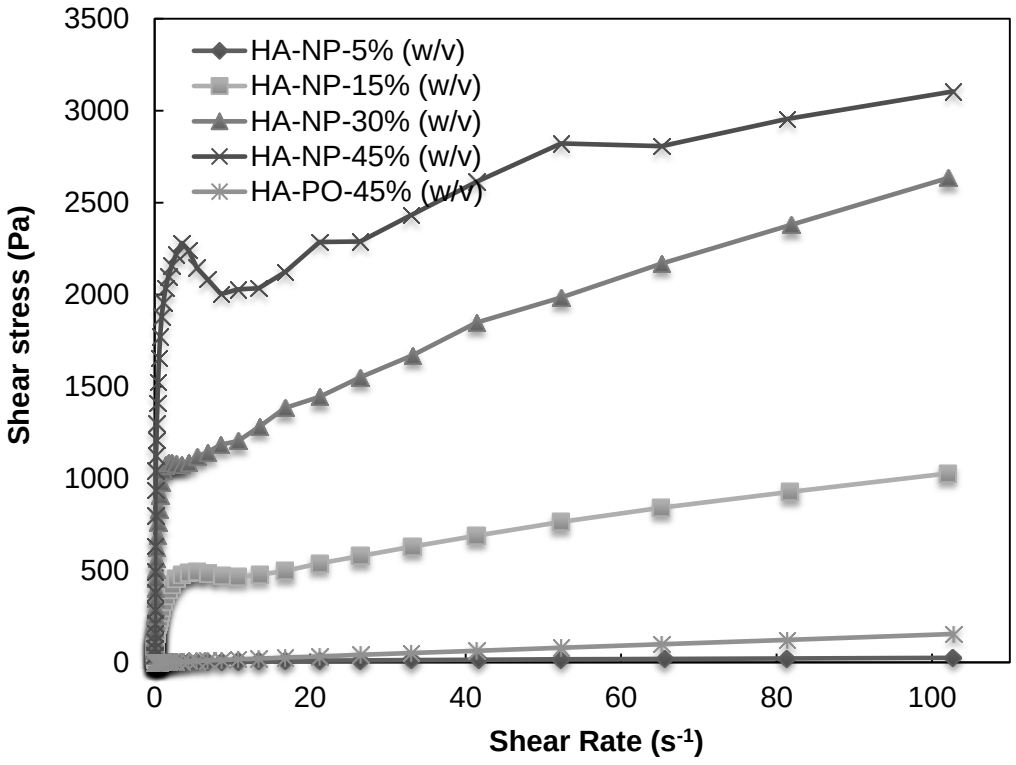

Figure (3-23) Rheological evaluation of HA-NP (17 kDa) for nanoparticles in deionized water. Increasing nanoparticle concentration increased shear stress.

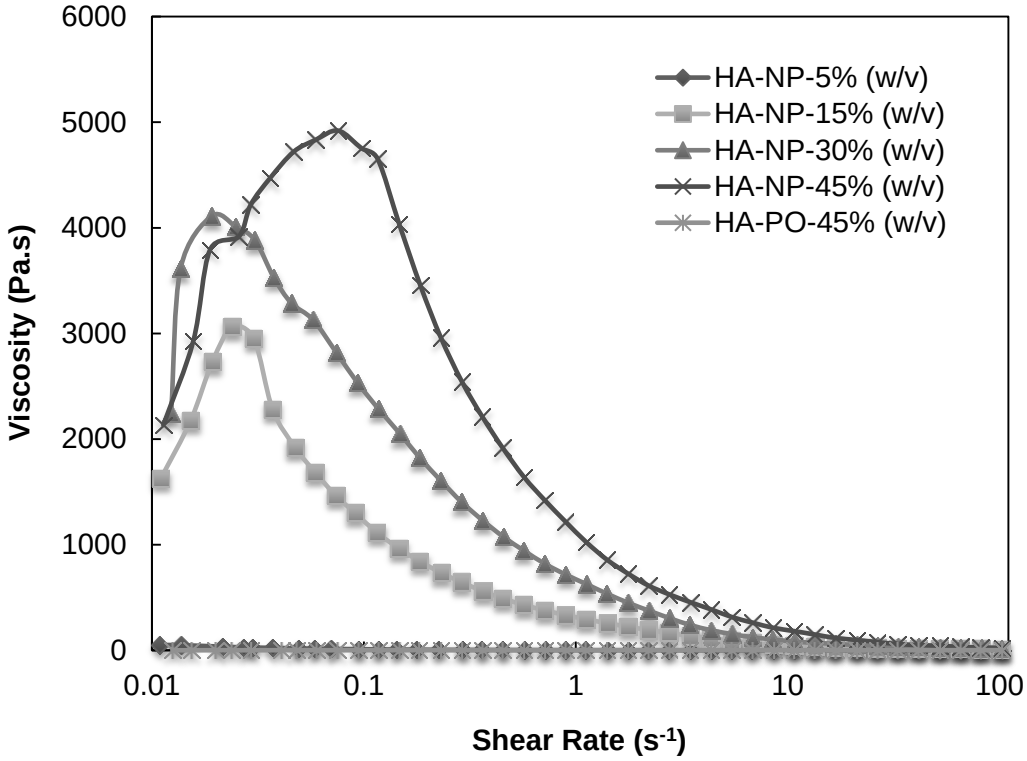

Figure (3-24) Rheological evaluation of HA-NP (17 kDa) for nanoparticles in deionized water. Increasing nanoparticle concentration increased viscosity.

3.3.8. HA colloidal gel recovery

3.3.8.1. Mechanical dynamics and recovery

Recovery of colloidal gels at 15%, 30%, and 45% w/v nanoparticle concentrations (17 kDa HA) tested after fabrication and after swelling in 0.1 M PBS. Representative stress-gap curves were collected for all the tested formulations (Figure 3-25). Results suggested that after the first cycle of compression/decompression, the height of the samples recovered back to the initial height. This might be due to the structural properties of the colloidal gel samples including chemical crosslinking in the nanoparticles, physical entanglement between nanoparticles, and the nature of HA itself. Mechanical dynamics and recovery did not depend on nanoparticle concentration.

Moreover, similar recovery behavior was observed for both conditions (after fabrication and after swelling samples in 0.1 M PBS). Due to the failure of samples swollen in deionized water at strains less than 30%, mechanical recovery experiments were not performed on these samples.

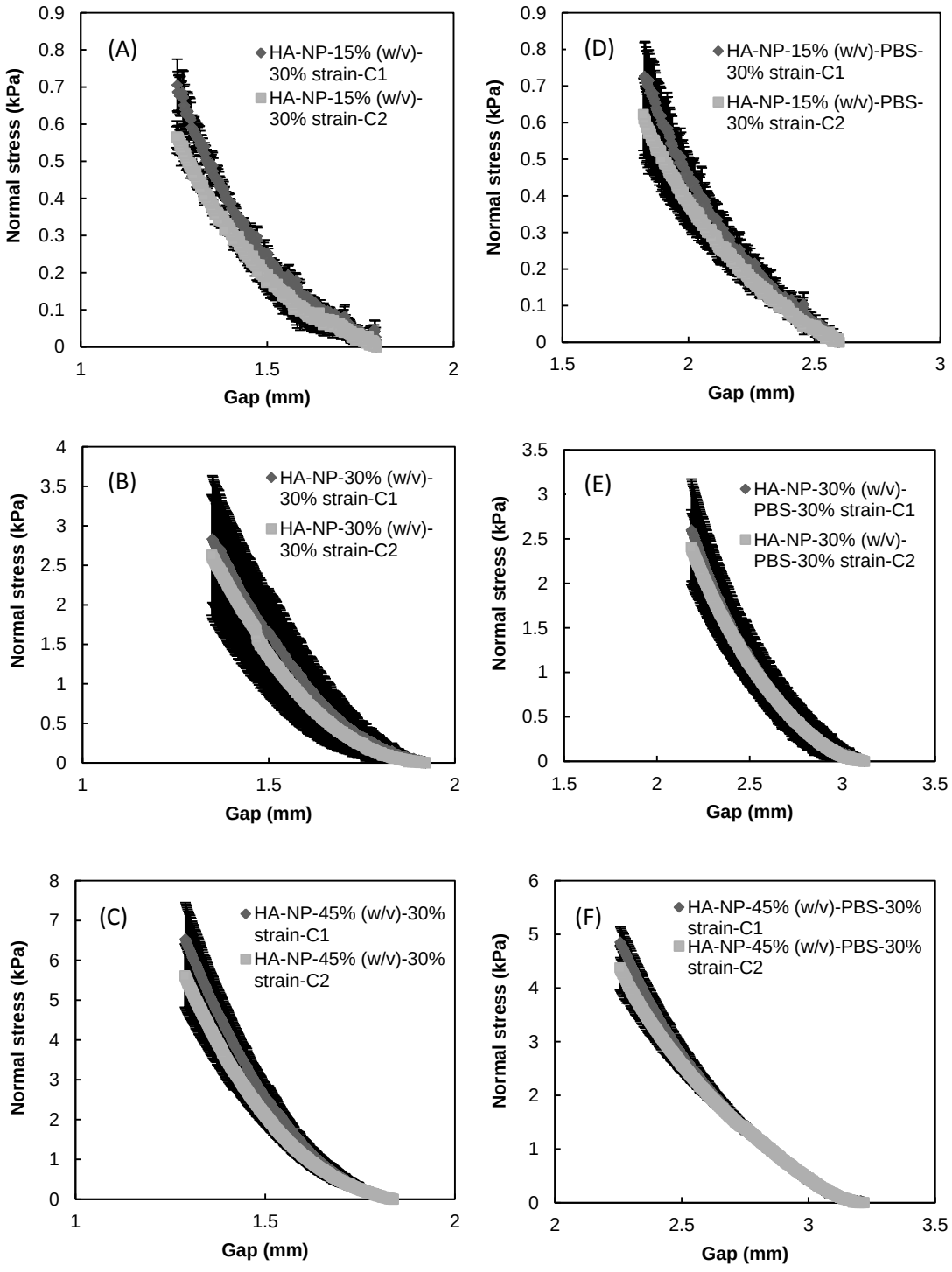

Figure (3-25) The recovery of colloidal gels (15%, 30%, and 45% w/v) after fabrication (A, B , and C) and swollen in 0.1 M PBS (D, E, and F) was determined by applying two compression\decompression cycles with 5 minutes delay time between cycles. Data represent the mean ± SD (n=3): C1: 30% strain, 0.005 mm/s. C2: 30% strain, 0.001 mm/s. Five preconditioning cycles were also applied before the recovery experiment at 6% strain, 0.005 mm/s.

3.3.8.2. Rheological recovery

The rheological recovery of samples at 15% w/v nanoparticle concentration was also evaluated after colloidal gel fabrication (Figure 3-26 and Figure 3-27). The viscosity of the colloidal gels was recoverable after applying shear stress to the samples. These results suggested that surface chains could re-associate after disruption by shear force. After applying shear force, samples still had similar rheological behavior compared to the initial material which suggests recovery of the colloidal gel network after applying shear. Studies have shown a reduction in the viscosity of HA solutions after applying shear stress and HA has been found to degrade under shear (15, 20-22). The slight drop in viscosity after the first sweep might be due to the degradation of HA or an insufficient delay between each run. The drop in viscosity was less after the second run (Figure 3-27).

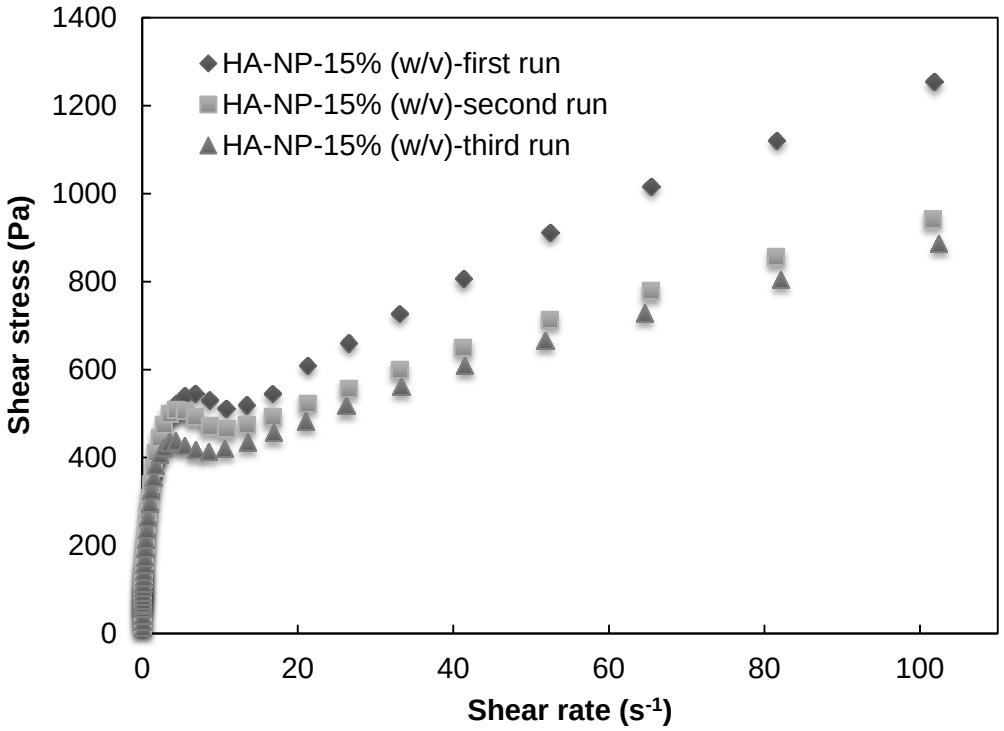

Figure (3-26) Colloidal gel recovery based on rheology. After applying shear stress to the sample (15% w/v nanoparticle concentration), shear recovery was observed after a one minute delay between cycles.

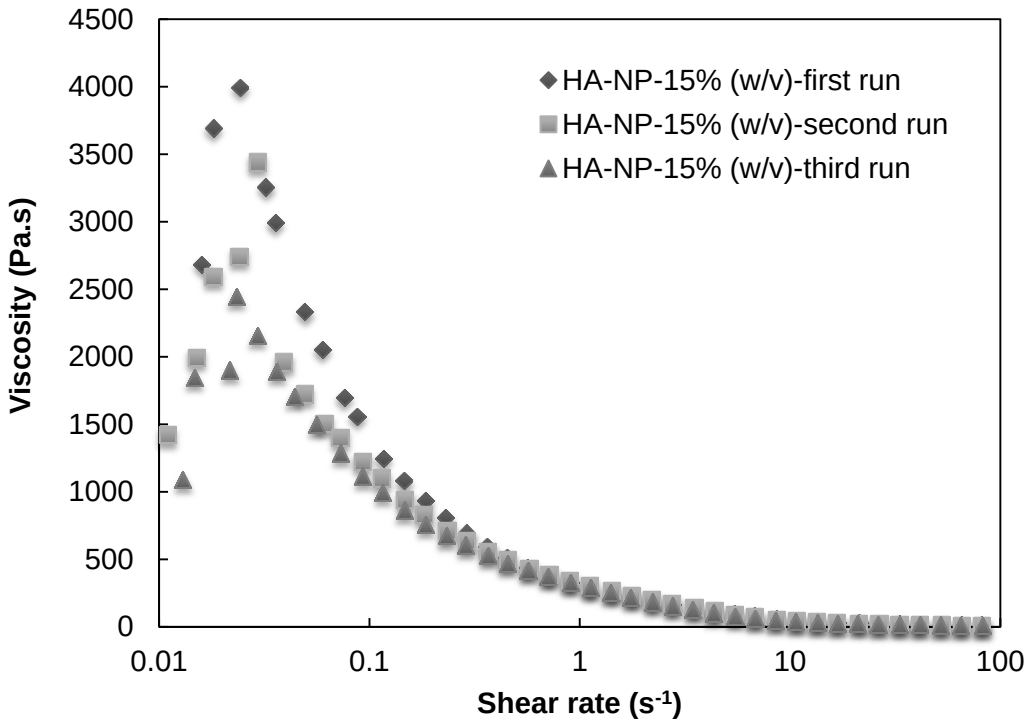

Figure (3-27) Colloidal gel recovery based on rheology. After applying shear stress to the sample (15% w/v nanoparticle concentration), shear recovery was observed after a one minute delay between cycles.

3.3.8.3. Physical recovery

Colloidal gels at 30% w/v nanoparticle concentration (17 kDa HA) formed a network after fabrication and after swelling in deionized water. The steps for performing this recovery experiment are shown in Figure 3-28. First, nanoparticles made from 17 kDa HA were used to make the colloidal gel at 30% w/v concentration. The colloidal gel was then swollen and equilibrated in deionized water for at least 24 hours. After swelling the sample, the colloidal gel was completely crushed. Then, the sample was transferred to a desiccator chamber and left to dry for at least 48 hours. Finally, the dried sample was again used to form a colloidal gel network at 30% w/v nanoparticle concentration in deionized water. A colloidal gel was again formed from the dried sample. These data

suggested that dangling chains available on nanoparticles could entangle with each other even after colloidal gel destruction.

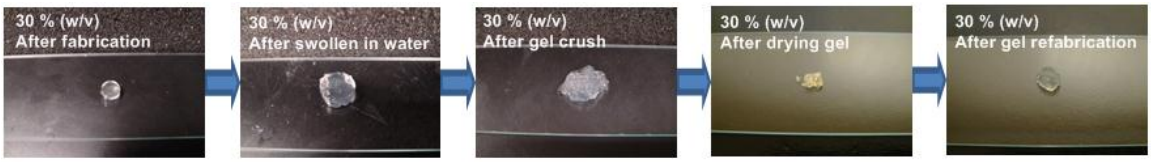

Figure (3-28) Physical recovery tests suggested that the colloidal gel networks could be reformed from destroyed colloidal gels.

3.4. Discussion

Colloidal gel networks were formed by addition of HA nanoparticles in deionized water. The type of polymer, molecular weight of polymer, and nanoparticle concentration significantly influenced nanoparticle-nanoparticle interactions and colloidal gel formation. Stable 3-D colloidal gel networks formed at 15%, 30%, and 45% concentrations when using nanoparticles fabricated with 17 kDa HA. At these concentrations, physical entanglement between 17 kDa HA nanoparticles with 'hairy' structure might be the reason for colloidal gel formation. After mixing nanoparticles with deionized water, dangling chains on the nanoparticles might entangle and interlock resulting in formation of stable colloidal gels. Colloidal gels did not form at 5% w/v when 17 kDa HA nanoparticles were used. This was likely due to insufficient nanoparticle concentration to achieve physical entanglement. On the other hand, HA nanoparticles made from 1500 kDa HA could not form colloidal gel networks even at high concentration probably due to the limited availability of dangling chains on these nanoparticles. Also, CS nanoparticles could not form colloidal gel networks probably due

to the nature of CS and the absence of physical entanglement or ‘self-association’ in this highly charged GAG.

Swelling experiments suggested that colloidal gel networks were stable upon dilution in an excess of deionized water and in 0.1 M PBS. The results also indicated that the swelling ratio was dependent on nanoparticle concentration and the nature of the swelling solution. Increasing nanoparticle concentration may increase physical entanglement between nanoparticles reducing the swelling ratio. Moreover, the presence of salt in swelling solution is known to reduce hydrodynamic radius of HA and physical entanglement. As a result, the swelling ratio of the samples in 0.1 M PBS was lower than the swelling ratio of the samples in deionized water. A comparison of HA colloidal gels and classic HA hydrogels including HA crosslinked via divinyl sulfone (DVS), photocrosslinked methacrylated HA, dual-crosslinked HA (photo crosslinked and chemically crosslinked), and HA via crosslinked disulfide bond formation, showed that the swelling ratio of the colloidal gels was in the range of a maximum swelling ratio of classic gels (i.e. a low degree of crosslinking) (10, 23-26).

In addition, compression testing also suggested that the mechanical properties of colloidal gels (Young’s and shear moduli) were influenced by nanoparticle concentration and sample condition. Increasing nanoparticle concentration made colloidal gels stiffer. Moreover, samples swollen in deionized water had greater Young’s modulus compared to the samples after fabrication or to samples swollen in 0.1 M PBS. These behaviors may also hinge on the physical entanglement between nanoparticles which was influenced by nanoparticle concentration and sample condition. In addition, compression testing indicated that colloidal gels behaved as a softer material compared to classic HA

hydrogels. Maximum Young's and shear moduli of the colloidal gels reached approximately 20 kPa; however, normal Young's and shear moduli values for HA crosslinked with DVS were in the range of several thousand kPa (23, 26). Comparing the shear modulus of colloidal gels with photocrosslinked methacrylated HA (20<G<60 kPa) also showed that the colloidal gels had softer mechanical properties (24). Only the initial portion of strain-stress curves, where the stress-strain function curves were linear, was used to calculate the mechanical properties of colloidal gels, where was though the colloidal gels have ideal elastic behavior. The compression testing data (E/G values) showed that the colloidal gels were elastomeric materials but did not behave as an ideal neo-Hookean elastomer.

In other studies, nanoparticle concentration had an important effect on rheological behavior of colloidal gels. Increasing nanoparticle concentration increased elastic modulus, viscous modulus, complex modulus, and tan delta of the samples after fabrication. Moreover, viscosity of the samples upon mixing nanoparticles with deionized water increased by increasing nanoparticle concentration. The shear stress and viscosity of the colloidal gels increased up to a yield point by increasing the shear rate. After the yield point, viscosity of the samples decreased by increasing the shear rate indicative of shear thinning behavior for the colloidal gels. Viscoelasticity measurements also indicated that colloidal gels had a similar elastic modulus, viscous modulus, and complex modulus compared to a classic hydrogel. Previous viscoelasticity evaluation of HA crosslinked via DVS showed that the elastic and loss moduli were in the range of several hundred to several thousand Pa and the colloidal gels had similar viscoelasticity (23).

Finally, recovery experiments revealed the dynamic properties of colloidal gels. Mechanical experiments suggested that the height of the samples was recoverable to the original height after compressing/decompressing samples independent of nanoparticle concentration. Rheological experiments also showed that the viscosity of the colloidal gels was recoverable after applying shear stress to the samples. These results support the notion that the interrupted physical entanglement between surface chains on nanoparticles could re-associate after removing shear force. A physical recovery experiment showed that destroyed, dried, and reconstituted colloidal gels can still form a colloidal gel network.

3.5. Conclusion

In conclusion, colloidal gel networks were formed by mixing HA nanoparticles in deionized water. The type of polymer, molecular weight of polymer, and nanoparticle concentration significantly influenced nanoparticle-nanoparticle interactions and colloidal gel formation. Stable 3-D colloidal gel networks formed at 15%, 30%, and 45% concentrations when using nanoparticles fabricated with 17 kDa HA due to physical entanglement between nanoparticles. CS nanoparticles and nanoparticles made from 1500 kDa HA could not form colloidal gel networks probably due to limited availability of surface chains to mediate nanoparticle-nanoparticle interactions. Mechanical and rheological experiments showed that Young's modulus, shear modulus, viscosity, and viscoelasticity of colloidal gels were influenced by nanoparticle concentration which might increase the chance of physical entanglement between 'hairy' nanoparticles and media type. These data also showed that the colloidal gels did not behave as an ideal neo-

Hookean elastomer. Finally, recovery experiments confirmed that colloidal gels had dynamic properties. Formation of stable 3-D colloidal gels using HA nanoparticles without any potentially toxic chemical reactions suggests a new approach for scaffold fabrication and tissue regeneration.

3.6. References

1. Wang Q, Wang J, Lu Q, Detamore MS, Berkland C., Injectable PLGA based colloidal gels for zero-order dexamethasone release in cranial defects, Biomaterials, 2010;31(18):4980-6.
2. Wang Q, Wang L, Detamore MS, Berkland C., Biodegradable colloidal gels as moldable tissue engineering scaffolds, Advanced Materials, 2008;20(2):236-9.
3. Kretlow JD, Klouda L, Mikos AG., Injectable matrices and scaffolds for drug delivery in tissue engineering, Advanced drug delivery reviews, 2007;59(4-5):263-73.
4. Yeo Y, Ito T, Bellas E, Highley CB, Marini R, Kohane DS., In situ cross-linkable hyaluronan hydrogels containing polymeric nanoparticles for preventing postsurgical adhesions, Annals of surgery, 2007;245(5):819.
5. Tan H, Marra KG., Injectable, biodegradable hydrogels for tissue engineering applications, Materials, 2010;3(3):1746-67.
6. Gutowska A, Jeong B, Jasionowski M., Injectable gels for tissue engineering, The Anatomical Record, 2001;263(4):342-9.
7. Wang Q, Jamal S, Detamore MS, Berkland C., PLGA chitosan/PLGA alginate nanoparticle blends as biodegradable colloidal gels for seeding human umbilical cord mesenchymal stem cells, Journal of Biomedical Materials Research Part A, 2011.
8. Berkland C, Wang Q., Biodegradable Colloidal Gels as Moldable Tissue Engineering Scaffolds, Google Patents; 2008.
9. DeKosky BJ, Dormer NH, Ingavle GC, Roatch CH, Lomakin J, Detamore MS, et al., Hierarchically designed agarose and poly (ethylene glycol) interpenetrating network hydrogels for cartilage tissue engineering. Tissue Engineering Part C: Methods, 2010;16(6):1533-42.
10. Zawko SA, Suri S, Truong Q, Schmidt CE., Photopatterned anisotropic swelling of dual-crosslinked hyaluronic acid hydrogels, Acta Biomaterialia, 2009;5(1):14-22.
11. Segura T, Anderson BC, Chung PH, Webber RE, Shull KR, Shea LD., Crosslinked hyaluronic acid hydrogels: a strategy to functionalize and pattern, Biomaterials, 2005;26(4):359-71.
12. Fransson J, Espander Jansson A., Local tolerance of subcutaneous injections, Journal of pharmacy and pharmacology, 1996;48(10):1012-5.
13. Gatej I, Popa M, Rinaudo M., Role of the pH on hyaluronan behavior in aqueous solution, Biomacromolecules, 2005;6(1):61-7.
14. Dornhofer W, Embrechts E., Injection solution for intramuscular and subcutaneous administration to animals, Google Patents; 1998.
15. Garg HG, Hales CA., Chemistry and biology of hyaluronan, 2004, Elsevier Science.
16. Barbucci R, Lamponi S, Borzacchiello A, Ambrosio L, Fini M, Torricelli P, et al., Hyaluronic acid hydrogel in the treatment of osteoarthritis, Biomaterials, 2002;23(23):4503-13.
17. Ghosh K, Shu XZ, Mou R, Lombardi J, Prestwich GD, Rafailovich MH, et al., Rheological characterization of in situ cross-linkable hyaluronan hydrogels, Biomacromolecules, 2005;6(5):2857-65.
18. Fam H, Kontopoulou M, Bryant J., Effect of concentration and molecular weight on the rheology of hyaluronic acid/bovine calf serum solutions, Biorheology, 2009;46(1):31-43.
19. Zhao X. Synthesis and characterization of a novel hyaluronic acid hydrogel, Journal of Biomaterials Science, Polymer Edition, 2006;17(4):419-33.
20. Šoltés L, Mendichi R, Kogan G, Schiller J, Stankovska M, Arnhold J., Degradative action of reactive oxygen species on hyaluronan, Biomacromolecules, 2006;7(3):659-68.
21. Stern R, Kogan G, Jedrzejas MJ, Soltés L., The many ways to cleave hyaluronan, Biotechnology advances, 2007;25(6):537-57.

22. Volpi N, Schiller J, Stern R, Soltes L., Role, metabolism, chemical modifications and applications of hyaluronan, Current medicinal chemistry, 2009;16(14):1718-45.
23. Ibrahim S, Kang QK, Ramamurthi A., The impact of hyaluronic acid oligomer content on physical, mechanical, and biologic properties of divinyl sulfone-crosslinked hyaluronic acid hydrogels, Journal of Biomedical Materials Research Part A, 2010;94(2):355-70.
24. Bencherif SA, Srinivasan A, Horkay F, Hollinger JO, Matyjaszewski K, Washburn NR., Influence of the degree of methacrylation on hyaluronic acid hydrogels properties, Biomaterials. 2008;29(12):1739-49.
25. Jha AK, Hule RA, Jiao T, Teller SS, Clifton RJ, Duncan RL, et al., Structural analysis and mechanical characterization of hyaluronic acid-based doubly cross-linked networks, Macromolecules, 2009;42(2):537-46.
26. Shu XZ, Liu Y, Luo Y, Roberts MC, Prestwich GD., Disulfide cross-linked hyaluronan hydrogels, Biomacromolecules, 2002;3(6):1304-11.

Chapter 4

Application of hyaluronic acid nanoparticles in colloidal suspensions as a potential osteoarthritis treatment

Chapter 4: Application of hyaluronic acid nanoparticles in colloidal suspensions as a potential osteoarthritis treatment

4.1. Introduction

Currently, the quality of life for ~33 million Americans is affected by osteoarthritis (OA) with about 70% of these individuals aged 65 and over (1-3). OA is a disease in which the degradation of joints results in pain and loss of joint function. Intra-articular treatments, such as hyaluronic acid (HA) injections into the synovial joint, are normally recommended to reduce the pain and increase joint function. HA is a major component of synovial fluid lubricating the joint and preventing joint erosion (4). HA viscosupplements such as Synvisc®, Orthovisc®, and Hyalgan® are available on the market (5-7). While these products have shown positive effects, reducing pain and increasing joint function, poor injectability or insufficient therapeutic effect remain a need (5-7).

To enhance injectivity, multiple studies have been conducted and several low viscosity products are available on the market. Using HA with lower molecular weights has been the primary means to reduce viscosity of vicosupplements; however, low molecular weight HA does not provide a sufficient therapeutic effect. Hyalgan® is one of these low molecular weight, uncrosslinked HA viscosupplements. More injections of Hyalgan® are required per treatment course to achieve a reasonable therapeutic effect (Table 1-5). On the other hand, treatment with crosslinked HA viscosupplements such as Synvisc® requires fewer injections per treatment course but their high viscosity impedes injection.

Here, HA nanoparticles were explored as a means to reduce the viscosity of viscosupplements using high molecular weight HA. Orthovisc® is made from uncrosslinked 1500 kDa HA and has the highest concentration of HA among the uncrosslinked viscosupplements (Table 1-5). In this study, HA nanoparticles were used to reduce the viscosity of HA solutions with similar molecular weight and concentration to Orthovisc®. Two experiments were designed to investigate the effect of nanoparticles on the rheological behavior (viscosity and viscoelasticity) of simulated Orthovisc®. A solution of 1500 kDa at 1.4% w/v was prepared as a model viscosupplement for osteoarthritis treatment. The effect of including nanoparticles at different ratios and changing the molecular weight of HA used for nanoparticle fabrication was evaluated rheologically.

4.2. Materials and Methods

4.2.1. Materials

Nanoparticles fabricated in chapter two (section 2.2.2.1) at 1X polymer concentration, 1:1 molar reactive site ratio, and three hours reaction time made from 17 kDa and 1500 kDa HA were used in this chapter for the experiments.

4.2.2. Methods

4.2.2.1. Application of HA nanoparticles simulated Orthovisc® formulation

4.2.2.2.1. Mixing HA nanoparticles with HA polymer to reach hyaluronic acid concentration simulated Orthovisc® formulation

To evaluate the effect of HA nanoparticles in a simulated Orthovisc® formulation, an overall HA concentration was set at 1.4 w/v which is the same concentration of hyaluronic acid (1500 kDa) in Orthovisc®. Two sets of samples were prepared by mixing nanoparticles made from 17kDa HA or nanoparticles made from 1500 kDa HA with 1500 kDa HA polymer at different nanoparticle: polymer ratios to reach the final HA concentration of 1.4% w/v in deionized water. Polymer to nanoparticle ratios were selected as: 100:0, 75:25, 50:50, 25:75, and 0:100. After removing the dry polymer and nanoparticles from the freezer and equilibrating them at room temperature, samples were prepared using these ratios by mixing them in deionized water. Control samples were also

prepared by mixing 1500 kDa HA polymer in deionized water at different concentrations (1.05%, 0.7%, and 0.35% w/v).

4.2.2.2.2. Using HA nanoparticle formulations at different concentrations

To evaluate the effect of nanoparticle concentration on the viscosity and viscoelasticity of HA nanoparticle suspensions, nanoparticles made of 1500 kDa HA were mixed at 1.4%, 5%, 10%, and 15% w/v concentrations with deionized water. 1500 kDa HA polymer at 1.4% w/v was also selected as a control (simulated Orthovisc®).

4.2.2.2. Viscosity measurement

To investigate the viscosity of samples made in sections 4.2.2.1.1. and 4.2.2.1.2., an AR 2000 rheometer (TA Instruments, Delaware) equipped with a 2°, 20 mm diameter cone-plate at 25 °C was employed. Similar to section 3.2.2.7., after loading samples under the rheometer, shear stress and viscosity of the samples were measured over a a shear rate sweep of 0.01-1000 s^{-1}.

4.2.2.3. Viscoelasticity measurement

To evaluate the viscoelasticity of samples prepared in sections 4.2.2.1.1. and 4.2.2.1.2., dynamic oscillatory rheological measurements were performed using an AR 2000 rheometer (TA Instruments, Delaware) equipped with a 2°, 20 mm diameter cone-

plate at 25 °C. Similar to section 3.2.2.6., first, strain sweep experiments were performed to determine the limit of viscoelasticity, where the rheological properties are strain dependent. Then, the viscoelastic properties of colloidal suspensions were evaluated using a frequency sweep from 0.1 to 10 Hz at 1% strain, which was in the linear viscoelastic region. This range includes the physiological frequencies of the knee, ranging from 0.5 Hz (walk) to 3 Hz (running) (1, 8-10). All experiments were performed in triplicate.

4.3. Results

All formulations were prepared as described and tested to evaluate their viscosity and viscoelasticity (Figure 4-1). A simulated Orthovisc® using a HA polymer solution (1500 kDa) at 1.4% w/v concentration was compared to a HA nanoparticle suspension (1500 kDa) at similar concentration. It was observed that the polymer solution was highly viscous; however, the nanoparticle suspension was more water-like. The nanoparticle formation obviously reduced the viscosity and increased the fluidity of HA at 1.4% w/v.

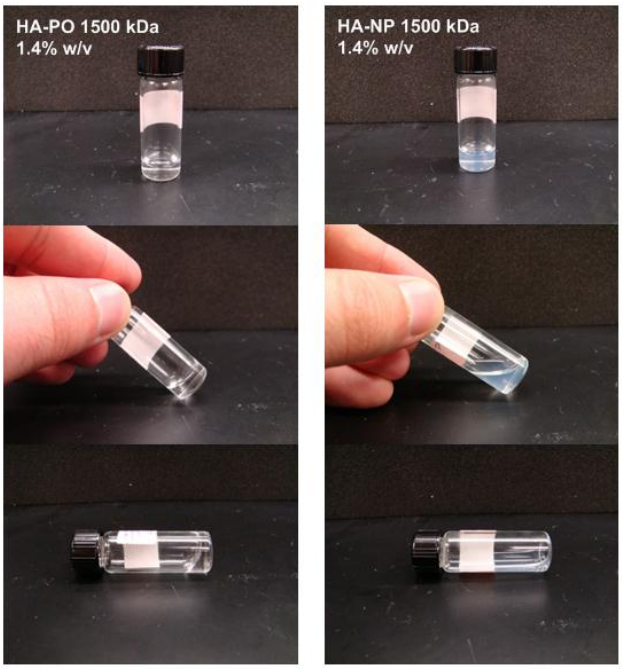

Figure (4-1) (Left): HA polymer solution (HA-PO 1500 kDa) at 1.4% w/v concentration. A viscous polymer solution was observed. (Right): HA nanoparticle suspension (HA-NP 1500 kDa) at 1.4% w/v concentration. Viscosity of the nanoparticle suspension was much lower than the polymer solution.

4.3.1. Viscosity measurement

4.3.1.1. Mixing HA nanoparticles with HA polymer to reach hyaluronic acid concentration in the Orthovisc® formulation

The rheological behavior of HA polymer/nanoparticle mixtures using 1500 kDa polymer and nanoparticles made from 17 kDa or 1500 kDa HA was explored. Increasing nanoparticle concentration reduced the shear stress and viscosity of the polymer/nanoparticle mixtures independent of the HA molecular weight used for nanoparticle fabrication. The highest shear rate and viscosity values were observed for the sample with 100% HA polymer. On the other hand, the lowest shear rate and

viscosity values were for the samples with 100% HA nanoparticles made from either 17 kDa or 1500 kDa HA.

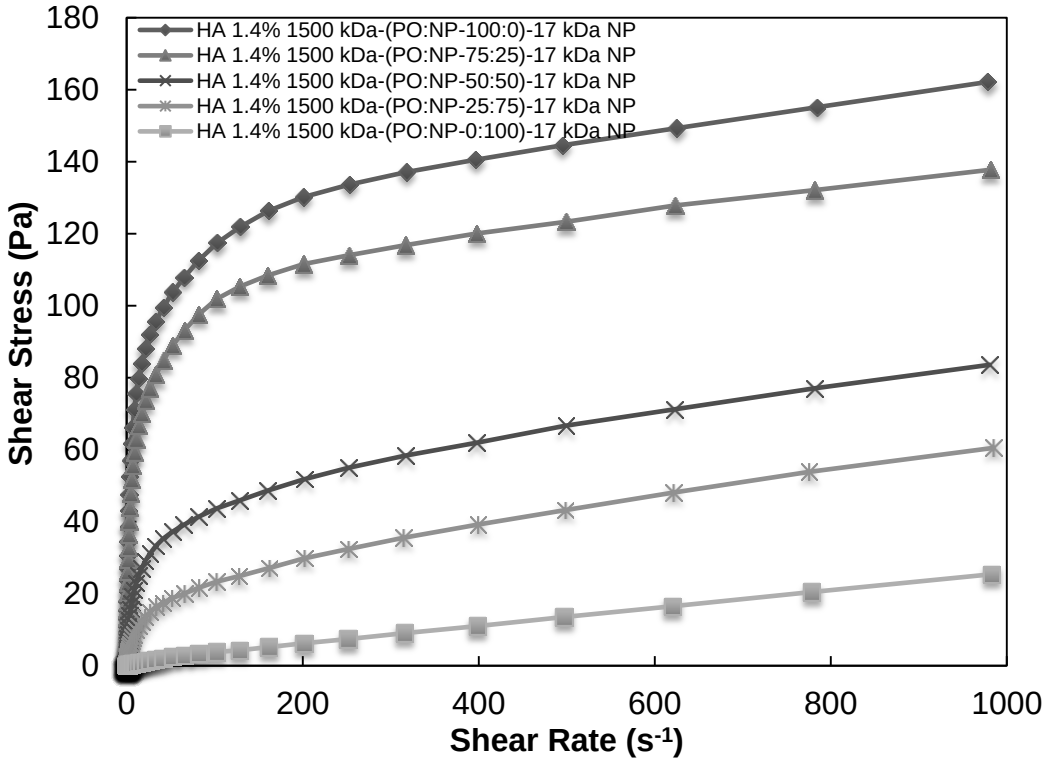

Figure (4-2) Rheological evaluation of HA polymer (1500 kDa) and HA nanoparticle (17 kDa) mixtures. Increasing nanoparticle content in the formulation decreased shear stress.

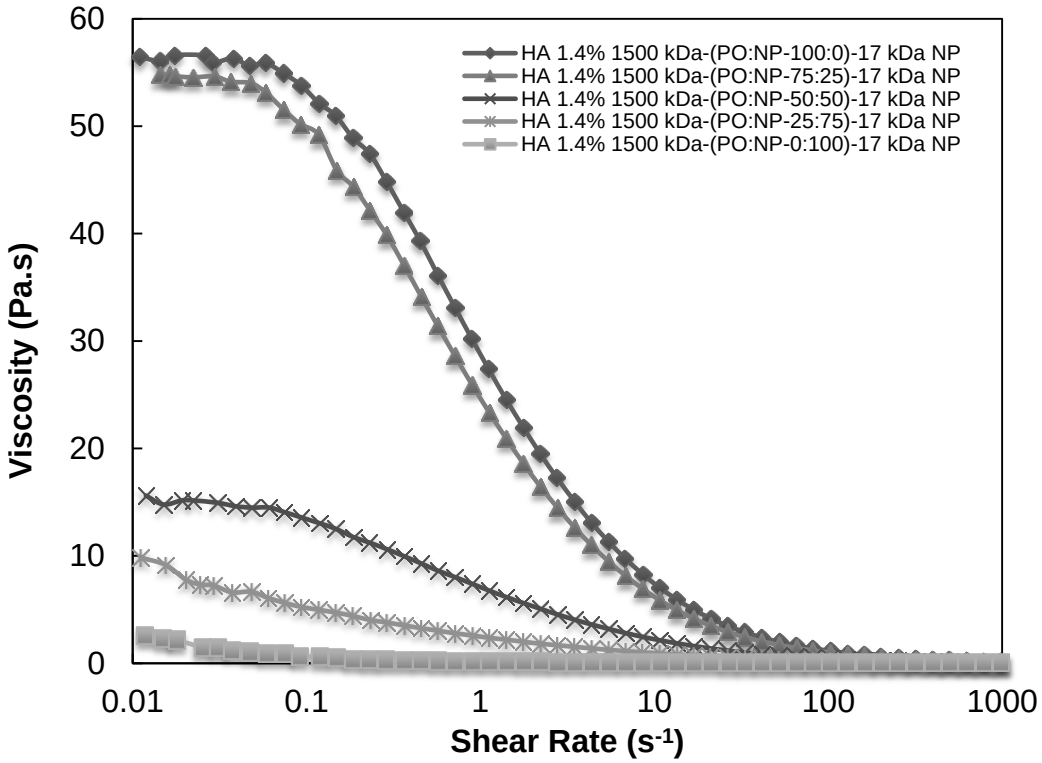

Figure (4-3) Rheological evaluation of HA polymer (1500 kDa) and HA nanoparticle (17 kDa) mixtures. Increasing nanoparticle content in the formulation decreased viscosity.

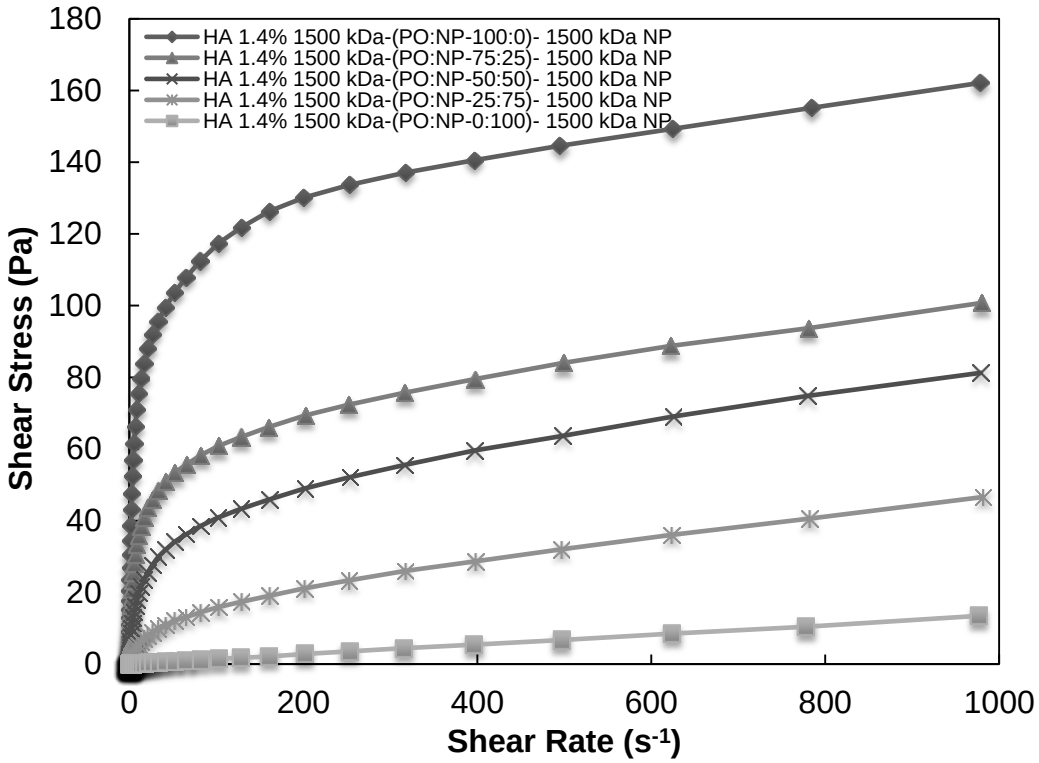

Figure (4-4) Rheological evaluation of HA polymer (1500 kDa) and HA nanoparticle (1500 kDa) mixtures. Increasing nanoparticle content in the formulation decreased shear stress.

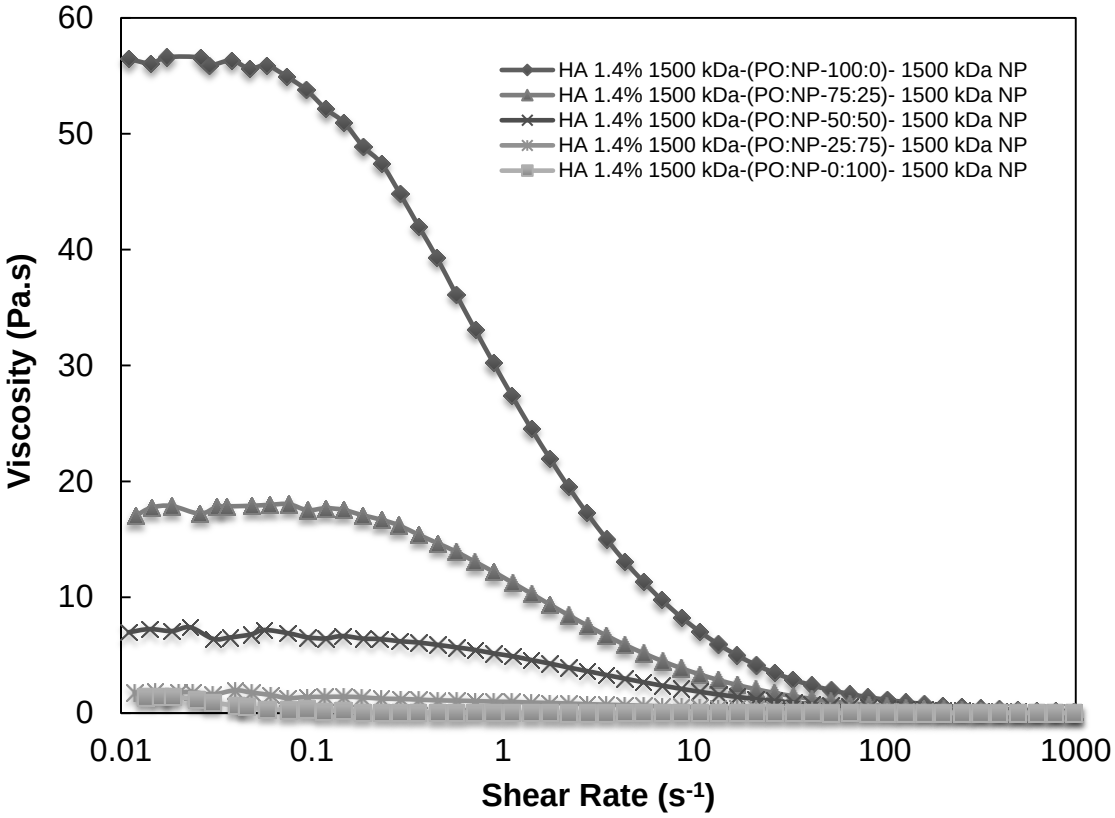

Figure (4-5) Rheological evaluation of HA polymer (1500 kDa) and HA nanoparticle (1500 kDa) mixtures. Increasing nanoparticle content in the formulation decreased viscosity.

Comparing polymer/nanoparticle mixtures made from either 17 kDa or 1500 kDa HA nanoparticles showed that samples containing 17 kDa HA nanoparticles had higher viscosity than samples made from 1500 kDa HA nanoparticles at all polymer: nanoparticle ratios (Figure 4-6). These results suggested that nanoparticles made from 17 kDa HA might interact more with 1500 kDa polymer chains resulting in greater viscosity. This interaction might be the result of dangling chains on the surface of 17 kDa nanoparticles. This hairy structure might facilitate entanglement with polymer chains resulting in greater viscosity values compared to the samples made from 1500 kDa HA nanoparticles at similar polymer: nanoparticle ratios. Lower viscosity samples made from

1500 kDa HA nanoparticles might be due to inhibiting polymer chain entanglement between HA molecules in solution. These data could also support the formation of colloidal gels using 17 kDa HA nanoparticles and the formation of paste-like materials using 1500 kDa HA nanoparticles observed in chapter three.

In addition, the difference in initial viscosity of samples using 17 kDa or 1500 kDa HA nanoparticles increased by increasing the concentration of HA polymer in the samples. The samples at a 75:25 ratio had the greatest initial viscosity difference comparing the two nanoparticle types (Figure 4-6). Increasing nanoparticle concentration decreased this viscosity difference as well as the overall viscosity of the samples. This might be due to more polymer-nanoparticle interaction and physical entanglement in the samples with higher polymer concentrations. Therefore, the viscosity of polymer/nanoparticle mixtures could be controlled using nanoparticles made from HA with different molecular weights.

Formulations containing 1500 kDa HA nanoparticles had viscosity values closer to the control samples at different polymer:nanoparticle ratios. Increasing the concentration of nanoparticles showed that the difference between the initial viscosity of the formulations and controls became lower. These results could suggest that the entanglement of free surface chains on nanoparticles was more dependent on the concentration of free polymer in the suspension. Moreover, the absence of sufficient dangling chains on 1500 kDa HA nanoparticles led to low interaction with either polymer chains or nanoparticles, thus reducing the viscosity the mixtures.

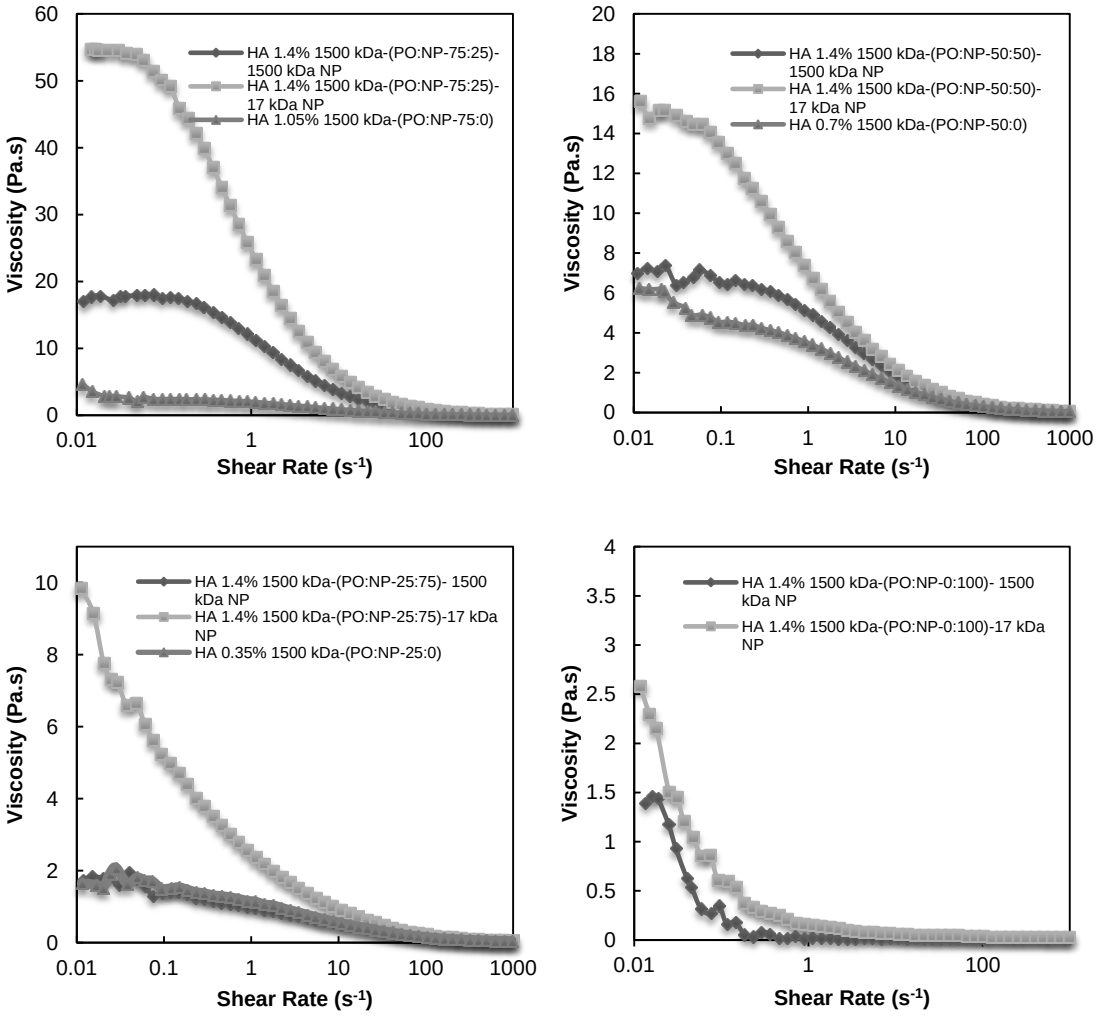

Figure (4-6) Rheological evaluation of HA polymer/nanoparticle mixtures. Viscosity of samples made with 17 kDa HA nanoparticles was greater than the viscosity of the samples made from 1500 kDa HA nanoparticles at all polymer: nanoparticle ratios.

4.3.1.2. Using HA nanoparticle formulations at different concentrations

In the previous experiment, the viscosity of suspensions made from 17 kDa and 1500 kDa HA nanoparticles was lower than the viscosity of HA polymer solution (1500 kDa) at 1.4% w/v. Here, the effect of increasing nanoparticle (1500 kDa HA) concentration from 1.4% w/v up to 15% w/v on the shear stress and viscosity of the

nanoparticle suspensions was investigated. The formation of colloidal systems from 1500 kDa HA nanoparticles (1.4% w/v up to 45% w/v) was presented in chapter three (Figure 3-1). Samples at 30% w/v and 45% w/v nanoparticle concentrations formed paste-like materials and the rheological properties could not be measured due to high viscosity of these samples. Therefore, nanoparticle concentrations up to 15% w/v were used for this experiment (Figures 4-7 and 4-8). The rheological behavior of HA nanoparticle (1500 kDa) samples at 1.4%, 5%, 10%, and 15% w/v concentrations were compared to HA polymer solution (1500 kDa) at 1.4% w/v.

Increasing nanoparticle concentration increased shear stress and viscosity as shear rate increased. These results indicated that even at 15% w/v nanoparticle concentration, shear stress and viscosity of the sample were still lower than the shear stress and viscosity of 1.4% w/v HA in solution. Nanoparticle formation not only reduced the viscosity of HA, but also it may also be used to increase the concentration of HA in formulations. Therefore, higher HA concentrations can be injected into the body with only a small increase in the formulation viscosity.

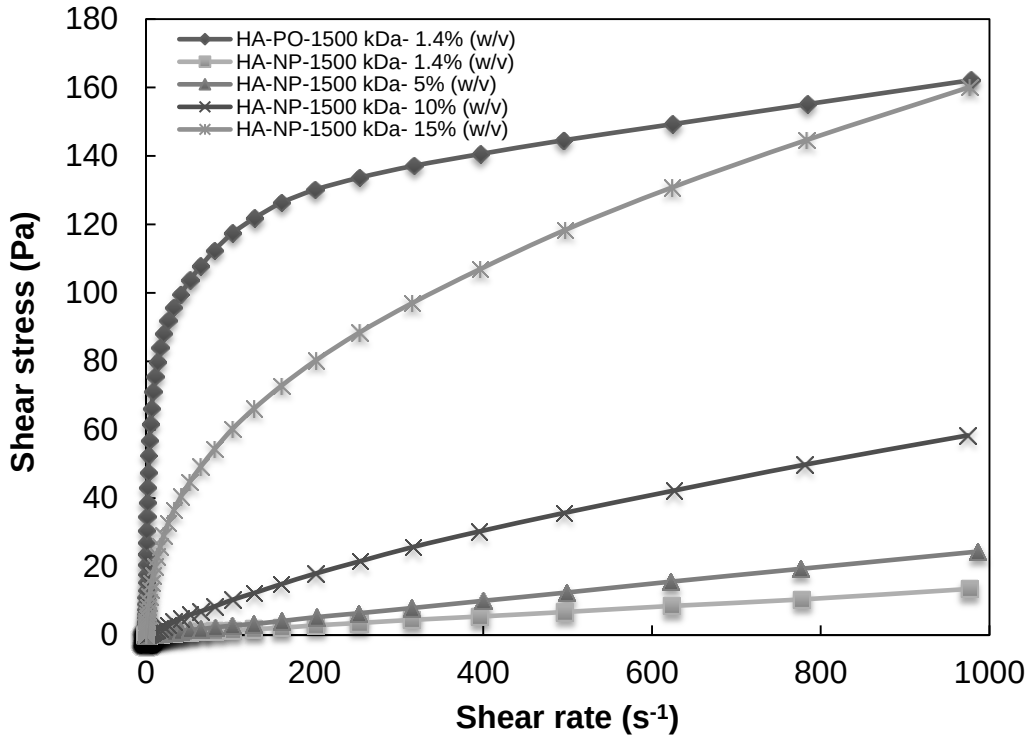

Figure (4-7) Rheological evaluation of HA nanoparticle (1500 kDa) suspensions at different nanoparticle concentrations. Increasing nanoparticle concentration increased shear stress.

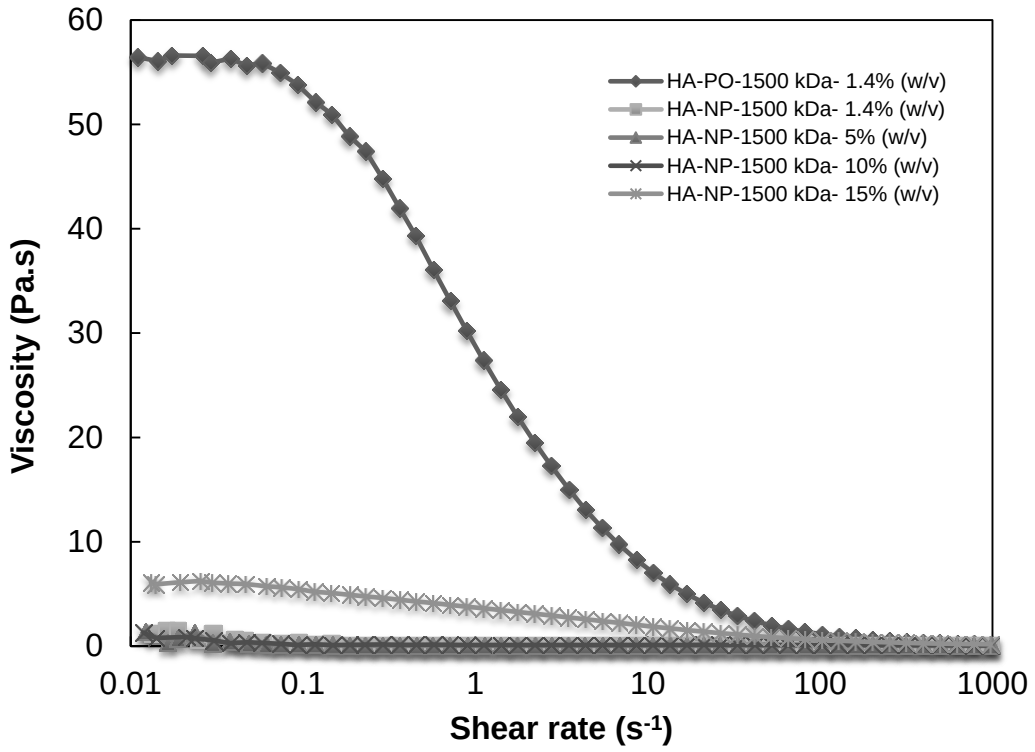

Figure (4-8) Rheological evaluation of HA nanoparticle (1500 kDa) suspensions at different nanoparticle concentrations. Increasing nanoparticle concentration increased viscosity.

4.3.2. Viscoelasticity measurement

4.3.2.1. Mixing HA nanoparticles with HA polymer to reach hyaluronic acid concentration in Orthovisc® formulation

The viscoelastic behavior of polymer/nanoparticle mixtures using 1500 kDa polymer and nanoparticles made from 17 kDa and 1500 kDa HA was evaluated (Figures 4-9 to 4-14). Increasing nanoparticle concentration lowered storage, loss, and complex moduli of the polymer/nanoparticle mixtures independent of the HA molecular weight used for the nanoparticles. The highest viscoelastic values were observed for the samples

with 100% HA polymer. In contrast, the lowest viscoelasticity was found for the samples with 100% HA nanoparticles made from either 17 kDa or 1500 kDa HA.

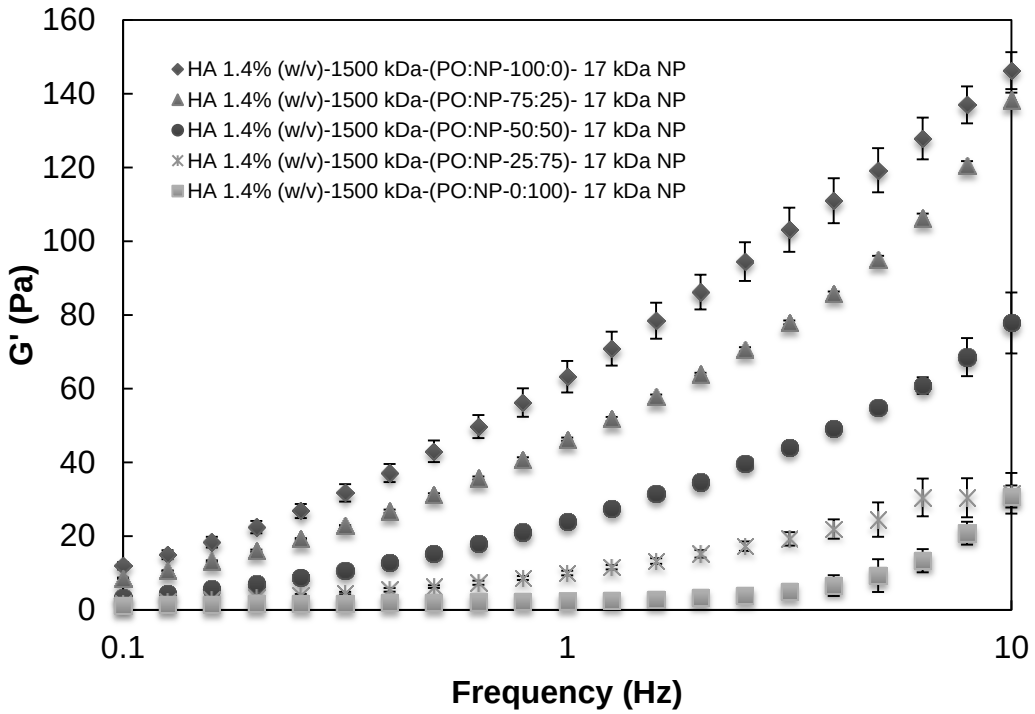

Figure (4-9) Viscoelasticity of HA polymer (1500 kDa) and HA nanoparticle (17 kDa) mixtures: elastic modulus over frequency range. Increasing nanoparticle concentration decreased elastic modulus.

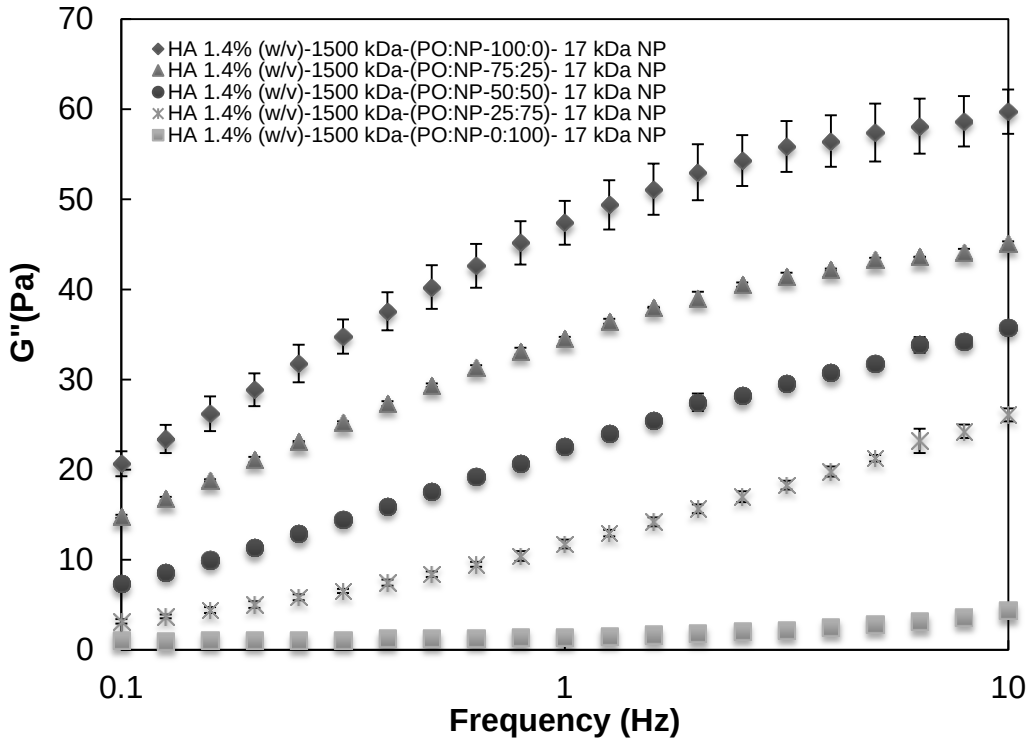

Figure (4-10) Viscoelasticity of HA polymer (1500 kDa) and HA nanoparticle (17 kDa) mixtures: viscous modulus over frequency range. Increasing nanoparticle concentration decreased viscous modulus.

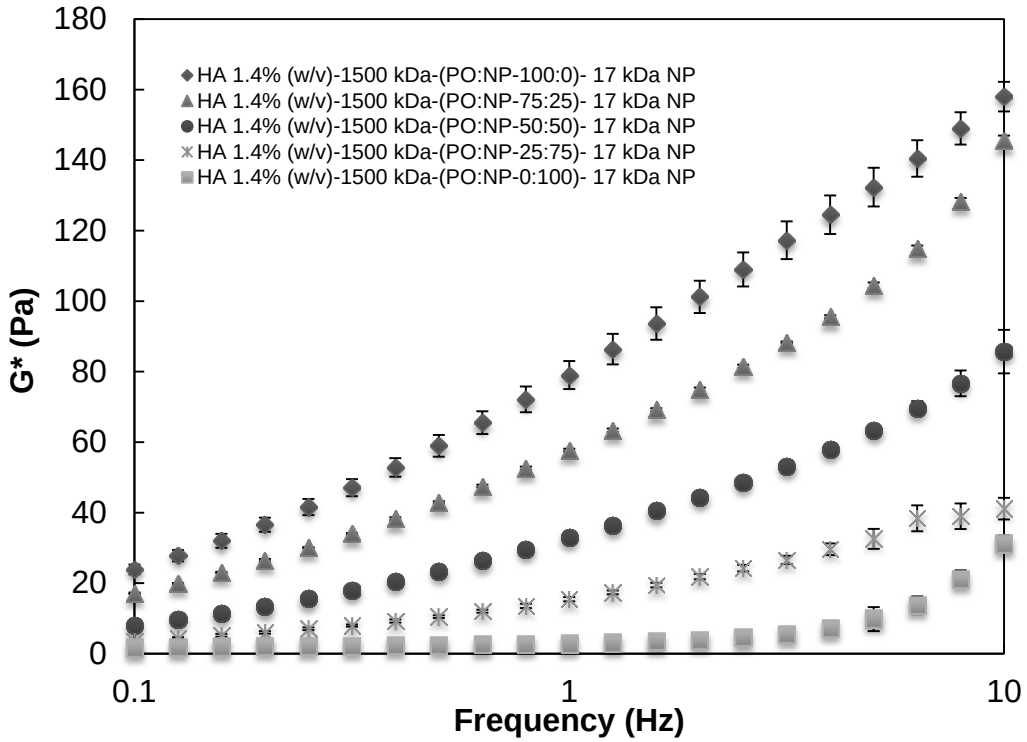

Figure (4-11) Viscoelasticity of HA polymer (1500 kDa) and HA nanoparticle (17 kDa) mixtures: complex modulus over frequency range. Increasing nanoparticle concentration decreased complex modulus.

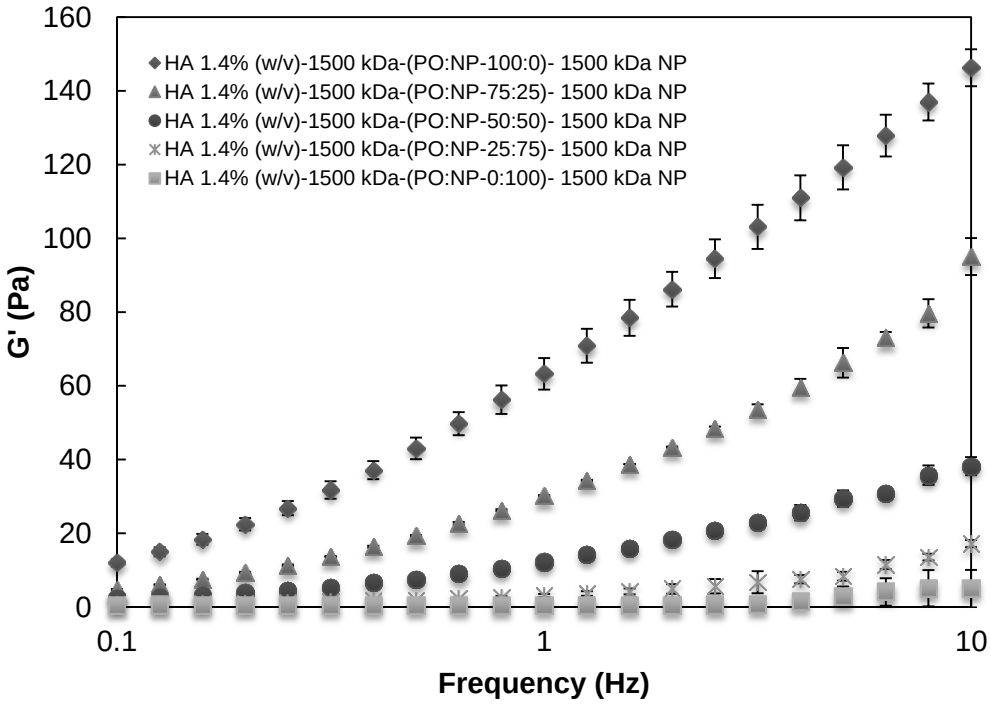

Figure (4-12) Viscoelasticity of HA polymer (1500 kDa) and HA nanoparticle (1500 kDa) mixtures: elastic modulus over frequency range. Increasing nanoparticle concentration decreased elastic modulus.

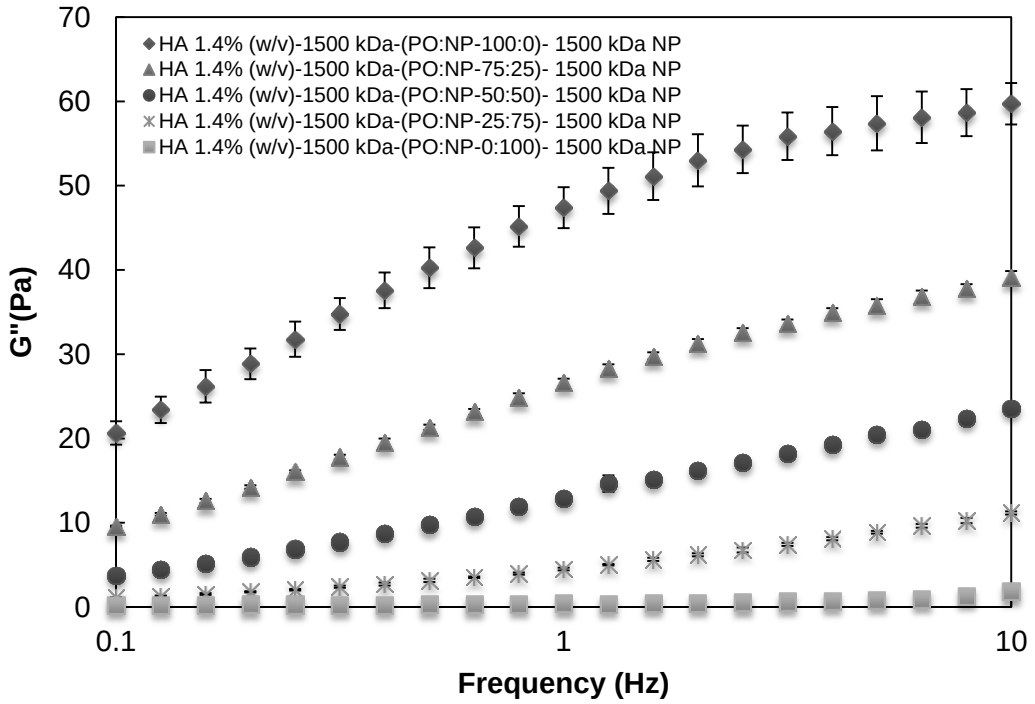

Figure (4-13) Viscoelasticity of HA polymer (1500 kDa) and HA nanoparticle (1500 kDa) mixtures: viscous modulus over frequency range. Increasing nanoparticle concentration decreased viscous modulus.

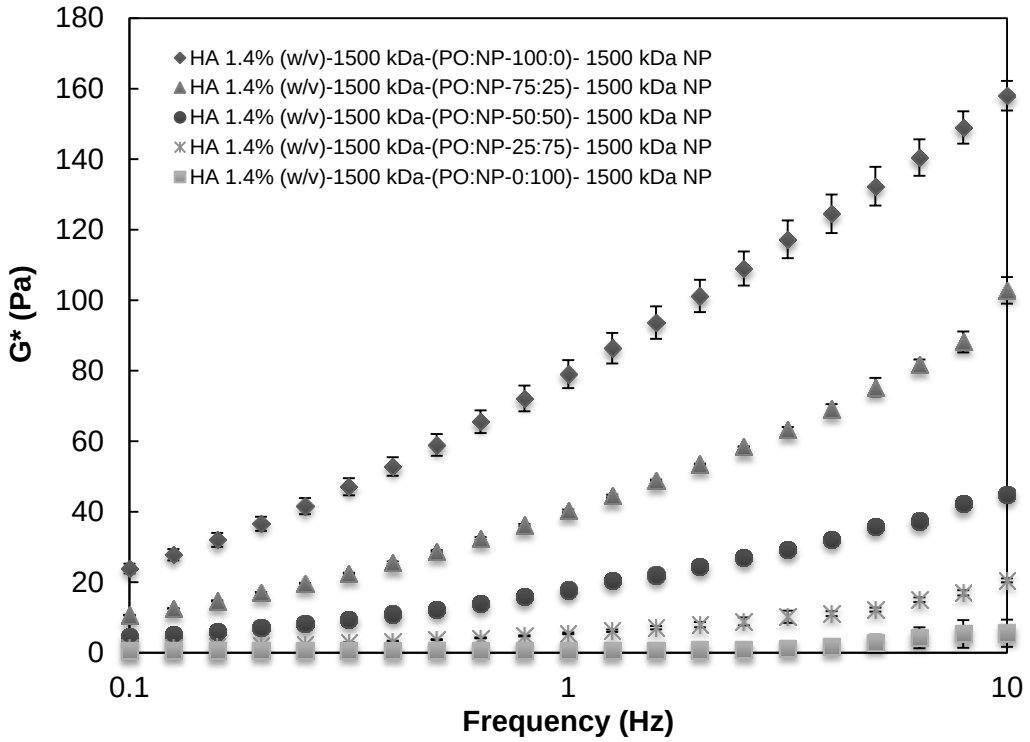

Figure (4-14) Viscoelasticity of HA polymer (1500 kDa) and HA nanoparticle (1500 kDa) mixtures: complex modulus over frequency range. Increasing nanoparticle concentration decreased complex modulus.

Polymer/nanoparticle mixtures made using 17 kDa HA nanoparticles showed a higher elastic, viscous, and complex moduli when compared to the samples made from 1500 kDa HA nanoparticles at all polymer: nanoparticle ratios (Figures 4-15, 4-16, and 4-17). Similar to viscosity measurements, these results also suggested that nanoparticles made from 17 kDa HA might interact more with HA polymer chains in solution resulting in greater viscoelasticity for the samples made from 17 kDa HA nanoparticles. The hairy structure of nanoparticles made from 17 kDa HA might physically entangle with HA polymer chains resulting in greater viscoelasticity values compared to 1500 kDa HA nanoparticles. On the other hand, nanoparticles made from 1500 kDa HA may behave more like a hard sphere or may even inhibit HA polymer-polymer interaction in solution.

Formulations containing 1500 kDa HA nanoparticles had the viscoelasticity values closer to the control samples at different polymer:nanoparticle ratios. Increasing the concentration of nanoparticles decreased the difference between the viscoelasticity of the formulations and controls.

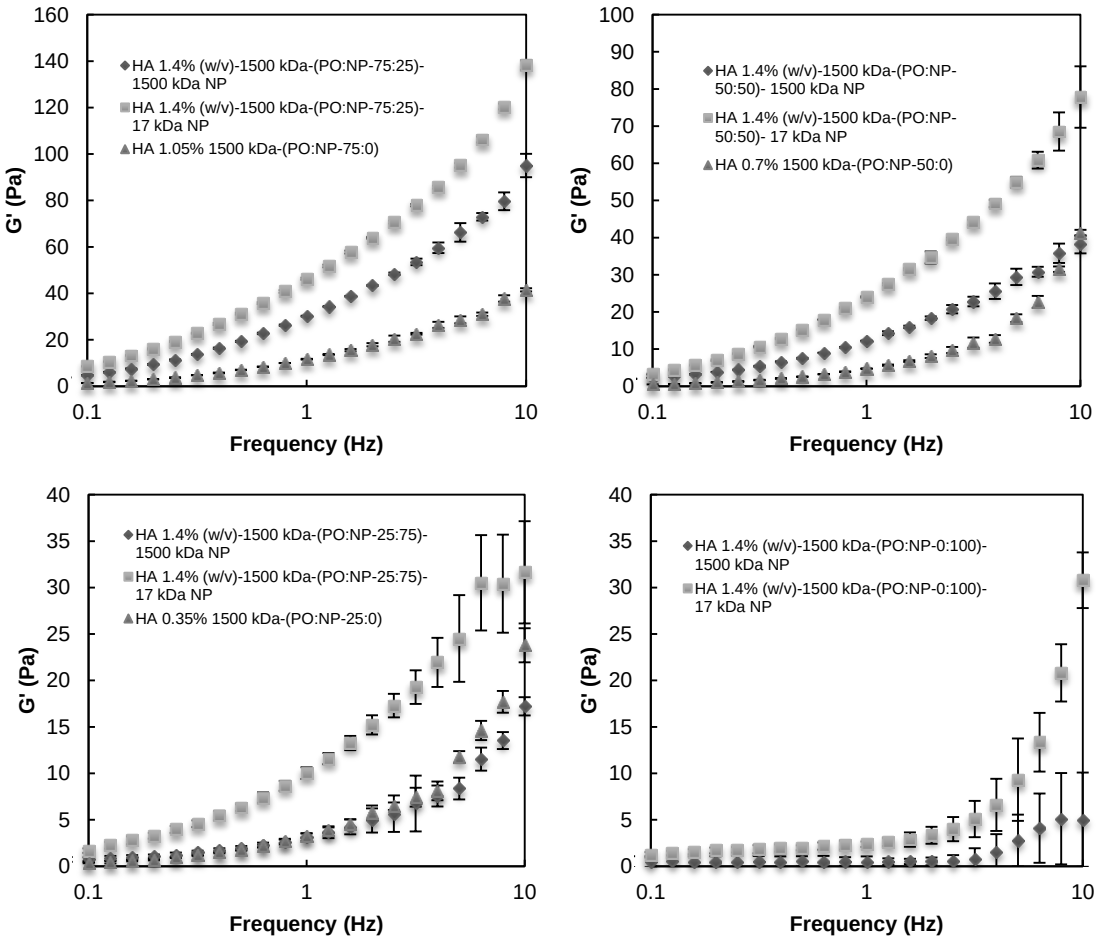

Figure (4-15) Viscoelasticity of HA polymer/nanoparticle mixtures: elastic modulus over frequency range. Elastic modulus of the samples composed of 17 kDa HA nanoparticles were greater than the elastic modulus of the samples made from 1500 kDa HA nanoparticles at all polymer: nanoparticle ratios.

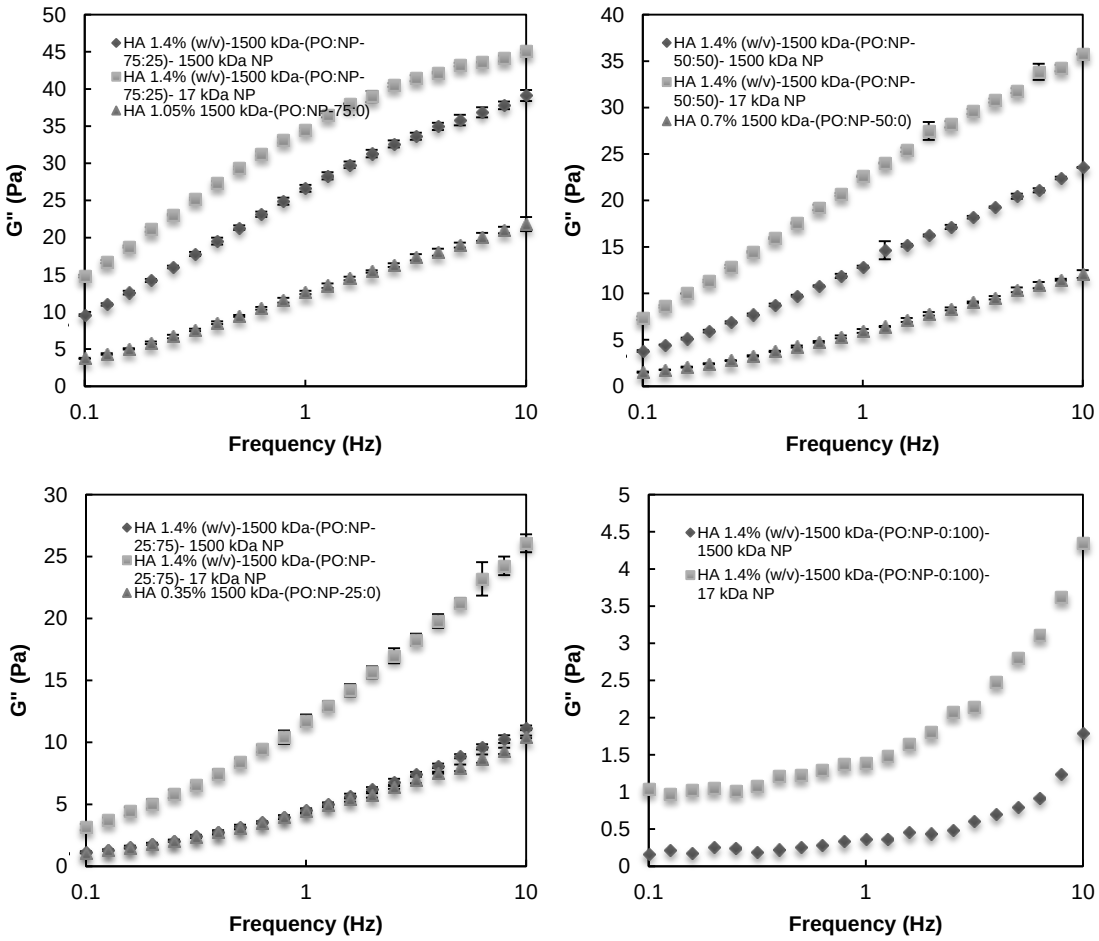

Figure (4-16) Viscoelasticity of HA polymer/nanoparticle mixtures: viscous modulus over frequency range. Viscous modulus of the samples composed of 17 kDa HA nanoparticles were greater than the viscous modulus of the samples made from 1500 kDa HA nanoparticles at all polymer: nanoparticle ratios.

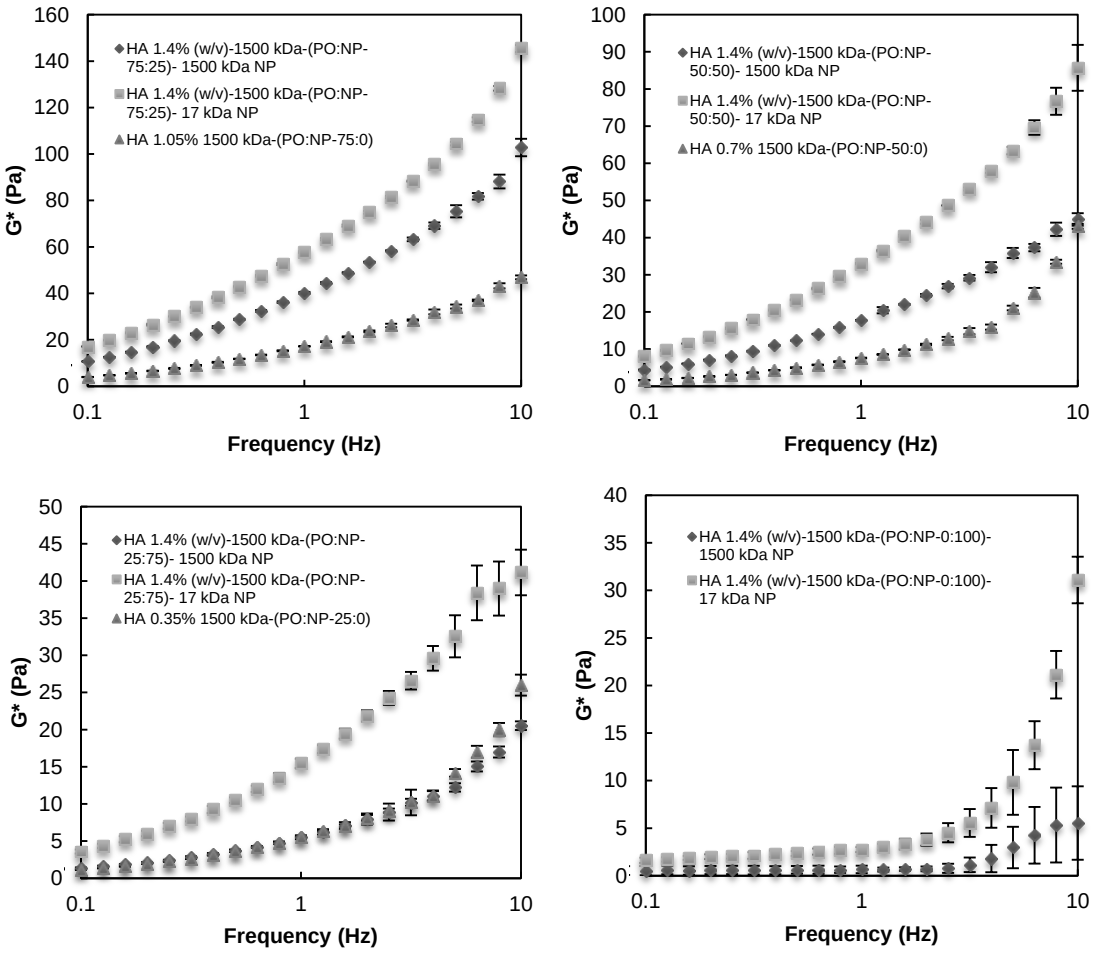

Figure (4-17) Viscoelasticity of HA polymer/nanoparticle mixtures: complex modulus over frequency range. Complex modulus of the samples composed of 17 kDa HA nanoparticles were greater than the complex modulus of the samples made from 1500 kDa HA nanoparticles at all polymer: nanoparticle ratios.

4.3.2.2. Using HA nanoparticle formulations at different concentrations

The effect of increasing nanoparticle (1500 kDa HA) concentration from 1.4% w/v up to 15% w/v on the viscoelasticity of the nanoparticle suspensions was also evaluated (Figures 4-18, 4-19, and 4-20). Increasing nanoparticle concentration increased storage, loss, and complex moduli of the colloidal suspensions. Therefore, viscoelastic

properties of colloidal suspensions could be controlled by changing the nanoparticle concentration in these formulations when compared to 1.4% polymer solution.

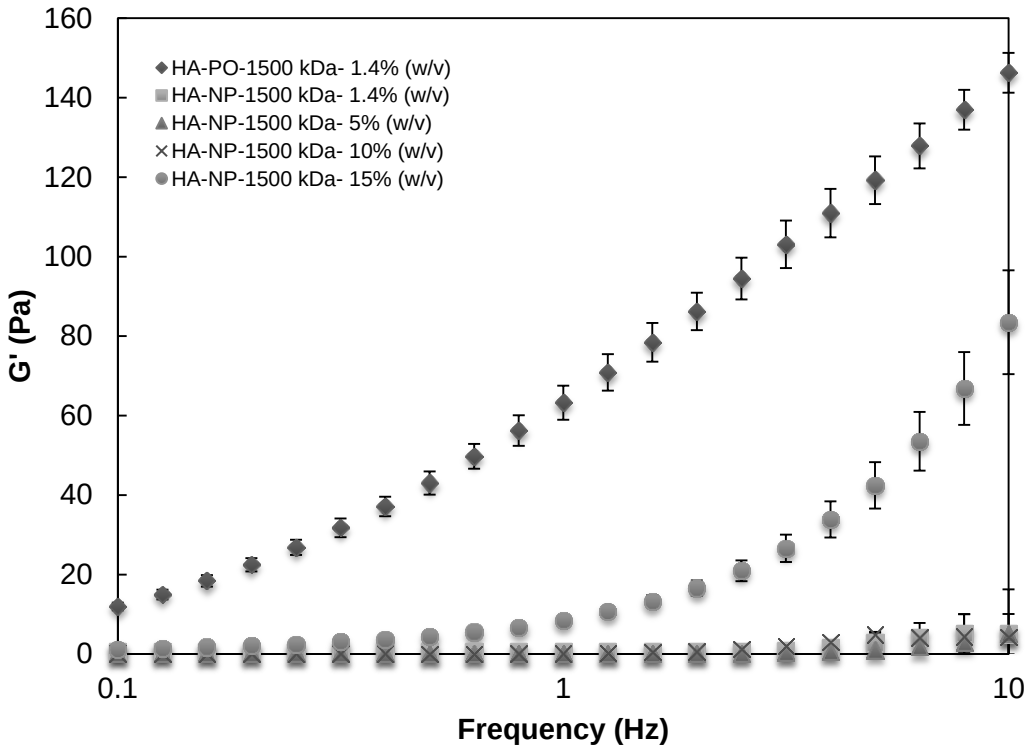

Figure (4-18) Viscoelasticity of HA nanoparticle suspensions at different nanoparticle concentrations: elastic modulus over frequency range. Increasing nanoparticle concentration increased elastic modulus.

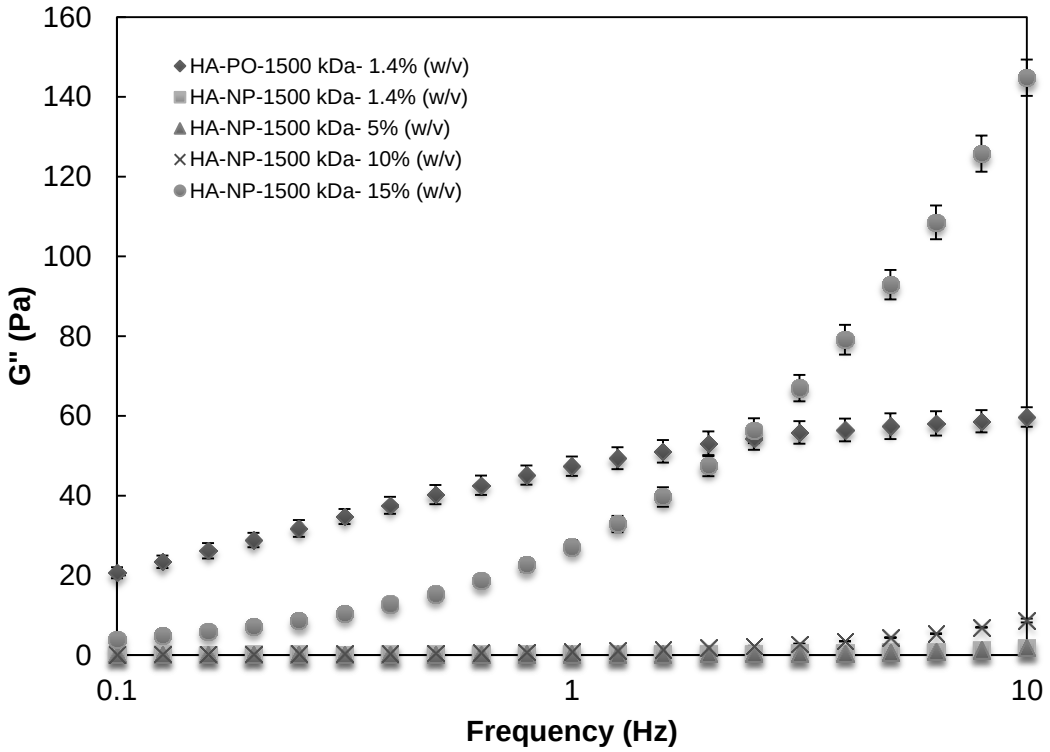

Figure (4-19) Viscoelasticity of HA nanoparticle suspensions at different nanoparticle concentrations: viscous modulus over frequency range. Increasing nanoparticle concentration increased viscous modulus.

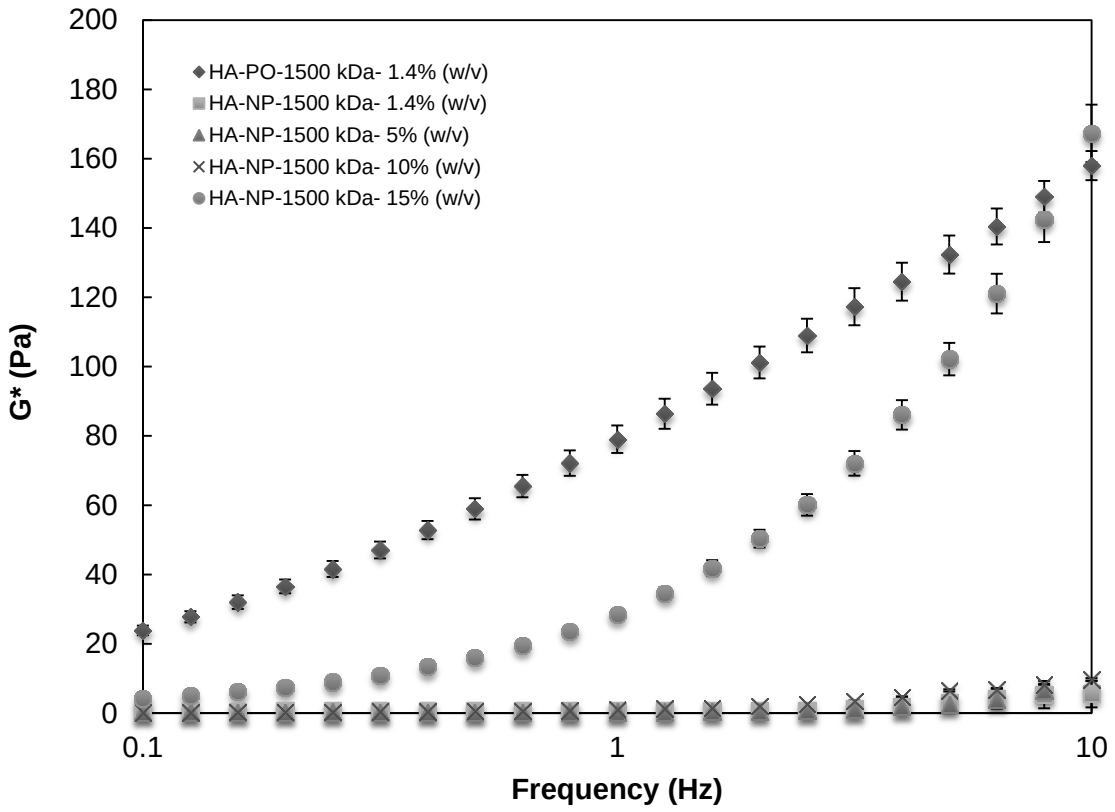

Figure (4-20) Viscoelasticity of HA nanoparticle suspensions at different nanoparticle concentrations: complex modulus over frequency range. Increasing nanoparticle concentration increased complex modulus.

4.4. Discussion

Our study showed that increasing nanoparticle concentration in polymer/nanoparticle mixtures (HA concentration of 1.4% w/v) reduced viscosity and viscoelasticity of the samples. This decrease was influenced by nanoparticles which were synthesized from HA with different molecular weights. The surface structure of nanoparticles, which was dependent on molecular weight of HA used for nanoparticle fabrication, might change the rheological properties of colloidal suspensions. Nanoparticles made from 17 kDa HA, which were presumed to have 'hairy' surface

structure, seemed to have more polymer-nanoparticle interaction and physical entanglement in polymer/nanoparticle mixtures compared to nanoparticles made from 1500 kDa HA. These interactions might be the reason for greater viscosity and viscoelasticity in the mixtures made from 17 kDa HA nanoparticles compared to the mixtures made from 1500 kDa HA nanoparticles at similar polymer/nanoparticle ratios. Rheological studies also showed that even 1500 kDa HA nanoparticles interacted with HA polymer influencing viscosity and viscoelasticity. This interaction depended on the polymer/nanoparticle ratio. At higher polymer concentrations, more physical interactions between nanoparticles (17 kDa or 1500 kDa) must have yielded a greater effect on rheological properties of samples. By increasing nanoparticle concentration in the formulations with 1500 kDa nanoparticles, the viscosity and viscoelasticity approached the viscosity and the viscoelasticity of control samples containing only polymer. Therefore, the rheological properties of the viscosupplements can be controlled via the type and the concentration of nanoparticles mixed into the formulation.

Application of nanoparticles to enhance rheological properties of fluids and to form formation of nanocomposites has been reported (11-13). One study suggested that the presence of a small amount of nanoparticles with large aspect ratio improved the fluidity of polymeric solutions under low shear rate. On the other hand, addition of a large amount of nanoparticles reduced the aspect ratio by aggregation and constrained polymer segment motion in solutions (11). Other studies also reported the application of inorganic nanoparticles such as clay nanoparticles in ophthalmic and otic pharmaceutical formulations to modify the rheological properties of the compositions to enhance the viscosity, flow characteristics, or lubricity of the products. The studies showed that

nanoparticles could enhance shear thinning behavior and fluidity (13, 14). These reports and others confirmed that nanoparticles can modify the rheological properties of solutions but the effect of surface structure of nanoparticles to control rheological properties of solutions has not been clearly reported. Here, the rheological properties of viscosupplements could be controlled via nanoparticles. Different types of nanoparticles (17 kDa or 1500 kDa HA) at different concentrations can be added to the viscosupplements to control the viscosity and viscoelasticity.

Moreover, increasing HA nanoparticle (1500 kDa) concentration increased viscosity and viscoelasticity properties (elastic and viscous moduli) of HA polymer solutions. Even at relatively high (15% w/v) nanoparticle concentration, the viscosity of the samples was lower than the control sample simulating Orthovisc® (1.4% w/v HA solution). At higher nanoparticle concentrations (30% and 45% w/v), formation of paste-like material was observed. Rheological measurement at these nanoparticle concentrations was difficult due to the high viscosity of these samples. Finally, nanoparticle formation not only reduced the viscosity of HA suspensions but also could be used to increase the total concentration of HA in the formulation. As a result, colloidal suspensions can be used to increase the HA concentration with a small increase in the viscosity of HA viscosupplements.

Particle fabrication is one of the techniques used to reduce the viscosity of a solution. Currently, crystallization, phase separation, and complexation have also been reported to enhance the viscosity and increase injectability of protein solutions, specifically monoclonal antibodies at high doses (15-19). Such particle fabrication approaches packed the proteins, reduced the concentration of free protein in solution, and

prevented interactions which typically caused an increase in viscosity. With nanoparticle fabrication, the viscosity of HA viscosupplements can be reduced and the injectability enhanced in addition to increasing the concentration of HA in formulation.

4.5. Conclusion

In conclusion, the ability of hyaluronic acid nanoparticles to modify the viscosity and viscoelasticity of a simulated viscosupplement was evaluated. Increasing nanoparticle concentration in polymer/nanoparticle mixtures (overall HA concentration of 1.4% w/v) reduced viscosity and viscoelasticity of the samples. The type of nanoparticles (17 kDa or 1500 kDa) influenced the nanoparticle-polymer interactions and controlled the rheological properties of the suspensions. In addition, the viscosity of suspensions that included 1500 kDa HA nanoparticles was lower when compared to simulated viscosupplement. The viscosity of suspensions containing 15% w/v of nanoparticles was also lower than the viscosity of simulated viscosupplement (1.4 w/v HA). Therefore, nanoparticle formations not only reduced the viscosity of HA suspensions but facilitated an increase in the HA concentration with minimal increase in the viscosity of viscosupplements in an effort to enhance injectability.

4.6. References

1. Barbucci R, Lamponi S, Borzacchiello A, Ambrosio L, Fini M, Torricelli P, et al., Hyaluronic acid hydrogel in the treatment of osteoarthritis, Biomaterials, 2002;23(23):4503-13.
2. Conrad BP., The effects of glucosamine and chondroitin on the viscosity of synovial fluid in patients with osteoarthritis, 2001, University of Florida, 2001.
3. Singh G, Miller JD, Lee FH, Pettitt D, Russell MW., Prevalence of cardiovascular disease risk factors among US adults with self-reported osteoarthritis: data from the Third National Health and Nutrition Examination Survey. population.7:17.
4. Yaszemski MJ., Tissue engineering and novel delivery systems, 2003, CRC Press.
5. Watterson JR, Esdaile JM., Viscosupplementation: therapeutic mechanisms and clinical potential in osteoarthritis of the knee, Journal of the American Academy of Orthopaedic Surgeons, 2000;8(5):277.
6. Altman R, Moskowitz R., Intraarticular sodium hyaluronate (Hyalgan) in the treatment of patients with osteoarthritis of the knee: a randomized clinical trial. Hyalgan Study Group, The Journal of rheumatology, 1998;25(11):2203.
7. Maheu E, Ayral X, Dougados M., A hyaluronan preparation (500-730 kDa) in the treatment of osteoarthritis: a review of clinical trials with Hyalgan, International journal of clinical practice, 2002;56(10):804.
8. Ghosh K, Shu XZ, Mou R, Lombardi J, Prestwich GD, Rafailovich MH, et al., Rheological characterization of in situ cross-linkable hyaluronan hydrogels, Biomacromolecules, 2005;6(5):2857-65.
9. Fam H, Kontopoulou M, Bryant J., Effect of concentration and molecular weight on the rheology of hyaluronic acid/bovine calf serum solutions, Biorheology, 2009;46(1):31-43.
10. Zhao X., Synthesis and characterization of a novel hyaluronic acid hydrogel, Journal of Biomaterials Science, Polymer Edition, 2006;17(4):419-33.
11. Yin H, Mo D, Chen D., Orientation behavior of attapulgite nanoparticles in poly (acrylonitrile)/attapulgite solutions by rheological analysis, Journal of Polymer Science Part B: Polymer Physics, 2009;47(10):945-54.
12. Shchipunov Y, Ivanova N, Silant'ev V., Bionanocomposites formed by in situ charged chitosan with clay, Green Chem, 2009;11(11):1758-61.
13. Ketelson HA, Meadows DL., Use of synthetic inorganic nanoparticles as carriers for ophthalmic and otic drugs. 2002, US Patent App. 20,050/003,014.
14. Ketelson HA, Meadows DL., Inorganic nanopartices to modify the viscosity and physical properties of ophthalmic and otic compositions, 2002, Google Patents.
15. Yang MX, Shenoy B, Disttler M, Patel R, McGrath M, Pechenov S, et al., Crystalline monoclonal antibodies for subcutaneous delivery, Proceedings of the National Academy of Sciences of the United States of America, 2003;100(12):6934.
16. Shire SJ, Shahrokh Z, Liu J., Challenges in the development of high protein concentration formulations, Journal of pharmaceutical sciences, 2004;93(6):1390-402.
17. Salinas BA, Sathish HA, Bishop SM, Harn N, Carpenter JF, Randolph TW., Understanding and modulating opalescence and viscosity in a monoclonal antibody formulation, Journal of pharmaceutical sciences, 2010;99(1):82-93.
18. Nishi H, Miyajima M, Nakagami H, Noda M, Uchiyama S, Fukui K., Phase Separation of an IgG1 Antibody Solution under a Low Ionic Strength Condition, Pharmaceutical research, 2010;27(7):1348-60.
19. Cooper C, Dubin P, Kayitmazer A, Turksen S., Polyelectrolyte-protein complexes, Current Opinion in Colloid & Interface Science, 2005;10(1-2):52-78.

Chapter 5

Conclusion and future directions

Chapter 5: Conclusion and future direction

Hyaluronic acid (HA) is one of the major naturally occurring components of body tissues. Many applications of HA have emerged in medicine including tissue engineering, dermatological fillers, and viscosupplementation for osteoarthritis treatment. The cytotoxicity of crosslinking techniques for scaffold fabrication and the high viscosity of viscosupplements have been issues impeding the development of products from HA. Thus, novel HA biomaterials for tissue engineering and improved properties of viscosupplements are in demand. Nanotechnology can be a useful tool to achieve these needs.

The aim of this study was to synthesize HA nanoparticles and use the fabricated nanoparticles to develop colloidal systems for these proposed biomedical applications. First, nanoparticles were successfully synthesized using a technique free of an oil and surfactant. This technique was also used to synthesize nanoparticles from other biomaterials such as chondroitin sulfate (CS). The size and charge of nanoparticles polymer type (HA or CS) depended on polymer concentration, HA molecular weight, reaction time, and the ratio of polymer to crosslinker. These factors may be optimized to reach a desired nanoparticle size and charge.

In the future, this nanoparticle fabrication technique should be tested to make nanoparticles from other polymers. This technique may be suitable to fabricate positively charged nanoparticles from polycations such as chitosan and poly-*L*-lysine. To synthesize nanoparticles, polycations primary amine groups can be crosslinked using a molecule such as an adipic acid crosslinker activated via carbodiimide reagents. Such nanoparticles

can be used to develop colloidal gels via electrostatic interactions with negatively charged nanoparticles.

HA and CS nanoparticles were also used to develop colloidal systems. The concentration of nanoparticles, type of nanoparticles and molecular weight of HA used for nanoparticle fabrication, effected the bulk properties of colloidal gels or colloidal suspensions. Colloidal gels are stable 3-D networks made from nanoparticles; in contrast, colloidal suspensions easily flow by applying shear force. Colloidal gels were formed by mixing 17 kDa HA nanoparticles in deionized water at 15%, 30%, and 45% w/v nanoparticle concentrations. On the other hand, mixing 17 kDa HA nanoparticles at 5% w/v concentration or 1500 kDa HA nanoparticles at concentrations up to 15% w/v concentration led to colloidal suspensions. Moreover, 1500 kDa nanoparticles at 30% and 45% w/v yielded of paste-like materials. CS nanoparticles could only formed colloidal suspensions, even at high nanoparticle concentrations (60% w/v).

The formation of colloidal gels resulted from the physical entanglement of surface chains between nanoparticles. Using 17 kDa HA seemed to yield dangling chains or ‘hairy’ nanoparticles. As a result, 17 kDa HA nanoparticles formed stable colloidal gel networks in deionized water at 15%, 30%, and 45% w/v. Colloidal gels swelled in an excess of deionized water or 0.1 M PBS, but did not dissociate. On the other hand, colloidal gels did not form when using 1500 kDa nanoparticles probably due to the absence of dangling chains on these nanoparticles.

Nanoparticle concentration influenced Young’s modulus, shear modulus, viscoelasticity and viscosity of colloidal gels. Mechanical testing also suggested that the pH and ionic strength of buffer used for colloidal gel fabrication affected Young’s

modulus and shear modulus of colloidal gels at different nanoparticle concentrations. However colloidal gels were elastomeric materials, they did not behave as an ideal neo-Hookean elastomer. Recoverably experiments showed that the samples could recover their initial shape after removing external force. Recovery was observed in both mechanical and rheological experiments performed to evaluate shape recoverability and viscosity recoverability. Finally, colloidal gels could be reformed after destruction.

This novel colloidal gel should be tested for tissue engineering applications in the future. HA colloidal gels self-assemble to form a stable 3-D biomaterial without any chemical reaction. Testing these colloidal systems in the presence of live cells will help to understand the potency of these biomaterials for scaffold fabrication. Different types of cells including chondrocytes and fibroblasts should be used. Mechanical and rheological characterizations in the presence of cells will also define the effect of biological environment on the properties of colloidal gels. Moreover, *in vivo* studies will identify the performance of these novel biomaterials as a means to generate specific tissues such as cartilage and skin in the body. Injectability of colloidal gels as a function of nanoparticle concentration, pH and ionic strength should be investigated in future to enhance the viscosity of the colloidal gels for injection and develop injectable scaffolds.

Rheological characterization of colloidal suspensions showed that the viscosity and viscoelasticity could be controlled. Generally, the viscosity and viscoelasticity of HA formulations could be reduced by including nanoparticles in place of polymer HA. The polymer: nanoparticle ratio and type of nanoparticles (17 kDa HA or 1500 kDa HA nanoparticles) were used to control the viscosity and viscoelasticity of HA formulations by influencing nanoparticle-polymer interactions. Moreover, higher concentration of HA

could be delivered with lower viscosity when using nanoparticles in place of HA polymer, which makes colloidal suspensions more convenient for injection.

The application of colloidal suspensions to enhance the properties of viscosupplements including dermal fillers and intra-synovial viscosupplements should be explored. Polymer solutions at 1.4% w/v of 1500 kDa HA were used as a model viscosupplement to evaluate the effect of nanoparticles on the viscosity and viscoelasticity of HA formulations. *In vivo* studies will help us define performance of modified viscosupplements containing HA nanoparticles to remove skin wrinkles and increase treatment duration upon administration subcutaneously. Moreover, intra-synovial injection of modified viscosupplements containing HA nanoparticles will identify their ability to reduce pain and increase joint function for osteoarthritis treatment.

Appendix

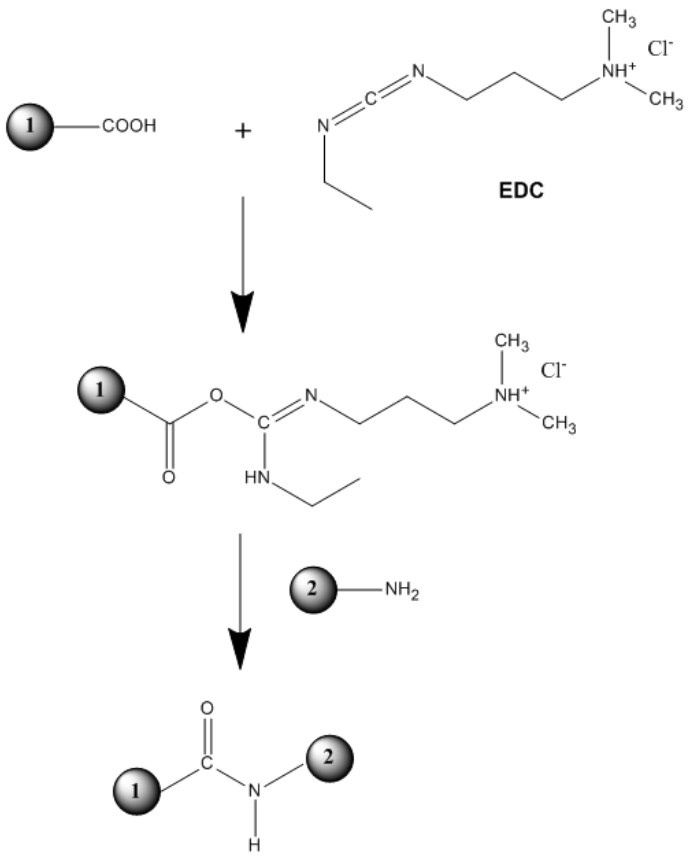

Figure (A-1) Carbodiimide chemistry for peptide bond formation. EDC activates carboxyl groups available on molecule (1) and provide reactive intermediates (O-acylisourea derivatives, extremely short-lived) which reacts with primary amine of molecule (2) forming peptide bond (Correlated to Figure 2-2).

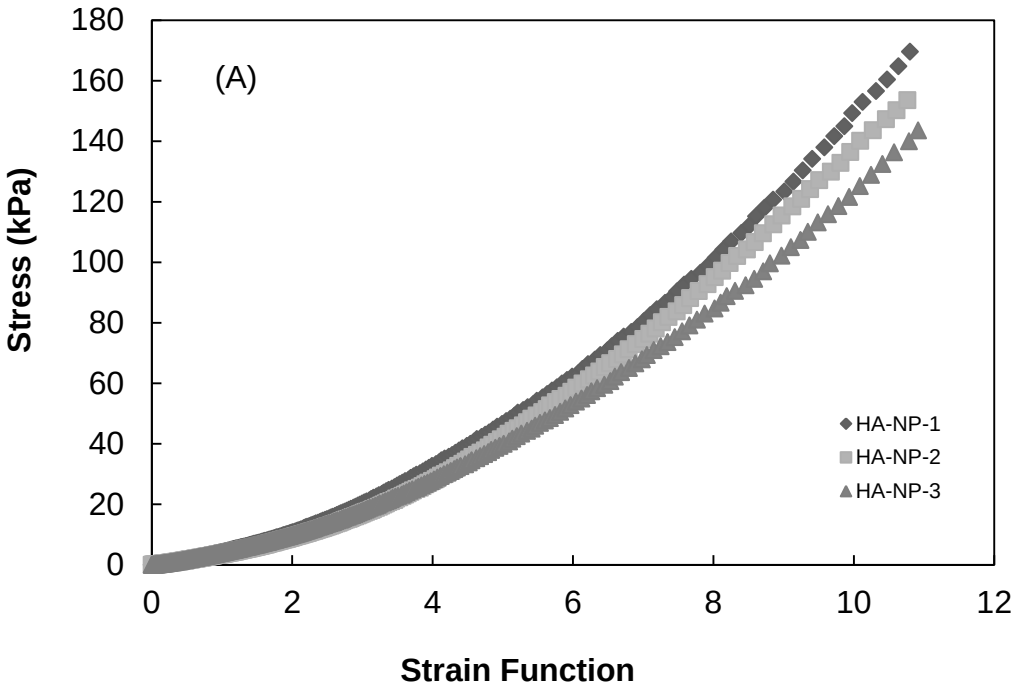

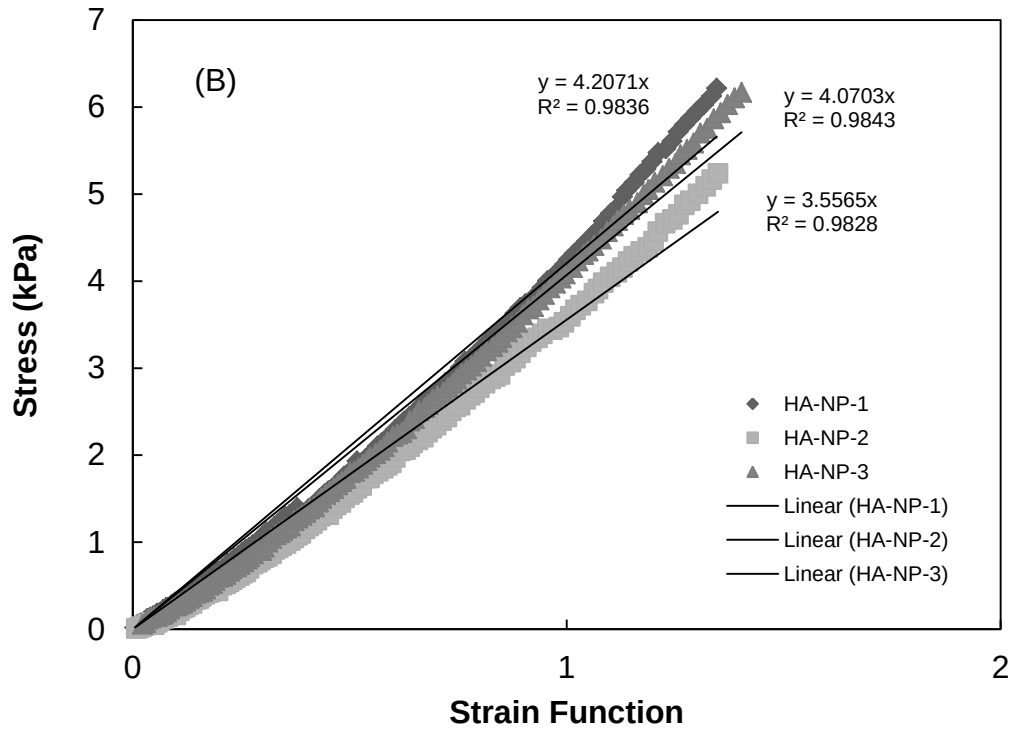

Figure (A-2) (A and B) Stress-strain function curves for 30% (w/v) colloidal gel samples after fabrication (Correlated to Figure 3-8).

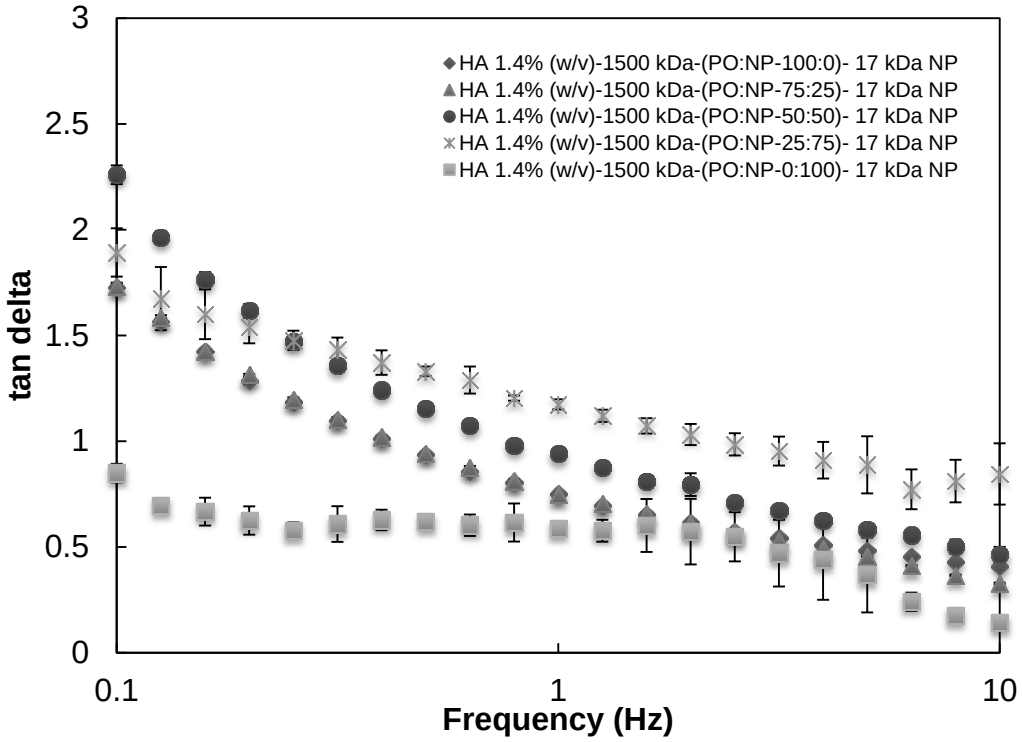

Figure (A-3) Viscoelasticity of HA polymer (1500 kDa) and HA nanoparticle (17 kDa) mixtures: tan delta over frequency range (Correlated to Figures 4-9, 4-10, and 4-11).

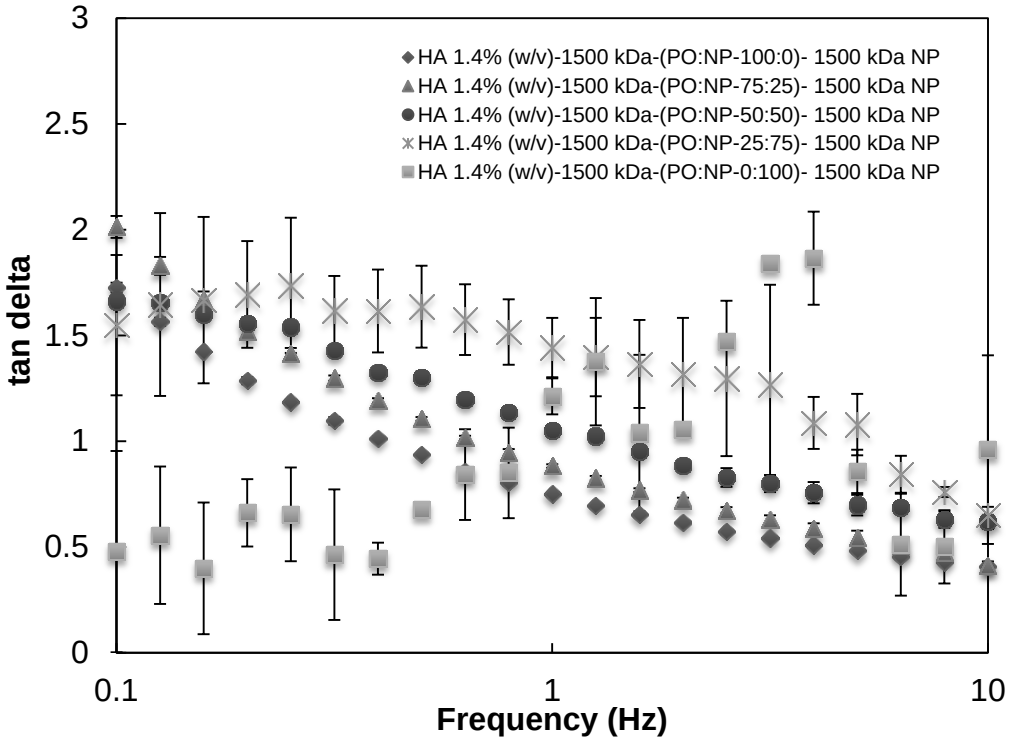

Figure (A-4) Viscoelasticity of HA polymer (1500 kDa) and HA nanoparticle (1500 kDa) mixtures: tan delta over frequency range (correlated to Figures 4-12, 4-13, and 4-14).

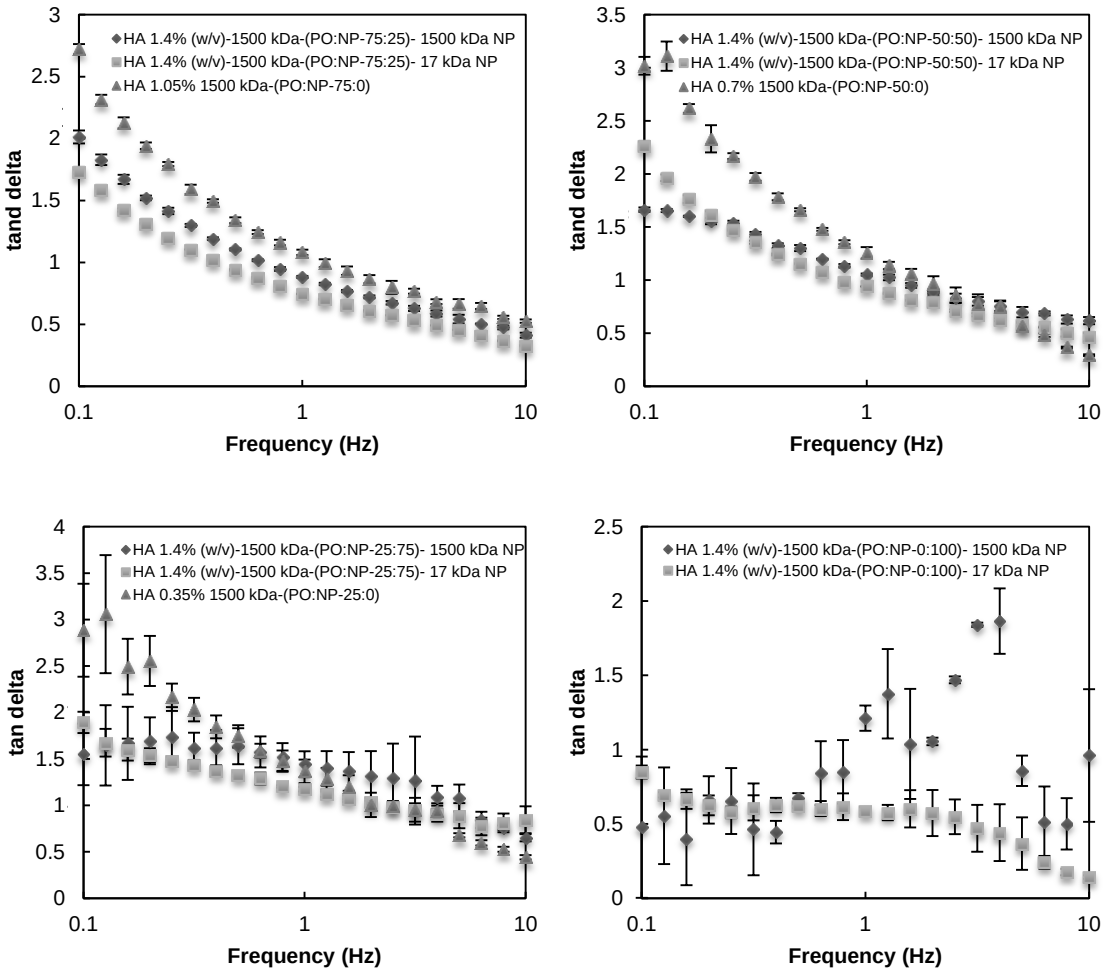

Figure (A-5) Viscoelasticity of HA polymer/nanoparticle mixtures: tan delta over frequency range (Correlated to Figures 4-15, 4-16, and 4-17).